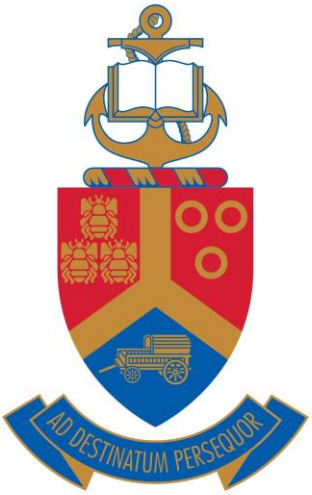

UNIVERSITEIT VAN PRETORIA
UNIVERSITY OF PRETORIA
YUNIBESITHI YA PRETORIA

Exploring the gene regulation response of multi-drug resistant, pathogenic *Escherichia coli* ATCC BAA-196 and *Staphylococcus aureus* ATCC BAA-39 exposed to synthesized iodine containing complexes used as potential antimicrobials

Submitted by
Setshaba Taukobong
u19368659

In partial fulfilment of the requirements, for the Degree MSc Bioinformatics
Centre for Bioinformatics and Computational Biology
Department of Biochemistry, Genetics and Microbiology
University of Pretoria

Submission Date: 07 February 2022

Declaration

1. I understand what plagiarism is and I am aware of the University's policy in this regard.
2. I declare that this final MSc Bioinformatics final thesis for BIF803 is my own original work. Where other people's work has been used (either from a printed source, Internet or any other source), this has been properly acknowledged and referenced in accordance with departmental requirements.
3. I declare that this work has not been submitted by me for a degree at any other University institution.
4. I have not used work previously produced by another student or any other person to hand in as my own.
5. I have not allowed, and will not allow, anyone to copy my work with the intention of passing it off as his or her own work.

SIGNATURE:

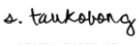

.....

DATE:

07 February 2022

.....

Acknowledgements

I would like to acknowledge and cordially thank my supervisor Dr Oleg N Reva for initiating and allowing me the opportunity to take on this project. It has been a very long and worthwhile journey. I would like to thank The Scientific Center for Anti-infectious Drugs for carrying out the experiments and providing the data for this project. I would also like to extend my gratitude to The National Research Fund and The University of Pretoria for providing the platform and financial support throughout my MSc journey.

Summary

Antibiotic resistance in infection-causing bacteria has been an increasing and persistent issue in healthcare facilities and communities. As a result, the development and production of new classes of antibiotics has been on the decline, rendering it necessary for research to find alternative ways to treat and reverse antibiotic resistance in infection-causing bacteria. The use of nanomolecular complexes as drug delivery systems in combination with existing biocides has shown promising results in addressing resistance in many pathogenic microorganisms. The lack of knowledge pertaining to the mechanism of action of certain drugs or biocides, including nanomolecular complexes, has, however, been a major limitation in the drug discovery process. Many of these drugs have been tested and proven to be effective however, the bioactivity of said drugs is often speculative or unclear. In this study, the transcriptional and metabolic pathway responses were evaluated to identify co-regulated genes and pathways that were affected in response to the exposure of three synthesized iodine-containing nanomolecular complex drugs denoted as KS25, KS33 and KS51 on model clinical isolates *Escherichia coli* ATCC BAA-196 (TEM-10) and *Staphylococcus aureus* ATCC BAA-39. Using DESeq2, with RNA sequence data from the two model microorganisms, a total of 444 and 539 differentially expressed genes (DEG) were identified in *E. coli* and *S. aureus*, respectively. Several major biological processes and pathways were observed in response to the three iodine-containing complexes, including the destruction of barriers, the induction of oxidative stress response genes, the activation and/or deactivation of several biosynthesis pathways such as a change in cellular respiration, amino acid, and nucleotide biosynthesis, mainly caused by halogen/iodine oxidation. The findings further indicated that the way in which the nanomolecular complexes exert their antibacterial effects is bacterial-growth-phase dependent *i.e.*, the effects of the complexes slightly differ in each growth-phase, in which the model organisms were treated at. The complexes were additionally, found to be influenced by the materials used to synthesize them and by their environmental surroundings *i.e.,* the presence of surrounding metal ions that could possibly bind to the nanomolecular complexes and further influencing their bioactivity. This study, therefore, aimed to evaluate the bioactivity of iodine entrapped in the three nanomolecular complexes. In analyzing the effects of these drug complexes on Gram-positive and Gram-negative model organisms, the mechanism of action, sensitivity, and factors influencing the bioactivity of iodine may have been determined, thus bettering the knowledge and the facilitation of the development of potential therapeutic antibacterial agents.

Keywords: Antibiotics, Antibiotic resistance, *Escherichia coli*, *Staphylococcus aureus*, Antibiotic resistance reversion, Combination therapy, Iodine, Nanomolecular complexes.

Table of Contents

Chapter 2: *E. coli* ATCC BAA-196 and *S. aureus* ATCC BAA-39 as model microorganisms for studying bacterial-nanomolecular complex interactions and identifying the factors influencing the bioactivity of complexes KS25, KS33, KS51 based on the transcriptional responses of the model microorganisms

List of Tables

Table S3. Pathways and biological processes of genes expressed during the lag and log phase (≥2 Log2FC, p-value 0.05) in *E. coli* strain ATCC BAA-196 in response to KS25, KS33 and KS51. Genes that were strongly upregulated (≥5 Log2FC) are highlighted in yellow and genes strongly downregulated are highlighted in green. For each pathway, associated genes are listed.

Table S4. Pathways and biological processes of genes expressed during the lag and log phase (≥2 Log2FC, p-value 0.05) in *S. aureus* ATCC BAA-39 in response to KS25, KS33 and KS51. Genes that were strongly upregulated (≥5 Log2FC) are highlighted in yellow and genes strongly downregulated are highlighted in green. For each pathway, associated genes are listed.

Table S5. Table S3. Fold change values of homologous genes differentially expressed in *E. coli* BAA-196 in comparison to *S. aureus* BAA-39 under the effect of three iodine-containing complexes, KS25, KS33 and KS51, in Lag and Log growth phases. Statistically reliable changes of gene expressing (|fold change| ≥ 2.0; p-value ≤ 0.05) are highlighted by yellow (upregulation) or green (downregulation) shading. Genes are ordered by clusters with similar patterns of expression.

Table S6. List of databases and tools used.

List of Figures

Figure 10. Volcano plot of differentially expressed genes identified between KS25, KS33 and KS51 treated variants of *E. coli* ATCC BAA-196 and control group, during the lag growth phase. A) Represents gene regulation in KS25 treated variant of E. coli versus the negative control, B) Represents gene regulation in KS33 treated variant of E. coli versus the negative control C) Represents gene regulation in KS51 treated variant of E. coli versus the negative control. Circles on the plot represent protein coding genes (CDS) plotted according to their negative (blue circles) and positive (orange circles) Log2FC values calculated in the Lag-experiment. The strongest regulated genes are labelled by their gene names. The thin vertical and horizontal lines within the plots separate genes with 1-fold or higher regulation. The panels denoted as -Inf and Inf represent genes that were only expressed in NC (-Inf) and only in treated samples (Inf), respectively.

Figure 11. Volcano plot of differentially expressed genes identified between KS25, KS33 and KS51 treated variants of *E. coli* ATCC BAA-196 and control group, during the lag growth phase. A) Represents gene regulation in KS25 treated variant of *E. coli* versus the negative control, B) Represents gene regulation in KS33 treated variant of *E. coli* versus the negative control C) Represents gene regulation in KS51 treated variant of *E. coli* versus the negative control. Circles on the plot represent protein coding genes (CDS) plotted according to their negative (blue circles) and positive (orange circles) Log_2FC values calculated in the Log-experiment. The strongest regulated genes are labelled by their gene names. The thin vertical and horizontal lines within the plots separate genes with 1-fold or higher regulation. The panels denoted as -Inf and Inf represent genes that were only expressed in NC (-Inf) and only in treated samples (Inf), respectively.

Figure 12. Volcano plot of differentially expressed genes identified between KS25, KS33 and KS51 treated variants of *S. aureus* ATCC BAA-39 and control group, during the lag growth phase. A) Represents gene regulation in KS25 treated variant of *S. aureus* versus the negative control, B) Represents gene regulation in KS33 treated variant of *S. aureus* versus the negative control C) Represents gene regulation in KS51 treated variant of *S. aureus* versus the negative control. Circles on the plot represent protein coding genes (CDS) plotted according to their negative (blue circles) and positive (orange circles) Log_2FC values calculated in the Lag-experiment. The strongest regulated genes are labelled by their gene names. The thin vertical and horizontal lines within the plots separate genes with 1-fold or higher regulation. The panels

denoted as -Inf and Inf represent genes that were only expressed in NC (-Inf) and only in treated samples (Inf), respectively.

Figure 13. Volcano plot of differentially expressed genes identified between KS25, KS33 and KS51 treated variants of *S. aureus* ATCC BAA-39 and control group, during the lag growth phase. A) Represents gene regulation in KS25 treated variant of *S. aureus* versus the negative control, B) Represents gene regulation in KS33 treated variant of *S. aureus* versus the negative control C) Represents gene regulation in KS51 treated variant of *S. aureus* versus the negative control. Circles on the plot represent protein coding genes (CDS) plotted according to their negative (blue circles) and positive (orange circles) Log_2FC values calculated in the Log-experiment. The strongest regulated genes are labelled by their gene names. The thin vertical and horizontal lines within the plots separate genes with 1-fold or higher regulation. The panels denoted as -Inf and Inf represent genes that were only expressed in NC (-Inf) and only in treated samples (Inf), respectively.

Figure 14. PheNetic network of transcriptional regulation of differentially expressed genes of *E. coli* BAA-196 and *S. aureus* ATCC BAA-39 treated with KS25, during the lag phase, grouped by functional or regulatory interactions between genes using upstream (A) which identifies the regulatory mechanisms that induced the observed differential expression and downstream (B) which identifies activated pathways in response to the treatments. Upregulated genes are depicted by pink/red nodes and downregulated genes by green nodes (vertices). The colour intensity indicates the level of regulation. Green edges show activation relations, blue edges show activities of inhibition relations. Direct regulations by transcriptional regulators are indicated by arrowheads. The genes are grouped regulons that are controlled by transcriptional regulators including; *lrp, purR, crp, narL, fnr, fur, rpoH, cra, phoB* and *pdhR.*

Figure 15. PheNetic network of transcriptional regulation of differentially expressed genes of *E. coli* BAA-196 and *S. aureus* ATCC BAA-39 treated with KS25, during the log phase, grouped by functional or regulatory interactions between genes using upstream (A) which identifies the regulatory mechanisms that induced the observed differential expression and downstream (B) which identifies activated pathways in response to the treatments. Upregulated genes are depicted by pink/red nodes and downregulated genes by green nodes (vertices). The colour intensity indicates the level of regulation. Green edges show activation relations, blue edges show activities of inhibition relations. Direct regulations by transcriptional regulators are

indicated by arrowheads. The genes are grouped regulons that are controlled by transcriptional regulators including; *rpoHS, ifhA, pdhR, fis, cytR, hns, hdfR, fihC, yafQ* and *dinJ*.

Figure 16. PheNetic network of transcriptional regulation of differentially expressed genes of *E. coli* BAA-196 and *S. aureus* ATCC BAA-39 treated with KS33, during the lag phase, grouped by functional or regulatory interactions between genes using upstream (A) which identifies the regulatory mechanisms that induced the observed differential expression and downstream (B) which identifies activated pathways in response to the treatments. Upregulated genes are depicted by pink/red nodes and downregulated genes by green nodes (vertices). The colour intensity indicates the level of regulation. Green edges show activation relations, blue edges show activities of inhibition relations. Direct regulations by transcriptional regulators are indicated by arrowheads. The genes are grouped regulons that are controlled by transcriptional regulators including; *isrR, purR, marAB, pepA, ryhB, rpoEH, ihfB, phoB, lrp, nsrR, soxS, oxyR* and *glnG*.

Figure 17. PheNetic network of transcriptional regulation of differentially expressed genes of *E. coli* BAA-196 and *S. aureus* ATCC BAA-39 treated with KS33, during the log phase, grouped by functional or regulatory interactions between genes using upstream (A) which identifies the regulatory mechanisms that induced the observed differential expression and downstream (B) which identifies activated pathways in response to the treatments. Upregulated genes are depicted by pink/red nodes and downregulated genes by green nodes (vertices). The colour intensity indicates the level of regulation. Green edges show activation relations, blue edges show activities of inhibition relations. Direct regulations by transcriptional regulators are indicated by arrowheads. The genes are grouped regulons that are controlled by transcriptional regulators including; *rpoEH, ryhB, glnG, soxS, ihfB, purR, micF, marAB* and *phoB*.

Figure 18. PheNetic network of transcriptional regulation of differentially expressed genes of *E. coli* BAA-196 and *S. aureus* ATCC BAA-39 treated with KS51, during the lag phase, grouped by functional or regulatory interactions between genes using upstream (A) which identifies the regulatory mechanisms that induced the observed differential expression and downstream (B) which identifies activated pathways in response to the treatments. Upregulated genes are depicted by pink/red nodes and downregulated genes by green nodes (vertices). The colour intensity indicates the level of regulation. Green edges show activation relations, blue edges show activities of inhibition relations. Direct regulations by transcriptional regulators are

indicated by arrowheads. The genes are grouped regulons that are controlled by transcriptional regulators including; *purR, fur, rpoEHS, fnr, arcA, glnG* and *crp*.

Figure 19. PheNetic network of transcriptional regulation of differentially expressed genes of *E. coli* BAA-196 and *S. aureus* ATCC BAA-39 treated with KS51, during the log phase, grouped by functional or regulatory interactions between genes using upstream (A) which identifies the regulatory mechanisms that induced the observed differential expression and downstream (B) which identifies activated pathways in response to the treatments. Upregulated genes are depicted by pink/red nodes and downregulated genes by green nodes (vertices). The colour intensity indicates the level of regulation. Green edges show activation relations, blue edges show activities of inhibition relations. Direct regulations by transcriptional regulators are indicated by arrowheads. The genes are grouped regulons that are controlled by transcriptional regulators including; *fnr, micA, fur, nsrR, nemR, gadEWX, phoB, appY, narL, ihfB, rpoH, gcvB, oxyR, kdpE, relE* and *pdhR*.

Figure 20. GO functional categories of genes upregulated and downregulated, from RNA-seq, organized based on GO biological, metabolic and cellular process terms, during the lag and log phase (≥2 Log2FC, p-value 0.05) in E. coli strain ATCC BAA-196 in response to KS25, KS33 and KS51. The number of genes for each functional category are listed. The x-axis represents the number of genes. Positive values indicate upregulation of genes and negative values indicate downregulation of genes.

Figure 20. GO functional categories of genes upregulated and downregulated, from RNA-seq, organized based on GO biological, metabolic and cellular process terms, during the lag and log phase (≥2 Log2FC, p-value 0.05) in *S. aureus* ATCC BAA-39 in response to KS25, KS33 and KS51. The number of genes for each functional category are listed. The x-axis represents the number of genes. Positive values indicate upregulation of genes and negative values indicate downregulation of genes.

Figure 22. Schematic drawing of Iodine, Copper and Cadmium ion uptake from the nanomolecular complexes and environment into bacterial cytoplasm. The Foldchange regulation of *Dps* are highlighted for KS25, KS33 and KS51, respectively and *AhpCF* for KS51.

Figure 23. Schematic representation of nucleotide excision repair in response to DNA damage caused by ROS in *S. aureus*.

Figure 24. Schematic drawing of the iodide induced gene expression for inducing chaperones and removing denatured proteins.

Figure 25. The structural differences between the cell envelope of Gram-positive (left) and Gram-negative bacteria (right) obtained and based on Clifton et al. 2013; Pajerski *et al*., 2019.

Figure 26. Plots of co-regulation of genes in the Lag experimental growth phases in A) *E. coli* BAA-196 vs *S. aureus* ATCC BAA-39 with both treated with KS25 compared with NC; B) *E. coli* BAA-196 vs *S. aureus* ATCC BAA-39 with both treated with KS33 compared with NC; and C) *E. coli* BAA-196 vs *S. aureus* ATCC BAA-39 with both treated with KS51 compared with NC. Circles represent protein coding genes (CDS) plotted according to their negative and positive Log_2FC values calculated in the *E. coli* ATCC BAA-196 (axis X) and *S. aureus* ATCC BAA-39 (axis Y). The outermost regulated genes are labelled by their names or CDS tag numbers. Thin vertical and horizontal lines within the plots separate genes with 1-fold or higher regulation and split the plots to sectors of genes of different categories depending on their coregulation. Numbers of CDS falling to different sectors are shown. Up- and down-coregulated genes, oppositely regulated genes and the genes regulated only in one experiment are depicted by different colours as depicted in the legends. The outermost co-regulated genes are labelled according to respective gene names. The color codes are represented in the key below.

Figure 27. Plots of co-regulation of genes in the Log experimental growth phases in A) *E. coli* BAA-196 vs *S. aureus* ATCC BAA-39 with both treated with KS25 compared with NC; B) *E. coli* BAA-196 vs *S. aureus* ATCC BAA-39 with both treated with KS33 compared with NC; and C) *E. coli* BAA-196 vs *S. aureus* ATCC BAA-39 with both treated with KS51 compared with NC. Circles represent protein coding genes (CDS) plotted according to their negative and positive Log_2FC values calculated in the E. coli ATCC BAA-196 (axis X) and S. aureus ATCC BAA-39 (axis Y). The outermost regulated genes are labelled by their names or CDS tag numbers. Thin vertical and horizontal lines within the plots separate genes with 1-fold or higher regulation and split the plots to sectors of genes of different categories depending on their coregulation. Numbers of CDS falling to different sectors are shown. Up- and down-coregulated genes, oppositely regulated genes and the genes regulated only in one experiment are depicted by different colours as depicted in the legends. The outermost co-regulated genes are labelled according to respective gene names. The color codes are represented in the key below.

Figure 28. Metabolic pathways affected each treatment and extracellular metal ions on the model microorganisms. A) Affected pathways in E. coli BAA-196 treated with KS25 and KS33; B) Affected pathways in E. coli BAA-196 treated with KS51; C) Affected pathways in S. aureus BAA-39 treated with KS25 and KS33; and D) Affected pathways in S. aureus BAA-39 treated with KS51. Up- and down-regulation of pathways are depicted respectively by arrows of yellow and green colours, respectively.

Abbreviations

A. baumannii	*Acinetobacter baumannii*
ABC	ATP-binding cassette
CBCB	Centre for Bioinformatics and Computational Biology
CDS	Coding sequence for protein
COG	Cluster of Orthologous Genes
CuO	Copper oxide
DEG	Differentially expressed genes
DNA	Deoxyribonucleic acid
E. coli	*Escherichia coli*
EAEC	Enteroaggregative *E. coli*
E. faecium	*Enterococcus faecium*
EHEC	Enterohemorrhagic *E. coli*
EIEC	Enteroinvasive *E. coli*
EPEC	Enteropathogenic *E. coli*
ETEC	Enterotoxigenic *E. coli*
ESBL	Extended spectrum β–lactamase
Fe-S clusters	Iron-sulfur clusters
GO	Gene ontology
H. influenzae	*Haemophilus influenzae*
H. pylori	*Helicobacter pylori*
HSPs	Heat shock proteins
K. pneumonia	*Klebsiella pneumonia*
KI	Potassium iodide
Lil	Lithium iodide
Log_2(Fold2change)	Log_2FC
LPS	Lipopolysaccharides
M. tuberculosis	*Mycobacterium tuberculosis*
MBC	Minimal bactericidal concentration
MDR	Multi-drug-resistant
MDR-TB	Multi-drug-resistant tuberculosis
MIC	Minimal inhibitory concentration
MRSA	Methicillin resistant *Staphylococcus aureus*

N. gonorrhoeae	*Neisseria gonorrhoeae*
NCBI	National Centre for Biotechnology Information
NMEC	Neonatal meningitis *E. coli*
NNIS	Nosocomial Infectious Surveillance System
NPs	Nanoparticles
OMPs	Outer membrane proteins
P. aeruginosa	*Pseudomonas aeruginosa*
PBPs	Penicillin-binding proteins
PFTs	Pore-forming toxins
RTF	Resistant transfer factor
RNA	Ribonucleic acid
PFTs	Pore-forming toxins
PVP-I	Povidone-iodine
RefSeq	Reference Sequences database
ROS	Reactive oxygen species
S. aureus	*Staphylococcus aureus*
S. pneumoniae	*Streptococcus pneumoniae*
SAgs	Superantigens
SCAID	The Scientific Centre for Anti-Infectious Drugs
SMR	Small multidrug resistance family
STEC	Shiga toxin-producing *E. coli*
TSST	Toxic shock syndrome
UPEC	Uropathogenic *E. coli*
Usp	Universal stress proteins
UTI	Urinary tract infection
VISA	Vancomycin-intermediate *S. aureus*
VRSA	Vancomycin-resistant *S. aureus*
Hetero-VRSA	Heterologous vancomycin-resistant *S. aureus*
WHO	World Health Organisation
XDR *Mycobacterium tuberculosis*	Extensively drug resistant *Mycobacterium tuberculosis*

Definitions

Free radicals: Radicals are oxygen containing molecules or ions that have one unpaired electron valence, making them extremely chemically reactive. Free radicals include hydroxyl radical, hydrogen peroxide, superoxide anion radical and hypochlorite.

Oxidative damage and stress: Oxidative stress is an imbalance between free radicals and antioxidants in biological systems. The high chemical reactiveness of free radicals can induce multiple chemical reactions called oxidation, which can be damaging if the free radicals outweigh the antioxidants.

Fenton reaction: A reaction that forms hydroxide (OH^-) and hydroxyl radicals from the decomposition of hydrogen peroxide (H_2O_2) ($Fe^{2+}+H_2O_2 \rightarrow Fe^{3+}+\bullet OH+^{-}OH$).

Upregulation (Positive regulation): Involves the activation of gene transcription/translation of protein.

Downregulation (Negative regulation): Involves the suppression of gene transcription/translation of protein.

Nanoparticles/Nanomolecular complexes: Are microscopic particles that are between 1 and 100nm in size and differ in shape, morphology and properties.

Hydrophobicity: A molecule that repels water.

Log_2Fold2change: The effect size estimate that informs how much gene expression has changed due to the treatment in comparison to the control.

P-value: Indicates whether the observed difference between the treatment and control is statistically and significantly different.

Chapter 1: Theoretical Background

1.1 Motivation and Problem statement

S. aureus and *E. coli* are major human pathogens responsible for various community and hospital-acquired infections. Antibiotics have been widely used to treat these infection-causing bacteria. The application of antibiotics, has however, shown major contradictory conflicts, namely, the desired effects of inhibiting bacterial growth, unavoidably leading to the undesired acquisition of bacterial resistance through evolution. When antibiotics were first discovered, Alexander Fleming warned that the inappropriate use and underdosing of penicillin could potentially lead to the development of resistance, therefore the potential of resistance was a well-known possibility even before the phenomenon had occurred (Fleming, 1945). As predicted, antibiotic resistance was reported, soon after their discovery in several disease causing and nosocomial infection-causing bacteria, including *M. tuberculosis, E. coli, S. aureus, A. baumannii* and *K. pneumonia*. As a result of said resistance, the number of developed and approved new classes of antibiotics have been declining over the years (Buckland, 2017), consequently leading to limited treatment options, an increase in medical costs, prolonged hospital stays, and increased mortality.

There has, therefore been, a need to design and develop better drug candidates to meet this challenge. New alternative treatment strategies that will yield novel, long-lasting therapies and methods to rationally utilize existing therapies alone and in combination to achieve the desired drug efficacy. Alternative strategies like antibiotic resistance reversion have since been considered. Antibiotic resistance reversion exploits active drugs that induce a counter-selection of resistant variants from populations of pathogens (Baym *et al.*, 2016). This has been done using combination therapy in efforts to achieve cumulative synergetic effects. The use of multiple antibiotics to impose a direct cost and select against drug-resistant strains is one example of this strategy. The use of antibiotics alongside substrates that select for enzymes that target antibiotics is another. Lastly, the use of antibiotics alongside antimicrobial substances entrapped in nanoparticles (NPs) in efforts to target multiple structures and pathways within the bacterial cells has also been studied and considered. These combination therapy strategies have since shown to be potential solutions in reversing antibiotic resistance in infectious causing bacteria. The synergistic activity between NPs and antibiotics suggests possible solutions in reversing antibiotic resistance in infection-causing bacteria and adjuvant in antimicrobial chemotherapy.

1.2 The history behind antibiotic development and activity

1.2.1 The early days

Bacteria are single celled microorganisms found in a wide range of environments. Some bacteria are known to be harmless, however there are those that are harmful and are known as pathogenic bacteria, meaning when they enter a body of living cells, they begin to cause a disease. Pathogenic bacteria can either be contagious or non-contagious *i.e.* can spread from person to person via skin contact, bodily fluids, airborne particles, contact with faeces, and touching a surface that has been touched by an infected person (Longhurst, 2019).
Contagious pathogenic bacteria have been known prominent threats since the early years of humanity. There are records of multiple infectious diseases caused by bacteria as far back as 3000 BC, affecting millions of people (Papagrigorakis *et al*., 2007). Today, infectious diseases caused by bacteria still remain a prominent threat and are among the leading causes of death worldwide, despite the advances made in medical and scientific research in efforts to treat.

Antibiotics are effective for the treatment of pathogenic bacteria, when prescribed appropriately and used correctly. Antibiotics are antibacterial agents that are capable of inhibiting bacterial growth (Millan, 2018). The idea of antibiotics stems from an observation and principle described by Paul Ehrlich that states; it is possible to create an agent or substance that can selectively target disease-causing bacteria without harming the host cell or other cells. He later came up with several systematic testing approaches alongside chemist Alfred Bertheim, to find drugs like arsphenamine, which is used to treat sexually transmitted infection syphilis caused by Spirochete *Treponema pallidium*. This led to the discovery of the first modern antibiotic even though he had referred to this treatment as chemotherapy (Williams *et al*., 2009). The screening approach introduced by Paul Ehrlich was a landmark event and became the standard approach for drug discovery in pharmaceutical companies. The first classified antibiotic, penicillin, was accidently discovered in 1928 by Alexander Fleming when he noticed a fungal species, *Penicillium notatum* had contaminated an uncovered plate cultured with *Staphylococcus*, preventing its growth (Millan, 2018). Microorganisms such as yeast and fungal species in the genus *Penicillium* produce a wide variety of antibiotics. These microorganisms have been known to produce antibiotics over time to gain a fitness advantage over competitors living in their environment. This discovery, among many, has therefore been, one of the most important tools in medicine and has led to the treatment of many bacterial infections that were once deadly. Today, there are well over 100 antibiotics available that treat

and kill many infection-causing bacteria (Stephens, 2019). Cell death caused by antibiotics is a complex process that involves the interaction between a drug molecule and a bacterium, followed by the disruption and alteration of several cellular components and essential pathways necessary for survival (Tortora *et al*., 2013).

1.2.2 Classification of Antibiotics based on mechanisms of action

Antibiotics target bacteria in several ways, mainly through interfering or inhibiting the cell wall, nucleic acid and protein biosynthesis, through the alteration of cell membranes and antimetabolite activity, ultimately leading to bacterial cell death (Kapoor *et al*., 2017), as illustrated in (Fig. 1). Antibiotics that inhibit cell wall biosynthesis target either penicillin-binding proteins (PBPs), peptidoglycan subunits or peptidoglycan subunit transport systems, therefore preventing the synthesis of the peptidoglycan layer, weakening the cell wall and membrane, leading to the cell undergoing lysis (Tortora *et al*., 2013). Antibiotics that inhibit nuclei acid synthesis interfere with RNA/DNA synthesis by targeting and inactivating folic acid synthesis enzyme, RNA-polymerase, topoisomerase II or DNA gyrase, bacterial enzymes involved in DNA synthesis and DNA/RNA replication, thus interfering with transcription (Hartmann *et al*., 2000). Antibiotics involved in the inhibition of protein synthesis interfere with the process at the 30S or 50S subunit of the ribosome. This prevents the tRNA from binding and adding its amino acid onto the growing polypeptide chain (Payseur, 2019). Antibiotics that disrupt cell membranes, work by permeabilizing the lipopolysaccharide in the outer membrane of the cell and damaging the integrity of the phospholipid bilayer of the inner membrane in Gram-negative bacteria. In Gram-positive bacteria, antibiotics work by increasing the permeability of the cell membrane, allowing unrestricted movement of inorganic substances such as Na^+, thus destroying the ion gradient between the cytoplasm and the extracellular environment (Delcour, 2009). Some antibiotics act as antimetabolites that inhibit certain metabolic pathways *e.g.* sulfonamides antibiotics target folic acid synthesis by inhibiting the enzyme involved in the production of dihydrofolic acid, subsequently, inhibiting production of pyrimidines and purines necessary for nucleic acid synthesis (Edwards, 1980).

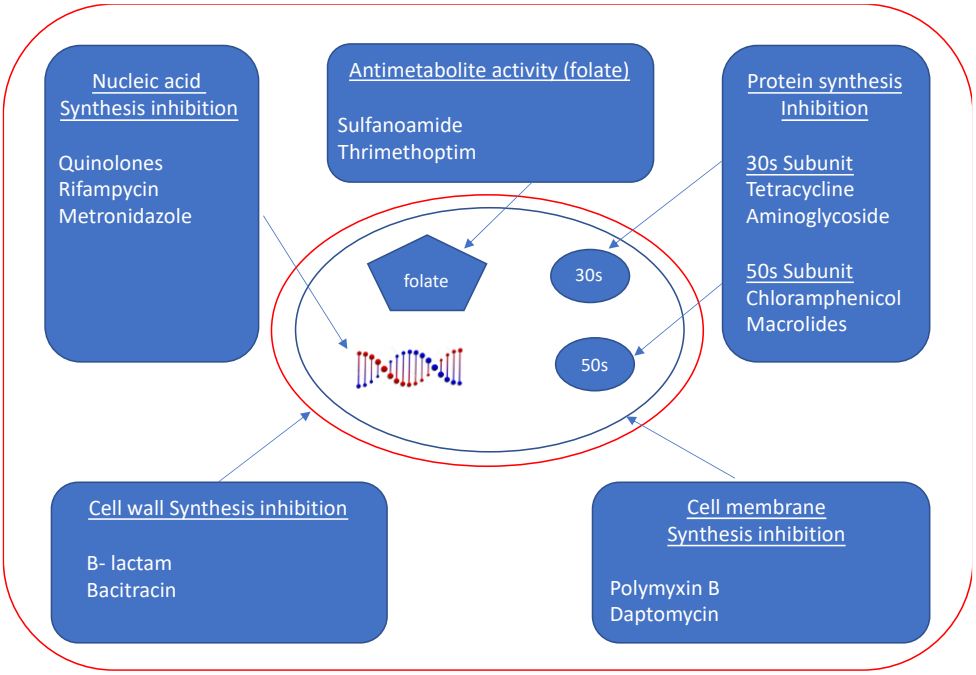

Figure 1. Antibiotics classification and modes of action modified based on Tortora *et al.*, 2013.

Antibiotic drugs have either a narrow or a broad-spectrum microbial activity. Broad-spectrum antibiotics act on both Gram-negative and Gram-positive bacteria when the causative bacteria is unknown (Kumar, 2012). Narrow spectrum antibiotics are used for specific infections when the causative bacteria is known (Kumar, 2012).

1.3 The history behind antibiotic resistance

Since the development of antibiotics, millions of deaths have been prevented; thus, making their discovery one of the biggest triumphs in medicine and science. Increasing resistance in bacteria however has been and is still a major problem. The overuse and misuse of antibiotics, in both humans and animals has been considered the main leading cause of increased multidrug-resistance in infection-causing bacteria. In much of the world, antibiotics are sold without prescription to treat inappropriate conditions. Even with appropriate use, treatment regimens are either shorter than needed to eliminate the infection entirely or patients do not finish the full regime of their prescribed antibiotics, thus encouraging the survival of resistant bacteria. In addition to the ill-use of antibiotics, mutations and horizontal gene transfer play a primary role in antibiotic resistance. This often leads to observed resistance in bacteria even before exposure *i.e.*, penicillin was introduced in 1943, however, penicillin resistance had

already been reported in penicillin-R *Staphylococcus* in 1940. Moreover, resistance has often been observed soon after exposure to an antibiotic *i.e.*, methicillin was introduced in 1960, however, resistance was soon reported in methicillin-R *Staphylococcus* in 1962, as illustrated in (Fig. 2). Consequently, as stated, this has led to the decline in the development of new classes of antibiotics by pharmaceutical companies due to their short lived efficacy, leading to lack the of return on investments (Sukker, 2013). Even with the widely used practise of using antibiotics in combination, this method has been shown to be ineffective in several other infection-causing, resistant bacteria, putting major strain on the health care systems.

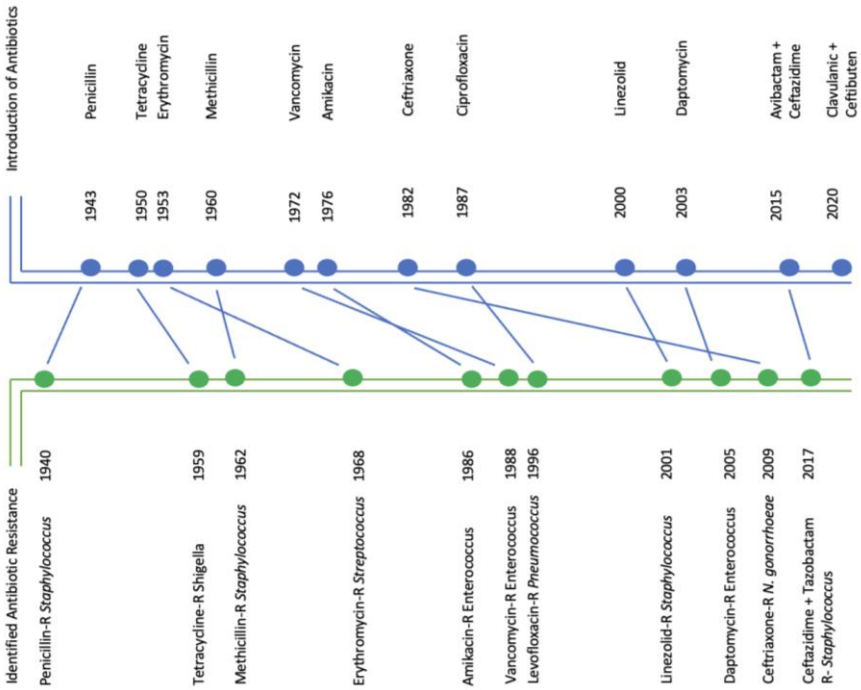

Figure 2. Timeline of antibiotic development and resistance. The top panel illustrates the date at which different antibiotics and classes of antibiotics were discovered and introduced. The bottom panel, illustrates the date at which resistance was observed for the given antibiotics. Modified based on the Centers for Disease Control (CDC). Antibiotic Resistance Threats in the United States, 2019. Atlanta, GA: U.S Department of Health and Human services, CDC, 2019.

1.4 Antibiotic resistance acquisition

1.4.1 Antibiotic resistance acquisition through mutations:

A mutation is change or alteration in a DNA sequence can occur spontaneously or can be induced. Spontaneous and antibiotic-Induced mutagenesis events related to resistance often occur as a response to natural selection incurring a survival advantage in the bacteria's environment (Woodford, 2007). There are several mechanisms of antibiotic resistance that are based on mutational events, like mutations in sequences of genes encoding the target of the antibiotics (Ruiz, 2003). Resistance to rifampicin and fluoroquinolones for instance, is caused by mutations in the target sites; *RpoB* and DNA-topoisomerases, respectively (Shaikh *et al*., 2015). The sites at which the antibiotics targets becomes altered in such a way that the antibiotics can longer bind to them and are otherwise made ineffective.

1.4.2 Antibiotic resistance acquisition through horizontal gene transfer:

Bacteria are able to pass their genetic material not only to their offspring but to other bacteria of the same species. The transfer of genes involves a donor cell giving a part of their gene to a recipient cell. The transferred genes are then incorporated into the recipient's DNA. Antibiotic resistance genes can be transferred by means of conjugation, transformation or transduction (Bello-López *et al*., 2019). Plasmids containing foreign DNA and resistant genes can be transferred to a bacterium from the environment by means of transformation or through being infected by a bacteriophage by means of transduction (Von Wintersdorff Christian *et al*., 2016). Transferal of resistance through conjugation is mediated with plasmids known as R-determinant and resistant transfer factor (RTF) plasmids (Bonnet, 2004). RTF is responsible for conjugal transfer. R-determinant plasmids have resistance genes that encode enzymes that inactivate certain drugs (Bonnet, 2004). Antimicrobial resistant islands are horizontally transferred DNA inserts that also carry resistant genes and are often horizontally transferred from one species to another (Ramsay *et al.*, 2017). horizontal gene transfer including conjugation, transduction and transformation or through spontaneous or induced mutations.

1.5 Mechanisms of antibiotic resistance

Major modes of antibiotic resistance mechanisms, include the following;

1.5.1 Enzymatic degradation or inactivation of antibiotics:

PBPs play an essential role in peptidoglycan synthesis, a key component of the bacterial cell wall. β-lactam antibiotics such as penicillin target PBPs (Bush, 2010). Several bacterial cells produce β-lactamase enzymes which target the β-lactam ring, hydrolyses it and destroys the structure (Bush, 2010). Resistance to β-lactam antibiotics in bacterial cells is mainly due to mutations in the PBPs or excessive synthesis of new PBPs that are insensitive to β-lactams antibiotics (Egorov *et al*., 2018). Resistance to β-lactams antibiotics has today, contributed to the spread of *E. coli* resistance to penicillins and *S. aureus* strains resistance to methicillin and cephalosporins.

1.5.2 Prevention of penetration to the target site within the microbe or limiting drug uptake:

Changes in the target site are often due to spontaneous mutations *i.e.,* resistance to rifamycin and quinolones are a result to mutations in RNA polymerase and DNA gyrase (Peter *et al*., 2005). Most Gram-negative bacteria are usually more resistant to antibiotic drugs due to the nature of their cell walls, which restricts absorption of certain substances through their porins. The bacteria are able to modify their porin openings in a manner that prevents antibiotics from entering the periplasmic space, thus limiting or preventing drug uptake (Munita *et al*., 2015). Methylation of the ribosomes for example, endows resistance to most ribosome-targeting antibiotics like tetracycline (Rev *et al*., 2014).

1.5.3 Rapid efflux of the antibiotic:

Bacteria have certain proteins in the plasma membrane that act as pumps that expel substances, preventing them from reaching a concentration high enough to be effective (Yang *et al*., 2004). These proteins include; the ATP-binding cassette (ABC) superfamily and the small multidrug resistance (SMR) family, which are activated in response to toxic substances (Yang *et al*., 2004).

1.5.4 The use of an alternative metabolic pathways to bypasses the action of antibacterial drug:

Several antibiotics target and block bacterial pathways. Bacterial cells can, however, adapt or use alternative pathways to overcome the antibacterial effects of antibiotics. This antibacterial mechanism has been reported to be somewhat effective as the antibiotics are able to slow down the bacterial growth (Porter, 2007).

1.6 The present and future prospects of antibiotics

In 2017, the World Health Organisation (WHO) announced its first ever list of multidrug-resistant bacteria that pose the greatest threat to human health, illustrated in (Table 1). The list is divided into three categories: critical, high and medium priority with the critical category being multidrug resistant bacteria that pose the most threat in hospitals and nursing homes. In the last 40 years, only one member of the synthetic oxazolidinone antimicrobial drug, linezolid has been introduced and clinically used in efforts to treat bacteria in the priority list. Linezolid was introduced in the market in 2000 (Leach *et al*., 2011) and used against only certain Gram positive bacteria listed in the WHO priority pathogens list, including; multidrug resistant enterococci, *S. pneumoniae*, methicillin resistant *S. aureus* (MRSA) and vancomycin-resistant *Enterococcus faecium*. It is involved in the inhibition of protein synthesis by interfering with the processes at the 50S subunit of the ribosome (Leach *et al*., 2011). Linezolid resistance in *S. aureus* and several enterococcus species has, however, been encountered clinically as well as *in vitro*, but has been reported to be a rare occurrence (Stefani *et al*.,2010). As of December 2019, 41 antibiotics were in development, with 15 in Phase I of clinical trials, 12 in Phase II, 13 in Phase III and 1 has been submitted for FDA approval (PEW, 2020).

In addition, the WHO added 3 new antimicrobials to its list of recommended medicines which are ceftazidime-avibactam, meropenem-vaborbactam, and plazomicin, drugs that are a combination of several existing antibiotics or a combination of existing antibiotics with biocide substrates that inhibit resistance mechanisms secreted by bacterial cells. These drugs are classified under "reserve or last resort" drugs that are only prescribed when all other options have failed. Despite the efforts of introducing new classes of antibiotics, antibiotic resistance in bacteria is an inevitable outcome, proving the process of developing new antibiotics in an effort to keep ahead of resistance, impractical and futile. Combining several existing antibiotics with other substrates has, however, shown to be a viable option to treat antibiotic-resistant bacteria. The benefits of using antibiotics in combination includes synergy, the is a reduced probability of simultaneous resistance against two drugs as compared to using a single drug and a wider range of bacteria can be targeted (Coates, 2019). The future of antibiotics therefore ultimately lies in either the combination of multiple antibiotics administered at once or a combination of antibiotics with certain antimicrobial biocides.

Table 1. List of drug-resistant bacteria that pose the greatest threat to human health. Based and obtained from: The drug-resistant bacteria that pose the greatest health threats (Willyard, 2017; WHO, 2017).

Priority	Bacteria	Antibiotics resistance	Health effects
Critical			
	A. baumannii	Carbapenem	Hospital infections
	P. aeruginosa	Carbapenem	Hospital infections
	Enterobacteriaceae	Carbapenem	Hospital infections
High			
	E. faecium	Vancomycin	Hospital infections
	S. aureus	Methicillin, Vancomycin	Sepsis, pneumonia, skin infection
	H. pylori	Clarithromycin	Stomach ulcers, cancer
	Campylobacter spp.	Fluoroquinolone	Diarrhoea
	Salmonellae	Fluoroquinolone	Diarrhoea
	N. gonorrhoeae	Cephalosporin, Fluoroquinolone	Gonorrhoea
Medium			
	S. pneumoniae	Penicillin	Pneumonia
	H. influenzae	Ampicillin	Pneumonia, meningitis
	Shigella spp.	Fluoroquinolone	Diarrhoea

1.7 Antibiotic resistance and virulent properties in *E. coli* and *S. aureus*

Among the many multidrug-resistant bacteria, methicillin-resistant *S. aureus* and extended spectrum β–lactamase (ESBL) producing *E. coli* are major causes of concern because of the reported public health threats worldwide. The Centre for Disease Control and Prevention has estimated that toxin strains of *E. coli* have been responsible for about 265 000 infections annually (Nicholl, 2019) and the annual incidence of *S. aureus* infections worldwide is approximately 10 to 30 per 100,000 person-years (Tong *et al*., 2015). Nosocomial infections have been reported to contribute to 0.7–10% of deaths occurring in hospitals (WHO, 2002), with *E. coli* responsible for 30% of these infections (Ferry *et al*, 2004) and an estimated 80 000 patients contracting MRSA infection after hospital admission per year as per Nosocomial Infectious Surveillance System (NNIS) (Bhat *et al*, 2014). Many efforts have been introduced to reduce the occurrence of nosocomial infections in hospitals such as encouraging health care providers to wash hands as often as possible with alcohol, disinfecting medical instruments with alcohol after every use, wearing masks, gloves and coats and utilize copper medical

equipment (Saloojee and Steenhoff, 2001;Buntz, 2013). Despite the efforts, nosocomial infections caused by *S. aureus* and *E. coli* still seem to be a persistent major problem.

1.7.1 *E. coli* pathotypes and mechanisms of resistance

E. coli is a Gram-negative, facultative anaerobic, rod-shaped bacterium that forms part of the human gastrointestinal microbiota and is usually harmless. Some strains of *E. coli* are, however, known to cause a spectrum of infections including; pneumonia, cholecystitis, cholangitis, peritonitis, cellulitis, osteomyelitis, infectious arthritis and neonatal meningitis (Pitout, 2012). Virulent pathotypes of *E. coli* strains include STEC, ETEC, EHEC, EPEC, EAEC, EIEC, UPEC and meningitis-associated *E. coli*, illustrated in (Table 2). STEC and EHEC produce Shiga toxins, which are known potent bacterial toxins, originally produced by *Shigella* spp (Melton-Celsa, 2014). EPEC strains have a type III secretion system to deliver effector virulence proteins into host cells leading to A/E lesion formation and diarrhoeal disease (Donnenberg *et al*., 2013). EAEC aggregates and adheres to the intestinal mucosa of animals, where they produce cytotoxins that damage host cells and induce inflammation, resulting in diarrhoea (Okhuysen *et al*., 2010). EIEC belongs to the same pathotype of *Shigella* and contains an invasion plasmid that encodes T3SS, a type III secretion system, which enables it to invade epithelial cells, multiply within the cytoplasm, take control over the cells actin-filament assembly machine and disperse from one cell to the other (Donnenberg, 2014).

UPEC and NMEC strains often affect the immune system by producing toxins, structural attachment components (P fimbriae encoding gene *pap* and Type I fimbriae encoding *fim*) and iron acquisition systems such as siderophores. Iron is an essential micronutrient that plays several roles in bacteria, more so, in proliferation and pathogenicity. Iron is needed for the expression of virulent determinants, therefore during iron starvation, bacteria synthesize and secrete high-affinity ferric iron chelators known as siderophores that scavenge iron from their surrounding environment, including their host and thus provides the itself with iron (Behnsen *et al*., 2016). This allows the infectious bacteria to persist longer in the host and express virulent determinants. Recent studies have shown that siderophores have additional functions. Enterobactin, for example, appears to protect Gram-negative bacteria from oxidative stress, thus contributing to resistance to certain stressors (Behnsen *et al*., 2016). UPEC strains have been reported to use yersiniabactins copper-binding properties as a mechanism to resist the toxic effects of copper, possibly rendering resistance to copper antimicrobial products

(Chaturvedi *et al*., 2012). Siderophores and the other above-mentioned virulence factors are often shared by horizontal gene transfer between species by means of plasmids and mobile genetic cassettes.

Table 2. Virulence factors and Clinical features of *E. coli* pathotypes.

Pathotypes	Virulence factors	Clinical features
STEC EHEC	Shiga-toxin, endotoxins, attachment and effacement	Bloody diarrhoea, haemorrhagic colitis, nausea, haemolytic uremic syndrome (Melton-Celsa, 2014)
ETEC	Heat stable and heat labile enterotoxins	Watery diarrhoea, nausea, vomiting, muscle aches (CDC, 2014)
EPEC	Type II secretion system, pili	Watery or bloody diarrhoea, vomiting (Donnenberg *et al*., 2013)
EAEC	Cytotoxins, pili	Watery or bloody diarrhoea with mucus, vomiting (Okhuysen *et al*., 2010)
EIEC	Invasion plasmid T3SS	Watery diarrhoea or dysentery (Donnenberg, 2014)
UPEC	P fimbriae, Type I fimbriae, lipopolysaccharides, iron acquisition systems, PAI	Cystitis, pyelonephritis, UTI (Aguiniga *et al*., 2016)
NMEC	K1 capsule, P fimbriae	Neonatal meningitis, sepsis (Gupta *et al.*, 2018)

The available treatment options for infections caused by the diverse pathogenic *E. coli* have included maintaining enough rehydration in instances of diarrhoea and a prescribed course of β-lactam antibiotics, nitrofurantoin, ciprofloxacin, aminoglycosides and trimethoprim-sulfamethoxazole (Alanazi *et al*., 2018). The mechanisms of resistance to β-lactam antibiotics have, however, been reported and observed. β-lactamases conferring resistance to cephalosporins were reported in numerous studies in *E. coli* (Jacoby *et al*.1988). Additional resistance to cephamycins and carbapenems soon followed after the emergence of AmpC β-lactamase (Philippon *et al*., 2010). β-lactamase enzymes can be traced back to millions of years ago in bacteria and have been reported to have emerged from environmental sources to protect bacteria from naturally occurring β-lactams (Bush, 2010). Their ancestors were believed to be penicillin-binding proteins that share sequence homology with β-lactamases that have an active-site serine (Bush, 2010). *E. coli* produces β-lactamases known as ESBL, which are a

group of chromosome-and-plasmid associated enzymes that are encoded by (*bla*) genes, responsible for resistance-mechanisms that prevent antimicrobial treatment (Shaikh *et al*., 2015). Well over 200 ESBLs have been characterized to date (Shaikh *et al*., 2015).

β-lactamases are classified under Ambler or Bush-Jacoby-Medeiro. These classifications are based on protein homology (amino acid similarity) (Ambler *et al*., 1991). Ambler's classes A, C and D are serine β-lactamase whereas class B enzymes are metallo-type β-lactamase (Ambler *et al*., 1991). Bush-Jacoby-Medeiro classification was based on the functional properties of the enzyme (Bush *et al*., 1995). The various ESBLs produced by *E. coli* were subdivided into the following classes; SHV, TEM, CTX and OXA. TEM-1 was first discovered in Greece in the 1960s followed by the discovery of other types of TEM varieties (Price, 2019). TEM-1 and TEM-2 types are able to hydrolyse penicillin as well as first generation cephalosporins however cannot hydrolyse oxyimino cephalosporins (Soughakoff *et al*., 1988). SHV hydrolyse β-lactams antibiotic penicillin and narrow spectrum cephalosporins (Jacoby *et al*., 2005).

OXA-1 enzymes have been reported to hydrolyse oxacillin and amoxicillin-clavulanic acid which are widely used antibiotics for treating infections caused by *E. coli* (Oteo *et al*., 2010). OXA-1 was originally discovered in *P. aeruginosa* isolates in Ankara hospital (Turkey) and later discovered in *E. coli* isolates thus showing evidence of possible spread of resistance between the two species of bacteria (Poirel *et al*., 2001). CTX types have been found and are more prevalent in *E. coli* and other species of *Enterobacteriaceae.* They hydrolyse cefotaxime and ceftazidime (Bradford *et al*., 1995). Studies have shown that the way in which CTX-M ESBLs were acquired by *E. coli* was by horizontal gene transfer from other bacteria using conjugative plasmids or transposons (Olson *et al*., 2005). The gene sequences encoding CTX-M enzymes of *E. coli* have shown to be very similar to those of β-lactamases of *Kluyvera* species and in addition to this, the gene sequences adjacent to the CTX-M genes of *E. coli* are also similar to those surrounding β-lactamases genes on the chromosome of *Kluyvera* species (Olson *et al*., 2005). CTX-M15 type on *E. coli* has been found to be located on highly mobile *IncFII* plasmids and associated with mobile genetic element IS26 (Woodford *et al*., 2011). Additionally, the activation of efflux pumps and plasmid-mediated resistance mechanisms like *qnr* genes have been reported to reduce fluoroquinolone sensitivity in *E. coli*, with high levels of resistance owing to the mutations within the quinolone resistance determining regions of *gyrA* and *parC* (Johnson *et al*., 2013). Medications used to treat ESBL producing *E. coli* has included carbapenems, fosfomycin, colistin and beta-lactamase inhibitors (Jewell, 2017).

However, resistance to carbapenems in *Enterobacteriaceae* (carbapenem-resistant *Enterobacteriaceae*) has been attributed to three major mechanisms including porin-mediated resistance that reduces the uptake of carbapenems, efflux pumps which expel carbapenems outside the cells and enzyme-mediated resistance *i.e.* carbapenemase genes that hydrolyse carbapenems (Elshamy and Aboshanab, 2020).

1.7.2 *S. aureus* pathogenicity and mechanisms of resistance

S. aureus is an opportunistic, Gram-positive, facultative aerobic bacterium, mostly commonly found on the skin, nose, and mucous membrane of humans. It is known to causes no harm, however, if it happens that it enters the human body through an opening such as a wound or is ingested, it can cause a wide range of deadly infections including endocarditis, food poisoning, cellulitis, mastitis, phlebitis, meningitis, urinary tract infections, toxic shock syndrome, skin and soft tissue infections, bone and joint infections, pneumonia and bloodstream infections (Tong *et al*., 2015). The success of infections caused by *S. aureus* is due to the production of several virulent factors including surface proteins that promote penetration, colonisation, bacterial adherence in the host cell, surface factors that inhibit phagocytic engulfment and host cell defence mechanisms, invasions that promote bacterial spread in tissues and the secretion of extracellular toxins and enzymes that destroy the host cell and tissues (Lowy, 1998).

1.7.2.1 Adherence to host cell

S. aureus express a wide range of surface proteins that are involved in adhering directly to the host cells, including fibrinogen binding proteins, serine aspartate repeat-containing protein D *SdrCDE*, clumping factor A *ClfA*, autolysin Atl, and serine-rich adhesin for platelets *SraP* (Josse *et al*., 2017).

1.7.2.2 Avoidance of host defence mechanisms

S. aureus has also evolved several immuno-modulatory mechanisms to resist phagocytosis. For instance, certain proteins are produced to regulate the binding of IgG antibodies to the bacterial surface protein A and immunoglobulins (Sbi) (Kuipers *et al*., 2016). Furthermore, capsular polysaccharide and extracellular fibrinogen binding protein (Efb) are secreted in efforts to protect the bacterial surface and surface-associated proteins like opsonins, from being recognized by phagocytic cells (Ko *et al*., 2013).

1.7.2.3 Enzymes and membrane damaging toxins

Some virulent factors produced by *S. aureus* can be described as toxins that are secreted in an attempt to 1) damage the host cell membrane, 2) interfere with receptor functions and 3) secrete enzymes that degrade host molecules or affect important host defence mechanisms (Otto *et al*., 2014). There are three main groups of toxins that are secreted by *S. aureus* including pore-forming toxins (Hemolysin-αβγδ, leukotoxins and phenol-soluble modulins), exfoliative toxins and superantigens. Pore-forming toxins (PFTs) are membrane-damaging toxins that cause cell lysis and leakage of vital molecules and metabolites. The lysis of the molecules and metabolites is dependent on receptor interaction (receptor-mediated) and those that interfere with membranes without receptor interaction (receptor-independent). Receptor meditated toxins include hemolysins (αβ), which are known to lyse red blood cells while leukotoxins are known to lyse white blood cells (Otto *et al*., 2014). Receptor-independent toxins include hemolysins (γδ) which are classified under phenol-soluble modulins and do not require a receptor for their hemolytic activity (Wang *et al*., 2007). Exfoliative toxins are exotoxin serine proteases that recognize and hydrolyze desmosome proteins in the human skin and are only produced by certain *S. aureus* strains. Exfoliative toxins in the host, have been associated with the loss of keratinocytes and cell-to-cell adhesion causing peeling and blister formation on host skin (Amagai *et al*., 2002). Superantigens (SAgs) are exotoxins that trigger T cells and proliferation resulting in the overproduction of cytokines, leading to systemic inflammation and shock (Xu *et al*., 2021). SAgs have been reported to be associated with food poisoning and toxic shock syndrome (TSST) (Grumann *et al*., 2014).

The available treatment options for infections caused by *S. aureus* have included beta-lactam antibiotics, ancomycin, aminoglycosides, tetracyclines, fluoroquinolones, macrolide (erythromycin), lincosamide (clindamycin), vancomycin, linezolid, and surgery if the infection has spread to some parts of the body such as the bones (Bush, 2021). Several strains of *S. aureus* have however, adapted effective mechanisms to avoid their antimicrobial effects. Penicillin, for instance, was introduced in 1940 to treat infections caused by staphylococci, penicillin-resistant staphylococci was, however, observed in 1942, first in hospitals and later in the community (Rammelkamp and Maxon, 1942). *S. aureus* resistance to β-lactam antibiotics is mediated by the *bla* gene, encoding β-lactamase enzymes and the *mecA* gene, encoding the penicillin-binding protein PBP-2a which has a low affinity for β-lactam antibiotics (Timothy *et al*., 2017). Penicillin-resistant *S. aureus* carry a plasmid-encoded penicillinase which hydrolyse the penicillin β-lactam ring, leading to penicillin resistance (Guo *et al*., 2020). An alternative antibiotic, methicillin was then introduced and applied in 1959, to

control infections caused by penicillin-resistant *S. aureus* (Rayner and Munckhof, 2005; Khoshnood *et al*., 2019). In the early 1960s however, isolates of methicillin-resistant *S. aureus* (MRSA) were reported, with this type of resistance owing to the *mecA* gene, encoding penicillin-binding protein PBP2a or PBP2′ integrated into the *Staphylococcal* cassette chromosome mec element (SCCmec) (Schulte and Munson, 2019), rendering it resistant to virtually all β-lactam antibiotics, including cephalosporins and carbapenems. MRSA has been identified as one of the most common nosocomial pathogens that cause a broad spectrum of persistent and deadly infections. Vancomycin has since been used as a first-line drug option to treat hospital- and community-acquired infections caused by MRSA.

In July 2002, the CDC in the United States of America reported the first strain of *S. aureus* that was resistant to both vancomycin and methicillin (CDC, 2002), carrying transposon Tn1546 that includes *vanAB* operons, reported to have been acquired from vancomycin-resistant *Enterococcus faecalis* (Zhu *et al*., 2013). Vancomycin-resistant *S. aureus* is divided into three types: vancomycin-resistant *S. aureus* (VRSA), vancomycin-intermediate *S. aureus* (VISA) and heterologous vancomycin-resistant *S. aureus* (hetero-VRSA), classified according to the minimal inhibitory concentration (MIC) of clinically isolated *S. aureus* to vancomycin (Amberpet *et al*., 2019; Baseri *et al*., 2018). The resistance mechanism of vancomycin is due to the *vanA*B operons, which encodes an enzymes that modifies, lowers affinity or eliminates the vancomycin-binding site, endowing resistance to vancomycin (Périchon *et al*., 2009). As it stands, glycopeptide-based antibiotics like teicoplanin, telavancin and daptomycin are being used as initial therapy drugs against MRSA, VISA and VRSA (Choo *et al*., 2016). Furthermore, ceftaroline has been used against MRSA and have been reported to be active against VISA and VRSA *in vitro* (Espedido *et al*., 2015).

1.8 Combination therapy to treat and combat antibiotic resistance in MDR bacteria

Considering the persistent antibiotic resistance problem in infection-causing bacteria, multiple studies and strategies have been carried out to minimize or invert the selective advantage of resistance in bacteria. Antibiotic resistance reversion has become a prospective approach to combat drug resistance in bacteria. In previous publications, antibiotic resistance reversion has been described as the suppression of antibiotic resistance proteins like drug pumps and/or antibiotic-degrading enzymes (Reading *et al*., 1977; Rodrigues *et al*., 2013). This approach has shown a considerable breakthrough in tackling resistance in many pathogenic microorganisms.

It has been demonstrated in studies where several antibiotics are administrated at the same time or are antibiotics are administrated in combination with other biocides in effort to impose a direct cost on resistance and select against drug-resistant strains. Research is now focused on steering towards preserving the efficacy of existing antibiotics instead of producing new antibiotic drugs. A review by Singh *et al*. (2017) identified and classified drug combinations that are effective in combating drug resistance, and identified considerable differences between the combined and individual effects of these drugs. The findings of the review suggested that antibiotic combinations with combined lowered effects than an individual antibiotic drug can reverse resistance. It was found that certain combinations of drugs are more powerful together than their individual effects, this was termed synergistic interactions (Singh *et al*., 2017). Other combinations, however, show less inhibition effects than their individual effects, this was termed antagonistic interactions (Singh *et al*., 2017). Within the antagonistic interactions, there are cases where the growth inhibition of bacteria by one antibiotic decreases when a second antibiotic is added, this is termed suppressive interactions (Singh *et al*., 2017). Strategies to combat resistance that use drugs in combination have shown to be effective therapies in HIV, tuberculosis, MRSA and some cancers (Shafer *et al*., 1999; Bozic *et al*., 2013). A standard treatment of the combination of isoniazid, rifampicin, ethambutol and pyrazinamide is still used today to treat tuberculosis (WHO, 2010). Additionally, some experts have recommended using TMP-SMX (trimethoprim-sulfamethoxazole) and rifampin in combination to treat infections caused by MRSA (Baorto, 2021).

The use of antibiotics in combination in bacteria, however, have some limitations *i.e.* some antibiotics often do not demonstrate synergy instead the effect of the antibiotic in combination

is more often equal to the effect of each antibiotic administrated alone or in most cases, the effect of the combination is less than each antibiotic administrated alone (antagonistic effect). Another proposed alternative strategy has been to use antibiotics in combination with substrates. *β*-lactamase inhibitors are drugs that are administrated in combination with *β*-lactam antibiotics. *β*-lactamase inhibitors are able to bind to *β*-lactamase enzymes and inactivate them, allowing the antibiotics to target respective proteins. These inhibitors are commonly referred to as suicide substrates which contain a β-lactam structure allowing them to bind reversibly on β-lactamase enzymes and thus inhibit their effect. Commercially-used inhibitors include clavulanate, sulbactam and tazobactam. (Bush *et al*., 2021). Clavulanic acid is used in combination with penicillin and cephalosporin, sulbactam with ampicillin and tazobactam with piperacillin. (Bush *et al*., 2021). This approach is, however, only limited to *β*-lactamase-producing bacteria.

1.8.1 Applications of Nanoparticles in antimicrobial therapy

The use of NPs as drug delivery systems has been shown to be effective in the treatment of resistant viral and bacterial infections. NPs are microscopic particles that are between 1 and 100nm in size, may differ in shape, morphology and properties. The concept and ideas of nanomaterials were first introduced and described by physicist Richard Feynman in 1959, where he described a process in which scientists would be able to manipulate and control individual atoms and molecules. The way in which nanomaterials such as NPs are synthesized depends on the materials used. They can either be carbon-, metal-, semiconductor-, ceramic-, polymeric-, liposomes-, micelles-, solid lipid-, nanostructured lipid carrier-, nanocapsule-, nanotube-, quantum dot-, dendrimer-, emulsion-, nanogel- or vesicle-based NPs (Ray, 2018). Today, NPs are used in medical applications, energy, electronics, environment applications, manufacturing and materials applications. The use of NPs has received much attention due to their higher surface to volume ratio, stability and ease of surface alteration in many industries (Syed *et al*., 2018). In medical applications, NPs used as drug delivery or antimicrobial systems are often synthesized using biological materials and the drug of interest is dissolved, trapped, absorbed, attached and encapsulated into a nano-matrix (Barratt., 2000; Couvreur *et al*., 1995). The NPs can either then be administrated orally, through an injection or by inhalation (Syed *et al*., 2018). NPs have been designed to pass through organ and tissue barriers to target cancer tumours, therefore delivering chemotherapy drugs to cancer cells. Several polymer/lipid and metal-based NPs containing the likes of titanium/gold/zinc/copper/silver have been

successfully administrated *in vitro* against virulent bacterial and viral agents, with the mechanisms illustrated in (Fig. 3) (Thukkaram, 2014). Polymer, metal and lipid bilayer-based NPs are primarily used due to their antimicrobial properties, ease in encapsulation and surface modification of drug in the NPs, making them easier to control and administer. Bobo *et al*., (2016) described a list of nanotechnology-based products approved to date by the FDA, illustrated in (Table 3).

Table 3. List of FDA-approved nanotechnology-based medicines combined with drugs or biologics used to treat microbial infectious (Bobo *et al*., 2016).

Name	**NP advantage**	**Material used (combined with drugs/biologics)**	**Treatment**	**Approval year**
Abelcet (Sigma-tau)	Reduced toxicity	Liposome-based NP	Fungal infections	1995
AmBisome (Gilead Sciences)	Reduced nephrotoxicity	Liposome-based NP	Fungal/protozoal infections	1997
PegIntron (Merck)	Improved stability of protein through PEGylation	Polymer-based NP	Hepatitis C	2001
Pegasys (Genentech)	Improved stability of protein through PEGylation	Polymer-based NP	Hepatitis B, Hepatitis C	2002
Nanotherm (MagForce)	Allows cell uptake and introduces superparamagnetism	Metal-based NP (Iron-oxide)	Glioblastoma	2010
Adynovate (Baxalta)	Improved stability of protein through PEGylatio	Polymer-based NP	Hemophilia	2015
Estrasorb (Novavax)	Controlled delivery of therapeutic	Micelle NP	Menopausal therapy	2003

To increase the efficacy and improve the antimicrobial activity of NPs, researchers have used and tested NPs with existing antibiotics *in vitro* as illustrated in (Table 4). The approach of using NPs in combination with existing antibiotics has been found to not only be effective in treating MDR bacteria but cost effective as novel antibiotics take a large sum of money and time to develop. The synergistic effect also allows NPs to act on bacteria through multiple targets and mechanisms; forming unique antimicrobial mechanisms and thus reducing the risk of antimicrobial resistance development. Several studies have reported and speculated that NPs

selectively disarm and sensitise pathogens, allowing the antibiotics to do their job, essentially restoring the effectiveness said antibiotics. The general mechanisms of NPs include the attachment of the NPs to the surface of the bacterial cell membrane, destroying the permeability and inactivating the membrane proteins (Kwakye Awuah *et al*., 2008). NPs further pass through the bacterial cells barrier and bind to the DNA, disrupting DNA replication. In addition, they are able to disrupt the electron transport chain and can affect ribosomal functioning by interfering with the translation of mRNA into protein and thus activating cytochrome b (Kwakye-Awuah *et al*., 2008). In most cases, however, the mode of action of NPs on microorganisms somewhat differ as the mechanisms often depend on type of NPs used, the drug of interest entrapped within the NP, the concentration, temperature, solvent type, the size and the shape. Often times, NPs made from natural polymers work best as drug delivery systems as they can be easily customized for targeted drug delivery, can be easily controlled in terms of drug release and can prevent bodily enzymes from degrading the drug (Zhang and Saltzman, 2013). The size of the NP also determine their biological activity. The suggested optimal size of NPs has been 100nm, with a large surface area to volume ratio (Syed *et al*., 2018). This is because NPs larger than 200nm tend to activate the lymphatic system and are quickly removed out the system (Prokop *et al*., 2008). It has also been reported that shapes of NPs greatly influence the bioactivity despite the fact that the outcome shape of NPs cannot be easily controlled.

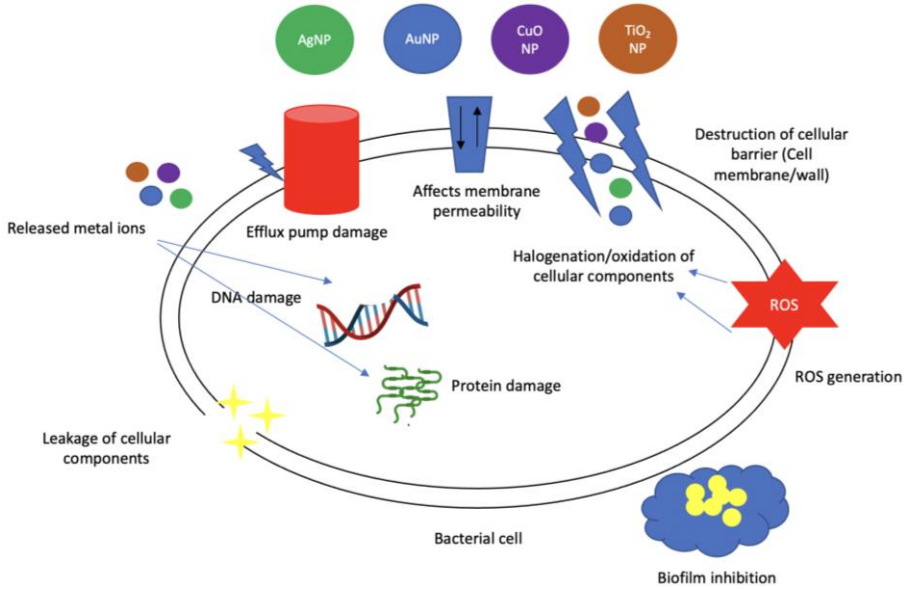

Figure 3. Antimicrobial activities of differently synthesized metal NPs modified based on Shaikh *et al.*, 2019.

Table 4. List of synthesized NPs and mechanisms of action against multi-drug resistant (MDR), clinical isolates administrated *in vitro*.

Nanoparticles (NPs) conjugated with antibiotics	Targeted bacteria	Antibacterial mechanisms	Factors affecting antibacterial mechanism	Citations
Copper (CuNP) with ampicillin, tetracycline, rifampin and ciprofloxacin	*A. Baumannii*, MDR *E. coli*, *S. aureus*, *B.* Pseudomonas spp, Shigella spp, *K. pneumoniae*	Lipid peroxidation, generation of reactive oxygen species (ROS), DNA degradation, protein oxidation	Size and concentration	Ingle *et al*., 2014; Chatterjee *et al*., 2014; Nene *et al*., 2019; Raheem *et al*., 2019
Silver (AgNP) with penicillin G, amoxicillin, erythromycin, clindamycin	MRSA, MDR *E. coli*, *K. pneumoniae*, carbapenem-resistant *P. aeruginosa*, ESBL-producing microorganisms, carbapenem and polymyxin B-resistant *A. baumannii*	Cell wall biosynthesis inhibition, lipid peroxidation, membrane disintegration, generation of ROS, cytochrome inhibition, membrane permeability, lipid and protein damage	Size and shape	Dizaj *et al*., 2014; Cavassin *et al*., 2015; Rudramurthy *et al*., 2016; Shahverdi *et al*., 2007
Gold (AuNP) with amoxicillin, clavulanic acid, ampicillin, Kanamycin	MSRA, MDR *E. coli*, *S. bovis*, *S. epidermidis*, *P. aeruginosa*	Inhibition of the subunit of ribosome, collapse membrane potential, membrane disruption, inhibit subunit of ribosome from binding tRNA, reduced ATPase activity, generation of holes in cell wall	Texture, shape and size	Chen *et al*., 2014; Dizaj *et al*., 2014; Rudramurthy *et al*., 2016; Hemeg, 2017; Payne *et al*., 2016
Zinc oxide (ZnoNP) with amoxicillin, penicillin G, ciprofloxacin and nitrofurantoin	*K. pneumoniae*, MRSA, ESBL-producing *E. coli*, Carbapenem-Resistant *A. baumannii*	Lipid peroxidation, and lipid and protein damage, generation of ROS, cell membrane disintegration	Size and concentration	Cavassin *et al*., 2015; Rudramurthy *et al*., 2016; Banoee *et al*., 2010
Iron oxide (FeNP) with tobramycin, β-lactam antibiotic	MRSA, MDR *E. coli*, *K. pneumoniae*, *P. aeruginosa*, *S. aureus*	Generation of ROS including; superoxide radicals, hydroxyl radicals, hydrogen peroxide	High chemical activity, size, interactions between NPs and cell membranes	Rudramurthy *et al*., 2016; Zaidi *et al*., 2017

1.8.2 Properties and the use of iodine in nanotechnology-based therapy

Halogens like chlorine and iodine have been known to have antimicrobial properties for decades. Povidone-iodine (PVP-I) is a commercially used wound healing agent and an effective disinfectant and sterilizer. It is a iodophore *i.e.* an agent consisting of a complex between iodine and a solubilizing polymer carrier, polyvinylpyrrolidone (Lachapelle *et al*., 2013;McDonnell *et al*., 1999). When in solution, free iodine (I_2) is released from the complex, is deactivated to iodide ions and then mediates microbicidal actions. Povidone-iodine has a broad spectrum activity (has been used against *S. aureus*, *N. gonorrhoeae*, *P. aeruginosa*, syphilis, hepatitis B virus, fungal biofilms), has the ability to penetrate biofilms, has anti-inflammatory benefits and low cytotoxicity on host cells (Bigliardi *et al*., 2017). The mechanism of action of povidone iodine has been reported to be due to the extensive halogen activity and strong oxidising ability (Capriotti *et al*., 2009). Strong oxidising agents like iodine are able to oxidise other substance *i.e.* accept their electrons (Clark, 2020). Iodine, being a halogen, has 7 electrons in its valence shell and needs one electron to complete its octet and to reach noble gas configuration. This allows iodine to penetrate the bacterial cell wall and membrane, oxidise nucleotides/fatty and amino acids, causing DNA denaturation, protein damage, membrane destabilisation and further slowdown or halt bacterial protein synthesis, disrupt electron transport and oxidative phosphorylation (Capriotti *et al*., 2009), with mechanisms illustrated in (Fig. 4). Iodine has a very high bioactivity, thus there has been no reported resistance development in bacteria and viruses thus far (Ilin *et al*., 2017). Considering the factors, iodine has shown to be a viable option in NP-based therapy to overcome the given problem of antibiotic resistance (Murdoch and Lagan, 2013).

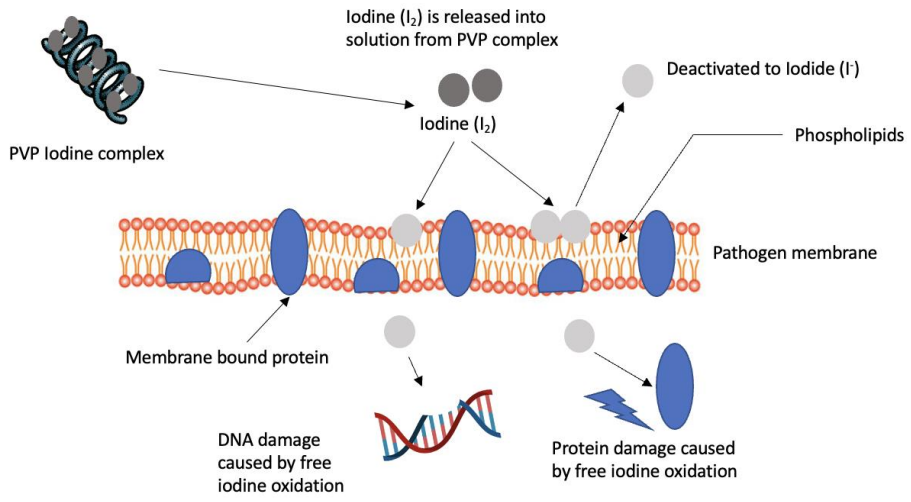

Figure 4. Mechanism of action of PVP-I modified based on Bigliardi *et al*., 2017.

A micelle NP complex drug *i.e.*, an aggregate of iodine and metal ions incorporated in a dextrin/polypeptide moiety, described as FS-1 was synthesized by The Scientific Centre for Anti-Infectious Drugs (SCAID), Almaty, Kazakhstan, in collaboration with The Centre of Bioinformatics and Computational Biology (CBCB), Pretoria, South Africa, in efforts to possibly induce antibiotic resistance reversion in bacteria (llin *et al*., 2017). The general formula of the FS-1 micelle is as follows:

$$[\{(L_n(MeJ_3)^+)_y\{Me(L_m)J]^+{}_x\}(Cl^-)_{y+x+k}] \qquad \text{Eq. 1}$$

where L–dextrin-polypeptide ligand; Me–Li/Mg ions, Cl^- - chloride ions, J - iodine ion, J_3 - triiodide; n, m, x, y,and k–variable integers ≥1. When blood plasma is treated with FS-1, the drug binds to blood albumins. This is followed by disintegration of FS-1, leading to the triiodide dissociating into iodine molecules, which have antimicrobial properties (Ilin *et al*., 2017).

The primary goal of the experiment was to evaluate whether FS-1 could possibly increase the effectiveness and induce sensitivity in resistant microbials,= to antibiotics; isoniazid, rifampicin, pyrazinamide, cycloserine, protionamide, capreomycin, and amikacin (Ilin *et al*., 2017), thus reversing antibiotic resistance. The FS-1 drug was shown to induce sensitivity in antibiotic-resistant and antibiotic-susceptible bacteria, including *S. aureus* ATCC BAA-39, *E. coli* ATCC BAA-196 and *A. baumannii* ATCC BAA-1790 *in-vitro*. The transcriptional response to FS-1 in model microorganisms *S. aureus* ATCC BAA-39, *E. coli* ATCC BAA-196 and *A. baumannii* ATCC BAA-1790 were seen in the activation of DNA repair genes, heavy metal ion-exporting ATPase subunits, nucleotide and protein biosynthesis, genes involved in osmotic stress response and a switch to anaerobiosis (Reva *et al*., 2020). Additional studies of FS-1 on model organism *M. tuberculosis* SCAID 187.0 *in vivo* found that the drug did not possess anaphylactogenicity, does evoke type I allergic reactions, does not have immunotoxic effects, and does not cause disorders/dysfunctions in the processes involved in normal maintenance of immune status in the then tested doses (Kulmanov *et al*., 2009). In addition, FS-1 was shown to possess a broad antimicrobial activity against mycobacteria, fungi, and viruses (Yuldasheva *et al*., 2015; Kulmanov *et al*., 2015). FS-1 is the first synthesized iodine nano-micelle that passed preclinical and clinical trials in 2015 and is currently in the 3rd round of clinical trials, in Kazakhstan (www.clinicaltrials.gov,acc. NCT02607449) as a potential

supplementary drug for MDR-TB (Korotetskiy *et al*., 2021). Much research has been done in using nanomolecular complexes in antimicrobial resistance reversion studies. The mechanisms of action of these complex drugs are, however, not well understood, including FS-1. The complex structure of FS-1 was found to be difficult to analyze because micelle was too big and problematic in terms of crystallization which then precluded further detailed investigation of interactions between components by X-ray crystallography. Therefore, the influence of the individual components within the drug on the overall bioactivity of FS-1 could not be determined.

1.9 References

1. Banoee M, Seif S, Nazari ZE, Jafari-Fesharaki P, Shahverdi HR, Moballegh A, Moghaddam KM, Shahverdi AR. ZnO nanoparticles enhanced antibacterial activity of ciprofloxacin against Staphylococcus aureus and Escherichia coli. J Biomed Mater Res B Appl Biomater. 2010 May;93(2):557-61.
2. Capriotti J, Shapiro A, Lilyestrom L. Iodine: An Elemental Force Against Infection. (2009). *Review of ophthalmology*.
3. Center for Disease Control and Prevention. Antibiotic Resistance Threats in the United States. (2019). CDC.
4. Katz A, Orellana O. Protein Synthesis and the Stress Response, Cell-Free Protein Synthesis. *IntechOpen*, DOI: 10.5772/50311.
5. Aguiniga LM, Yaggie RE, Schaeffer AJ, Klumpp DJ.2016. Lipopolysaccharide domains modulate urovirulence. *Infect. Immun*. 84, 3131-3140. 10.1128/IAI.00315-16.
6. Alanazi MQ, Alqahtani FY, Aleanizy FS. An evaluation of *E. coli* in urinary tract infection in emergency department at KAMC in Riyadh, Saudi Arabia: retrospective study. *Ann Clin Microbiol Antimicrob*. doi: 10.1186/s12941-018-0255-z
7. Amagai M, Yamaguchi T, Hanakawa Y, Nishifuji K, Sugai M, Stanley JR. *Staphylococcal* exfoliative toxin B specifically cleaves desmoglein 1. *J. Invest. Dermatol*. 2002,118:845–850.
8. Ambler RP, Coulson AF. Frere JM, Ghuysen JM, Joris B, Forsman M. A standard numbering schemed for the class A β -lactamase. *Biochem J*. 1991;276:269-70.
9. Barratt, GM. Therapeutic applications of colloidal drug carries. *Pharmaceut Sci Tech Today*. 2000;3:163-171.
10. Baym M, Stone L, Kishony R. Multidrug evolutionary strategies to reverse antibiotic resistance. *Science*. 2016 January 01; 351(6268): aad3292.
11. Behnsen J, Raffatellu M. Siderophores: more than stealing iron. (2016) mBio7(6):e01906-16. Doi:10.1128/mBio.01906-16
12. Bello-López JM, Cabrero-Martínez OA, Ibáñez-Cervantes G, *et al*. Horizontal Gene Transfer and Its Association with Antibiotic Resistance in the Genus *Aeromonas* spp. *Microorganisms*. 2019;7(9):363.
13. Bigliardi PL. Alsagoff SAL, El-Kafrawi HY, Pyon JK, Wa CTC, Villa MA. Povidone iodine in wound healing: A review of current concepts and practices, International Journal of Surgery. Volume 44, Pages 260-268, ISSN 1743-9191, https://doi.org/10.1016/j.ijsu.2017.06.073.
14. Bobo D, Robinson KJ, Islam J, Thurecht KJ, Corrie SR. Nanoparticle-based medicines: a review of FDA-approved materials and clinical trials to date. *Pharm Res*. 2016;33:2373–87
15. Bonnet R. Growing group of extended-spectrum β-lactamase; the CTX-M enzymes. *Antimicrobiology Agents Chemotherapy*. 2004;48(1):1-14
16. Bozic I, Reiter JG, Allen B, Antal T, Chatterjee K, Shah P, Moon YS, Yaqubie A, Kelly N, Le DT, Lipson EJ, Chapman PB, Diaz LA Jr, Vogelstein B, Nowak MA. Evolutionary dynamics of cancer in response to targeted combination therapy. *Elife*. 2013 Jun 25; 2():e00747.

17. Bradford PA. Extended-spectrum β-lactamase in the 21st centuary: characterization, epidemiology and detection of this important resistance threat. *Clin. Microbiol. Rev*: 14 933-951. 10.1128/CMR.14.4.933-951.1995
18. Brandl K, Plitas G, Mihu CN, Ubeda C, Jia T, Fleisher M, Schnabl B, DeMatteo RP, Pamer EG. Vancomycin-resistant enterococci exploit antibiotic-induced innate immune deficits. *Nature.* 2008 Oct 9; 455(7214):804-7.
19. Buckland D. Antimicrobial resistance and the race to find new antibiotics. (2017). *Prescriber*. 28. 12-15. 10.1002/psb.1528.
20. Bush LM. *Staphylococcus aureus* Infections. (2021). *MSD Manual*.
21. Bush K. The coming of age of antibiotics: discovery and therapeutic value. *Ann. N. Y. Acad.Sci*. 1213:1-4
22. Bush K, Jacoby GA, Medeiros AA. A functional classification scheme for β-lactamases and its correlation with molecular structure. *Antimicrob Agents Chemother*. 1995;39:1211-33.
23. Caster JM, Patel AN, Zhang T, Wang A. Investigational nanomedicines in 2016: a review of nanotherapeutics currently undergoing clinical trials. *Wiley Interdiscip Rev*. 2016;2017:9.
24. Cavassin ED, De Figueiredo LF, Otoch JP, Seckler MM, De Oliveira RA, Franco FF, *et al*. Comparison of methods to detect the in vitro activity of silver nanoparticles (AgNP) against multidrug resistant bacteria. J. Nanobiotechnology 13, 64. 10.1186/s12951-015-0120-6
25. Chatterjee AK, Chakraborty R, Basu T. Mechanism of antibacterial activity of copper nanoparticles. *Nanotechnology* 25, 135101.
26. Chaturvedi KS, Hung CS, Crowley JR, Stapleton AE, Henderson JP. 2012. The siderophore yersiniabactin binds copper to protect pathogens during infection. *Nat Chem Biol* 8:731–736.
27. Chen CW, Hsu CY, Lai SM, Syu WJ, Wang TY, Lai PS. Metal nanobullets for multidrug resistant bacteria and biofilms. *Adv. Drug Deliv. Rev*. 78, 88–104.
28. Choo EJ, Chambers HF. Treatment of Methicillin-Resistant *Staphylococcus aureus* Bacteremia. *Infect Chemother*. 2016;48(4):267-273.
29. Clark, J. Halogens as Oxidizing Agents. (2020). LibreTexts.
30. Coates A. The future of antibiotics lies in combination treatments. (2019). FUTURE DRUG DISCOVERY VOL. 1, NO. 1. https://doi.org/10.4155/fdd-2019-0012
31. Couvreur P, *et al*. Controlled drug delivery with nanoparticles: current possibilities and future trends. *Eur J Pharm Biopharm*. 1995;41:2-13.
32. Delcour AH. Outer membrane permeability and antibiotic resistance. *Biochim Biophys Acta*. 2009;1794(5):808-816.
33. Dizaj SM, Lotfipour F, Barzegar-Jalali M, Zarrintan MH, Adibkia K. Antimicrobial activity of the metals and metal oxide nanoparticles. *Mater. Sci. Eng. C Mater. Biol. Appl.* 44, 278–284.
34. Donnenberg MS. Enterobacteriaceae. (2014). ScienceDirect. https://doi.org/10.1016/B978-1-4557-4801-3.00220-4

35. Donnenberg MS, Finlay BB. Combating enteropathogenic *Escherichia coli* (EPEC) infections: the way forward. *Trends Microbiol*. 2013;21(7):317-319.

36. World Health Organization. (2002). Prevention of hospital-acquired infections : a practical guide / editors : G. Ducel, J. Fabry and L. Nicolle, 2nd. ed. World Health Organization.
37. Edwards D. Antibacterial Agents 5. Antimetabolites and Synthetic Drugs. (1980). In: Antimicrobial Drug Action. Palgrave, London. https://doi.org/10.1007/978-1-349-16360-1_10

38. Egorov AM, Ulyashova MM, Rubtsova MY. Bacterial Enzymes and Antibiotic Resistance. *Acta Naturae*. 2018;10(4):33-48.
39. Espedido BA, Jensen SO, van Hal SJ. 2015. Ceftaroline fosamil salvage therapy: an option for reduced-vancomycin-susceptible MRSA bacteraemia. *J Antimicrob Chemother*. 2015 Mar; 70(3):797-801
40. Ferry SA, Holm SE, Stenlund H, Lundholm R, Monsen TJ. The natural course of uncomplicated lower urinary tract infection in women illustrated by a randomized placebo controlled study. *Scand J Infect Dis.* 2004;36(4):296–301.
41. Fleming A. Penicillin, Nobel lecture,1945. The Noble Price.
42. Grumann D, Nübel U, Bröker BM. *Staphylococcus aureus* toxins—Their functions and genetics. *Infect. Genet. Evol.* 2014;21:583–592.

43. Gupta G. Neonatal meningitis. (2018). Medscape.

44. Hartmann G, Behr W, Beissner KA, Honikel K, Sippel A. Antibiotics as inhibitors of nucleic acid and protein synthesis. Angew Chem Int Ed Engl. 1968 Sep;7(9):693-701.
45. Hemeg HA. Nanomaterials for alternative antibacterial therapy. *Int. J. Nanomed.* 12, 8211–8225.
46. Ingle AP, Duran N, Rai M. Bioactivity, mechanism of action, and cytotoxicity of copper-based nanoparticles: A review. *Appl Microbiol Biotechnol* **98,** 1001–1009 (2014).
47. Jacoby GA, Munoz-Price LS. The new β-lactamases. *N Engl J Med* 2005; 352:380.
48. Kapoor G, Saigal S, Elongavan A. Action and resistance mechanisms of antibiotics: A guide for clinicians. *J Anaesthesiol Clin Pharmacol*. 2017;33(3):300-305.
49. Ko YP, Kuipers A, Freitag CM, *et al*. Phagocytosis escape by a *Staphylococcus aureus* protein that connects complement and coagulation proteins at the bacterial surface. *PLoS Pathog*. 2013;9(12):e1003816.
50. Kuipers A, Stapels DAC, Weerwind LT, Ko Y, Ruyken M, Lee JC, Van Kessel KPM and Rooijakkers, SHM. 2016. The *Staphylococcus aureus* polysaccharide capsule and Efb-dependent fibrinogen shield act in concert to protect against phagocytosis. *Microbiology (Reading)*. 2016 Jul; 162(7): 1185–1194.
51. Kulmanov ME, Kerimzhanova BF, Chernousova LN, Bocharova IV, Lepekha LN, Ilin AI. Efficiency of the new medication of FS-1 in the treatment of experimental tuberculosis. *Tuberculosis and Lung Diseases*. 2015;12:50-56

52. Kulmanov ME, Bogdanov AY, Bogdanova TM, Kalyikova AS, Dubeshko SY, *et al*. The study of immunotoxicity of pharmaceutical drug of FS-1. *Zdorove i bolezn*. 2009;4:138-149.

53. Kumar A, Verma AK, Malik S, Gupta MK, Sharma A, Rahal A. Occurrence of extended spectrum beta-lactamases producing alpha hemolytic Escherichia coli in neonatal diarrhea. Pak J Biol Sci. 2014 Jan 1;17(1):109-13.
54. Kwakye Awuah B, Williams C, Kenward M, *et al*. Antimicrobial action and efficiency of silver-loaded zeolite X. *J Appl Microbiol*. 2008; 104(5):1516-24.
55. Lachapelle JM, Castel O, Casado AF, Leroy B, Micali G, Tennstedt D, Lambert J. Antiseptics in the era of bacterial resistance: a focus on povidone iodine. *Clin Pract* 10:579–592.
56. Leach KL, Brickner SJ, Noe MC, Miller PF. Linezolid, the first oxazolidinone antibacterial agent. *Annals of the New York Academy of Sciences*, 1222: 49-54.

57. Longhurst, AD. What You Need to Know About Pathogens and the Spread of Disease. (2019). HealthLine.

58. Ilin AI, Kulmanov ME, Korotetskiy IS, Islamov RA, Akhmetova GK, Lankina MV, Reva ON. Genomic Insight into Mechanisms of Reversion of Antibiotic Resistance in Multidrug Resistant *Mycobacterium tuberculosis*Induced by a Nanomolecular Iodine-Containing Complex FS-1. *Front Cell Infect Microbiol*. 2017 May 8;7:151.
59. Magnusson KE, Bayer ME. Anionic sites on the envelope of Salmonella typhimurium mapped with cationized ferritin. *Cell Biophys*. 1982;4:163–75.

60. McDonnell G, Russell AD. Antiseptics and disinfectants: activity, action, and resistance. *Clin Microbiol Rev*. 1999 Jan; 12(1):147-79.[

61. Melton-Celsa AR. Shiga Toxin (Stx) Classification, Structure, and Function. Microbiol Spectr. 2014 Aug;2(4):EHEC-0024-2013.
62. San Millan A, Santos-Lopez A, Ortega-Huedo R, Bernabe-Balas C, Kennedy SP, Gonzalez-Zorn B. Small-plasmid-mediated antibiotic resistance is enhanced by increases in plasmid copy number and bacterial fitness. *Antimicrob Agents Chemother*. 2015;59(6):3335-3341.
63. Munita JM, Arias CA. Mechanisms of antibiotic resistance. Doi: 10.1128/microbiolspec.VMBF-0016-2015. NCBI. Department of Internal Medicine, Division of infectious diseases, University of Texas Medical School at Houston, Texas.
64. Murdoch RL, Lagan, KM. "The role of povidone and cadexomer iodine in the management of acute and chronic wounds." *Physical Therapy Reviews* 18 (2013): 207 - 216.
65. Nene A, Tuli HS. Synergistic effect of copper nanoparticles and antibiotics to enhance antibacterial potential. Bio-Material and Technology. ISSN 2582 – 2324.
66. Okhuysen PC, DuPont HL. Enteroaggregative Escherichia coli (EAEC): A Cause of Acute and Persistent Diarrhoea of Worldwide Importance. The Journal of Infectious Diseases, Volume 202, Issue 4, 15 August 2010, Pages 503–505.

67. Olson AB, Silverman M, Boyd DA, McGeer A, Willey BM, Pong-Porter V, Daneman N, Mulvey MR. Identification of a progenitor of the CTX-M-9 group of extended spectrum β-lactamase from kluyvera georgiana isolated in Guyana. *Antimicrob. Agents Chemother.* 49, 2112-2115
68. Oteo J, Cercenado E, Cuevas O, Bautista V, Delgado-Iribarren A, Orden B, *et al*. AmpC β-lactamases in *Escherichia coli*: emergence of CMY-2-producing virulent phylogroup D isolates belonging mainly to STs 57, 115, 354, 393, and 420, and phylogroup B2 isolates belonging to the international clone O25b-ST131. *Diagn. Microbiol. Infect.* Dis. 67 270–276. 10.1016/j.diagmicrobio.2010.02.008.
69. Otto M. *Staphylococcus aureus* toxins. *Curr Opin Microbiol*. 2014;17:32-37.
70. Papagrigorakis MJ, Synodinos PN, Yapijakis C. Ancient typhoid epidemic reveals possible ancestral strain of *Salmonella enterica serovar Typhi*. *Infect Genet* Evol 7 (2007): 126–7, Epub 2006 Jun.
71. Patra JK, Das G, Fraceto LF, Campos EVR, Rodriguez-Torres MDP, Acosta-Torres LS, Diaz-Torres LA, Grillo R, Swamy MK, Sharma S, Habtemariam S, Shin HS. Nano based drug delivery systems: recent developments and future prospects. *Journal of Nanobiotechnology* volume 16, Article number: 71 (2018).
72. Payne JN, Waghwani HK, Connor MG, Hamilton W, Tockstein S, Moolani H, Chavda F, Badwaik V, Lawrenz MB, Dakshinamurthy R. Novel Synthesis of Kanamycin Conjugated Gold Nanoparticles with Potent Antibacterial Activity. *Front Microbiol*. 2016 May 2;7:607.
73. Payseur B. 2019. Protein synthesis inhibitors. Chapter 4. Study.com.
74. Peter L. Bacterial resistance to antibiotics: Modified target sites. *Advanced drug delivery reviews*. 57. 1471-85. 10.1016/j.addr.2005.04.003.
75. PEW. Tracking the Global Pipeline of Antibiotics in Development. https://www.pewtrusts.org/en/research-and-analysis/issue-briefs/2020/04/tracking-the-global-pipeline-of-antibiotics-in-development
76. Philippon A, Labia R, Jacoby G. Extended-spectrum β-lactamases. *Antimicrob. Agents Chemother.* 33 1131–1136.
77. Poirel L, Girlich D, Naas T, Noordmann P. An extended-spectrum variant of OXA-10 β-lactamase, from *Pseudomonas aeruginosa* and its plasmid- and- integron- located gene. *Antimicrobial Agents Chemotherapy*. 2001;45:447-453.
78. Porter, S. 2007. Antibiotic resistance: taking the bypass. Digital World Biology
79. Price LSM. 2019. Extended Spectrum β-lactamases. UpToDate.
80. Prokop A, Davidson JM. Nanovehicular intracellular delivery systems. *J. Pharm. Sci*. 2008;97(9):3518–3590.
81. Ramsay JP, Ronson CW, Sullivan, JT. Symbiosis Islands, in Maloy, S. and Hughes, K. (ed), Brenner's Encyclopedia of Genetics. pp. 598-600. London, UK: Elsevier.
82. Ray, U. 2018. *What are the Different Types of Nanoparticles?*. AZoNano, viewed 10 May 2020, https://www.azonano.com/article.aspx?ArticleID=4938.
83. Reading C, Cole M. Clavulanic acid: a beta-lactamase-inhiting beta-lactam from Streptomyces clavuligerus. Antimicrob Agents Chemother. 1977 May;11(5):852-7. doi: 10.1128/AAC.11.5.852.

84. Rev, N. Wilson DN. Ribosome-targeting antibiotics and mechanisms of bacterial resistance. *Nat Rev Microbiol*. 2014 Jan;12(1):35-48.

85. Reva ON, Korotetskiy IS, Joubert M, Shilov SV, Jumagaziyeva AB, Suldina NA, Ilin AI. The Effect of Iodine-Containing Nano-Micelles, FS-1, on Antibiotic Resistance, Gene Expression and Epigenetic Modifications in the Genome of Multidrug Resistant MRSA Strain *Staphylococcus aureus* ATCC BAA-39. *Front Microbiol*. 2020 Oct 22;11:581660.
86. Roberts JA, Abdul-Aziz MH, Lipman J, Mouton JW, Vinks AA, Felton TW, Hope WW, Farkas A, Neely MN, Schentag JJ, Drusano G, Frey OR, Theuretzbacher U, Kuti JL, International Society of Anti-Infective Pharmacology and the Pharmacokinetics and Pharmacodynamics Study Group of the European Society of Clinical Microbiology and Infectious Diseases. Individualised antibiotic dosing for patients who are critically ill: challenges and potential solutions. *Lancet Infect Dis*. 2014 Jun; 14(6):498-509.

87. Rudramurthy GR, Swamy MK, Sinniah UR, Ghasemzadeh A. Nanoparticles: Alternatives Against Drug-Resistant Pathogenic Microbes. Molecules. 2016 Jun 27;21(7):836.
88. Ruiz J. Mechanisms of resistance to quinolones: target alterations, decreased accumulation and DNA gyrase protection. *J Antimicrob Chemother*. 2003 May;51(5):1109-17.
89. Shafer RW, Vuitton DA. Highly active antiretroviral therapy (HAART) for the treatment of infection with human immunodeficiency virus type 1. *Biomed Pharmacother*. 1999 Mar; 53(2):73-86.
90. Shahverdi AR, Fakhimi A, Shahverdi HR, Minaian S. Synthesis and effect of silver nanoparticles on the antibacterial activity of different antibiotics against Staphylococcus aureus and Escherichia coli. *Nanomedicine*. 2007 Jun;3(2):168-71.
91. Shaikh S, Fatima F, Kamal MA. Antibiotic resistance and extended spectrum beta-lactamases: Types, epidemiology and treatment. *Saudi J Biol Sci*. 2015 Jan;22(1):90-101.
92. Shaikh S, Nazam N, Rizvi SMD, *et al*. Mechanistic Insights into the Antimicrobial Actions of Metallic Nanoparticles and Their Implications for Multidrug Resistance. *Int J Mol Sci*. 2019;20(10):2468.
93. Schenone M, Dancik V, Wagner BK, Clemons PA. Target identification and mechanism of action in chemical biology and drug discovery. *Nature Chemical Biology* 9(4):232-240.
94. Singh N, Yeh PJ. Suppressive drug combinations and their potential to combat antibiotic resistance. *J Antibiot* (Tokyo). 2017 Nov; 70(11): 1033-1042.
95. Sougakoff W, Goussard S, Courvalin, P. 1988 TEM-3 β-lactamase which hydrolyses broad-spectrum cephalosporins is derived from TEM-2 penicillinases by two amino acid substitutions. *FEMS Microbiol*. Lett. 1988;56:343-348.
96. Stefani S, Bongiorno D, Mongelli G, Campanile F. Linezolid Resistance in *Staphylococci*. *Pharmaceuticals (Basel)*. 2010;3(7):1988-2006.
97. Stephens, E. 2019. Antibiotics (Side Effects, List, Types). INFECTIONS CENTER Medicine Health.

98. Sukker, E. 2013. Why are there so few antibiotics in the research and development pipeline? The Pharmaceutical journal. The royal pharmaceutical society. Pharmaceutical-journal.com.
99. Sun S, Selmer M, Andersson DI. Resistance to β-lactam antibiotics conferred by point mutations in penicillin-binding proteins PBP3, PBP4 and PBP6 in *Salmonella enterica*. *PLoS One*. 2014;9(5):e97202.

100. Rizvi SAA, Saleh AM. Applications of nanoparticle systems in drug delivery technology. *Saudi Pharm J*. 2018;26(1):64-70. doi:10.1016/j.jsps.2017.10.012
101. Thukkaram M, Sitaram S, Kannaiyan SK, Subbiahdoss G. Antibacterial Efficacy of Iron-Oxide Nanoparticles against Biofilms on Different Biomaterial Surfaces. *Int J Biomater*. 2014;2014:716080.
102. Foster, TJ. Antibiotic resistance in *Staphylococcus aureus*. Current status and future prospects, *FEMS Microbiology Reviews*, Volume 41, Issue 3, May 2017, Pages 430–449.

103. Tong SY, Davis JS, Eichenberger E, Holland TL, Fowler VG. 2015. *Staphylococcus aureus* infections: epidemiology, pathophysiology, clinical manifestations, and management. *Clin Microbiol Rev*. 2015 Jul;28(3):603-61.
104. Tortora GJ, Funke, BR, Case, CL. Microbiology: An Introduction. 2013.

105. von Wintersdorff CJ, Penders J, van Niekerk JM, Mills ND, Majumder S, van Alphen LB, Savelkoul PH, Wolffs PF. Dissemination of Antimicrobial Resistance in Microbial Ecosystems through Horizontal Gene Transfer. Front Microbiol. 2016 Feb 19;7:173.
106. Wang R, Braughton KR, Kretschmer D, Bach TH, Queck SY, Li M, Kennedy AD, Dorward DW, Klebanoff SJ, Peschel A, DeLeo FR, Otto M. 2007. Identification of novel cytolytic peptides as key virulence determinants for community-associated MRSA. *Nat Med*. 2007 Dec; 13(12):1510-4.

107. Williams KJ. The introduction of 'chemotherapy' using arsphenamine - the first magic bullet. *J R Soc Med*. 2009;102(8):343-348.
108. Willyard, C. The drug-resistant bacteria that pose the greatest health threats. *Nature***543,** 15 (2017).
109. WHO. Guidelines for treatment of tuberculosis. ISBN: 9789241547833.
110. World Health Organization. WHO Publishes List of Bacteria for which new antibiotics are urgently needed. 2017. Available from: //www.who.int/news-room/detail/27-02-2017-who-publishes-list-of-bacteria-for-which-new-antibiotics-are-urgently-needed.
111. Woodford N, Ellington MJ. 2007. The emergence of antibiotic resistance by mutation. Clinical Microbiology and infection volume 13, issue. *ScienceDirect*. Doi.org./10.1111/j.1469-0691.2006.01492.x
112. Woodford N, Turton JF, Livermore DM. Multi resistant gram-negative bacteria: the role of high-risk clones in the dissemination of antibiotic resistance. *FEMS Microbiol. Rev*. 2011;35:736-755.

113. Xu SX, McCormick JK. *Staphylococcal* superantigens in colonization and disease. *Front Cell Infect Microbiol*. 2012;2:52.

114. Yael NS, Jason A, Häfeli, UO, Horacio B. Metal nanoparticles: understanding the mechanisms behind antibacterial activity. *Nanobiotechnol* (2017) 15:65.

115. Yang W, Moore IF, Koteva KP, Bareich DC, Hughes DW, Wright GD. TetX is a flavin-dependent monooxygenase conferring resistance to tetracycline antibiotics. *J.Biol.Chem*. 2004;279:52346-52352.

116. Yuldasheva G, Argirova R, Ilin A. Inhibition of HIV-1 integrase active catalytic center by molecular iodine complexes with bioorganic ligands and lithium halogenides. *Journal of AIDS and Clinical Research*. 2015;6:2-6.

117. Zaidi S, Misba L, Khan AU. Nano-therapeutics: A revolution in infection control in post antibiotic era. *Nanomedicin*e. 2017 Oct;13(7):2281-2301.

118. Zhang J, Saltzman M. Engineering biodegradable nanoparticles for drug and gene delivery. *Chem Eng Prog*. 2013 Mar;109(3):25-30.

1.10 Research Aims and Objectives

On account of the complex structure of the FS-1 drug and the inability to determine the influence of the individual components on the activity of the drug, SCAID synthesized three simpler and well-controlled iodine-containing nanomolecular complexes, synthesized with amino acids and metal ions. The newly synthesized complexes were denoted as KS25, KS33 and KS51. The structure of the complexes were confirmed and resolved by X-ray crystallography and deposited in the structural database of the Cambridge Crystallographic Data Centre.

The Aim of this study was to therefore, investigate the changes in gene transcription in model microorganisms *E. coli* ATCC BAA-196 and *S. aureus* ATCC BAA-39, treated with three iodine-containing complexes in sub-lethal concentrations (0.5 Minimal bactericidal concentration (MBC)), at two time-points during growth (lag and exponential growth phase). *E. coli* ATCC BAA-196 was exposed to the three complexes for 10 min at the end of the lagging growth phase (1 h after inoculation) and at the middle of the logarithmic growth phase (6 h after inoculation). *S. aureus* ATCC BAA-39 was exposed to the three complexes for 10 min at the end of the lagging growth phase (2.5 h after inoculation) and at the mid of the logarithmic growth phase (9 h after inoculation).

The specific objectives of the study were as follows:

- Chapter 1: Identify positively/negatively coregulated genes, metabolic pathways and networks influenced by each iodine-containing nanomolecular complex on *E. coli* and *S. aureus* in different growth phases, thus evaluating the bioactivity of each individual complex.
- Chapter 2: Evaluate the effects of the iodine-containing nanomolecular complex treatments by comparing the gene regulation results of distantly related Gram-negative *E. coli* to Gram-positive *S. aureus* and then identify the factors influencing the biological activity of iodine in both model microorganisms, compared to each other.

1.11 Ethical clearance

The research in this study was conducted with the approval from The Faculty of Natural and Agricultural Sciences Ethics Committee, University of Pretoria (See Appendix A).

Chapter 2: *E. coli* ATCC BAA-196 and *S. aureus* ATCC BAA-39 as model microorganisms for studying bacterial-nanomolecular complex interactions and identifying the factors influencing the bioactivity of complexes KS25, KS33, KS51 based on the transcriptional responses of the model microorganisms

2.1 Introduction

E. coli ATCC BAA-196 is a clinical strain, isolated in 1988 from a chronic-care facility in Boston, Massachusetts. It is characterized by producing ESBL TEM-10, endowing resistance to β-lactam antibiotics (Korotetskiy *et al*., 2019). *S. aureus* ATCC BAA-39 is a natural MDR clinical strain, isolated in 2010 from a nasal clinical sample (Joubert *et al.,* 2019). It is characterized by having a cassette chromosome mec element (SCCmec) containing the *mecA* gene, which encodes the penicillin-binding protein 2a (Joubert *et al.,* 2019), endowing resistance to cefuroxime, erythromycin, clindamycin, gentamycin, oxacillin, tetracycline, tobramycin, cefaclor, and penicillin (Holden *et al*., 2004). The *E. coli* K-12 variant strain forms part of the human intestinal flora. It is not virulent nor resistant, therefore this suggests that the BAA-196 strain gained its resistance and pathogenicity through horizontal gene transfer from other species. *E. coli* ATCC BAA-196 originates from *E. coli* J53-2 (K-12 related strain) and was laboratory designed by inserting multiple antibiotic resistant plasmid pMG223 from *K. pneumonia.* Phylogenetic analysis and clustering confirmed that *E. coli* ATCC BAA-196 was related to *E. coli* K-12 related strains; *E. coli* K-12 DH10B, *E. coli* K-12 W3110 strain and *E. coli* K-12 NC 000913 (Korotetskiy *et al*., 2021). Furthermore, the large plasmid and genomic islands within the strain were aligned against BLASTN for sequence comparison and was found to have 90-99% sequence similarity with a plasmid from *K. pneumonia* (pKP64477b) (Cassu-Corsi *et al*., 2018).

The first complete genome sequence of *E. coli* K12, strain MG1655, was published in 1997 by Frederick Blattner and co-researchers (Blattner *et al*., 1997). The first complete genome of *S. aureus* was first published in 2001 by Kuroda *et* al., 2001 and deposited at the National Centre for Biotechnology Information (NCBI) Reference Sequences (RefSeq) database. The complete genome assembly of *E. coli* ATCC BAA-196, was published in 2019 (GCA_008033295.1) and the whole-genome assembly comprising 83 contigs of *S. aureus* ATCC BAA-39 was published in 2010 (GCA_000146385.1). Based on the premise that both microorganisms have a high

level of annotated, complete and known genomes, this makes them desirable model microorganisms for transcriptomics, genomics and proteomics studies. Additionally, both microorganisms are fast growing, can be easily manipulated in the lab and there is a plethora of bioinformatics tools available, containing information on each strain. *E. coli* ATCC BAA-196 and *S. aureus* ATCC BAA-39 clinical isolates were, therefore, used as model microorganisms in studies by Korotetskiy *et al.*, 2019, Joubert *et al.*, 2019 and Reva *et al*., 2020 to test the transcriptional effects of iodine-containing NP micelle denoted as FS-1. The micelle was characterized by having an aggregate of triiodide, negative iodine, chloride ions and metal ions; positive lithium and magnesium ions, incorporated in dextrin/polypeptide ligands (Ilin *et al*., 2017). When blood plasma is treated with FS-1, the drug binds to blood albumins, followed by the disintegration of FS-1, leading to the triiodide dissociating into iodine molecules, which have antimicrobial properties (Ilin *et al*., 2017). Like FS-1, the antimicrobial effects of NPs are primarily to due to the entrapped drug. The materials used and the process of synthesising the NPs however, also play a crucial step in antimicrobial therapy because this determines the effectiveness of the drug. Factors such as the ease and control in loading the antimicrobial agent, long-term stability and durability, biosafety and achieving the target area for treatment have to be considered to achieve the best outcome of the drug. Conjugating NPs with amino acids, forming NPs-amino acid complexes for example, has shown to influence the stability and bioactivity of NPs. The increase in bioactivity and stability of NPs conjugated with amino acids, is believed to be due to amino acids exhibiting zwitterionic behaviour, molecular chirality and them being easily controlled (Sharma,2020; Nidya *et al*., 2015). Furthermore, the interaction between NPs and amino acids are believed to have formed through the NH_2 and COOH groups and with some exceptions, the R-group or side chain (Deschamps *et al*., 2003; Badetti *et al*., 2019).

Additionally, amino acids have shown to be ideal when synthesizing NPs because they have proven to allow for control over shape and size of NPs, they exhibit high biosafety and do not have harmful effects (Sharma, 2020). Hydrophobic amino acids, in particular, have been of interest as compared to hydrophilic amino acids. This is because, hydrophilic NPs have been shown to likely remain in the solvent column during treatments (Crandon *et al*., 2020), whereas hydrophobic NPs have an increased uptake potential within organism systems and the hydrophobicity nature of NPs dictates the attachment and interaction between the surface of the NP and biological components such as the bacterial lipid bilayer (Crandon *et al*., 2020;

Aggarwal *et al*., 2009). Moreover, the NPs-amino acid complex within the bacterial environment, interacts with carbohydrates, proteins, fats and nucleic acids, directly increasing the toxicity and bioaccumulation (Kim *et al*., 2013). Studies have shown that amino acids can function as ligands that can attach to the surface of NPs and contribute to the slow release and dissolution of NPs through ligand-assisted ion release (Badetti *et al*., 2019), further increasing the toxicity effect. A study by Badetti *et* al., 2019) demonstrated that the antimicrobial activity of copper oxide (CuO)-NPs against Gram-positive bacterium *S. epidermidis* ATCC 35984 (a model microorganism known to produce biofilms) was highly influenced by the presence of amino acids. The (CuO)-NPs-amino acid complexes were formed using amino acids L-Arginine, L-Aspartate, L-Glutamate, L-Cysteine, L-Valine, L-Leucine, L-Phenylalanine and L-Tyrosine. The amino acids were found to bond to (CuO)-NPs in different ways in terms of stoichiometry (Cu : amino acid) *i.e.*, the interaction between (CuO)-NPs and the amino acids were influenced by the functional groups (amino group, carboxyl group and or with some exceptions, the charge of the amino acidic side chains). The study showed that polar amino acids L-cysteine and L-glutamate exhibited the greatest antimicrobial activity at low concentration. This finding was directly linked to the charge of the amino acidic side chain and how they were better suited to form a bond with copper.

Surrounding metal ions from the environment have also been reported to form interactions with NPs and possibly form ligands with the amino acids interacting with the NPs. When NPs enter a certain environments, they come across natural organic matter such as polysaccharides and ions, which gravitate towards and attach to NPs, forming dynamic coronas (Zhu *et al*., 2013). The ions, then alter the surface charge of NPs, therefore influencing their bioactivity (Zhu *et al*., 2013). The surface charge of NPs then influence their uptake within bacterial cells as liposaccharides and teichoic acids attract positively charged substances.

In this chapter, the effects of three iodine-containing synthesized nanomolecular complexes (KS25, KS33 and KS51) on model microorganisms; *E. coli* ATCC BAA-196 and *S. aureus* ATCC BAA-39 were determine. Iodine-containing complex KS25 was synthesized with amino acid glycine, KS33 was synthesized with alanine and complex KS51 was synthesized with isoleucine. Glycine is the simplest known amino acid, consisting of an amino group, carboxyl group and a single hydrogen atom as its side chain. Alanine is the second simplest known

amino acid consisting of an amino, carboxyl and a methyl group as its side chain. Isoleucine is characterised by having an amino group, carboxyl group and hydrocarbon, branched chain, as illustrated (Fig. 4). All three amino acids are aliphatic *i.e.* contain an aliphatic side chain functional group, making them non-polar and hydrophobic. The hydrophobicity of amino acids generally increases as the number of carbon atoms on the hydrocarbon chain increases, thus making isoleucine the most hydrophobic amino acid.

A number of studies have been carried out to evaluate the antimicrobial activity of iodine as a potential candidate for nano-therapy in bacteria. FS-1 was tested on *E. coli* ATCC BAA-196 and *S. aureus* ATCC BAA-39 to evaluate the transcriptional response to iodine, in which mechanisms of oxidative stress response, the activation or deactivation of several biosynthesis pathways such as a change in cellular respiration, amino acid, and nucleotide biosynthesis were induced. Additionally, a study by Gao *et al*., 2017 demonstrated and reported on hydrophobic Povidone-iodine NPs (PVP-I_2 NPs) that showed stronger antibacterial activity against *E. coli* and *S. aureus in vivo* as compared to PVP-I_2 NPs synthesized with hydrophilic antibacterial additive agents. The study further reported that the concentration of the free iodine had a significant role in the bactericidal activity of PVP-I_2 NPs. Moreover, the antimicrobial mechanism was described to be associated with the deactivation of I_2 to I^-, when in solution. Free iodine is able to kill off bacterial cells when in solution. It, however, needs to reach a certain sufficient threshold concentration to be bactericidal and the survival rate of bacteria will decrease with increasing concentration of iodine (Bigliardi *et al*., 2017). PVP-I_2 NPs was also reported to release free iodine into solution slowly and continuously, thus maintaining the antimicrobial capacity for longer periods (Sriwilaijaroen *et al*., 2009; He *et al*., 2014; Edis *et al*., 2019) and found to be uniform in *S. aureus* in *in vitro* and *ex vivo* models regardless of any antibiotics or antiseptic resistance (Kunisada *et al*., 1997; Haley *et al*., 1998; Block *et al*., 2000). Lastly, the use of PVP-I NPs was reported to not induce iodine or cross-resistance to antibiotics or other antiseptics (Lepelletier *et al*., 2020).

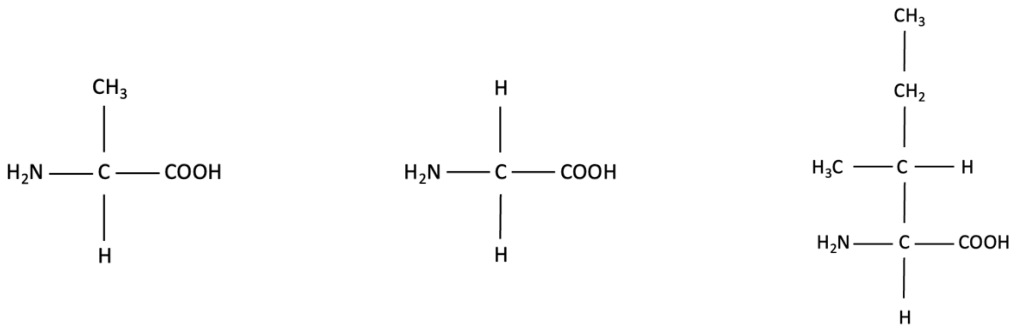

Alanine Glycine Isoleucine

Figure 5. Amino acids chemical structures showing their functional group characteristics.

A novel hypothesis for this chapter and study may be that the amino acids, the surrounding metal ions and the form of iodine in the complex are the factors influencing the bioactivities of the complexes. The way in which the amino acids interact with the iodine-containing nanomolecular complexes may be due to the hydrophobicity of the amino acid side chain and thus influences the antibacterial activity of the NP. The nanomolecular complex synthesized with isoleucine, may possibly exhibit a different antimicrobial activity mechanism due to it being the most hydrophobic amino acid of all amino acids. Additionally, the functional groups (side chain group) involved in the coordination with iodine may possibly influence the bioactivity of the nanomolecular complexes. The surrounding metal ions, may, in addition, interact with the surface of the NPs, influence the bioactivity of the NPs and possibly aid in causing significant damage to the bacterial cell barriers. Lastly, when in solution, iodine will be deactivated to iodide and then proceed to target the biological components. The antimicrobial mechanism of action of the iodine containing nanomolecular complexes will likely adhere to one of three models: oxidative stress induction, metal ion release and transport, or non-oxidative mechanisms. This is followed by changes in cell structure, metabolism, and transport patterns. The objective for the work presented in this chapter is to therefore, evaluate the positively/negatively coregulated genes and networks influenced by each iodine-containing complex on both *E. coli* and *S. aureus*. Additionally, identify the pathways and functional categories affected by each complex on *E. coli* and *S. aureus*. Furthermore, this chapter will characterise the three iodine-containing nanomolecular complexes and compare the bioactivity of each complex based on gene transcription.

2.2 Methods

2.2.1 Bacterial cultures and maintenance and growth conditions

All the experimental wet lab work was conducted by The SCAID using model microorganisms; ESBL (TEM-1) producing *E. coli* ATCC BAA-196^{TM} and MDR *S. aureus* ATCC BAA-39^{TM}, obtained from the American Type Culture Collection (ATCC) (https://www.lgcstandards-atcc.org/en.aspx). The bacterial strains were cultivated on Mueller-Hinton (MH) liquid or solid media (Himedia, India) with *S. aureus* cultivated without antibiotics and *E. coli* cultivated in the medium supplemented with ceftazidime 10 µg/ml as recommended from the ATCC product sheet. Before supplementing the bacterial cultures with the iodine-containing nanomolecular complexes, the bacterial strains were twice passaged on MH medium and maintained in a freezer at −80°C for long term storage.

2.2.2 Cultivation of bacterial cultures with iodine-containing complexes KS25, KS33 and KS51

Bacterial inoculate *E. coli* ATCC BAA-196 was then incubated and maintained at 37ºC for 1 hour (the end of the lagging growth phase, termed Lag-experiment) and for 6 hours (the middle of the logarithmic growth phase, termed Log-experiment) and *S. aureus* ATCC AA-39 for 2.5 hours (Lag experiment) and 9 hours (Log experiment) at 37°C. Lag and Log growth phases were estimated based on the strain specific growth curves on MH medium, which were determined in the previous study (Korotetskiy *et al*., 2021). After incubation, the experimental cultures were supplemented with iodine-containing nanomolecular complexes; KS25, KS33 and KS51, separately, whereas the negative control samples were left un-supplemented. The experimental cultures were then incubated for 5 minutes, at 37°C while shaking. All the metabolic processes within the cells were then stopped by the killing buffer (2.0 ml of 1 MTris-HCl, pH 7.5; 0.5 ml of 1 M MgCl2, 1.3 g of NaN_3; 997.5 ml of water) added in the ratio of 1:1 (Howden *et al*., 2013). All experiments were performed in three replicates (see Table 5). Bacterial cells were collected for RNA extraction by centrifugation at 5,000 g for 10 min.

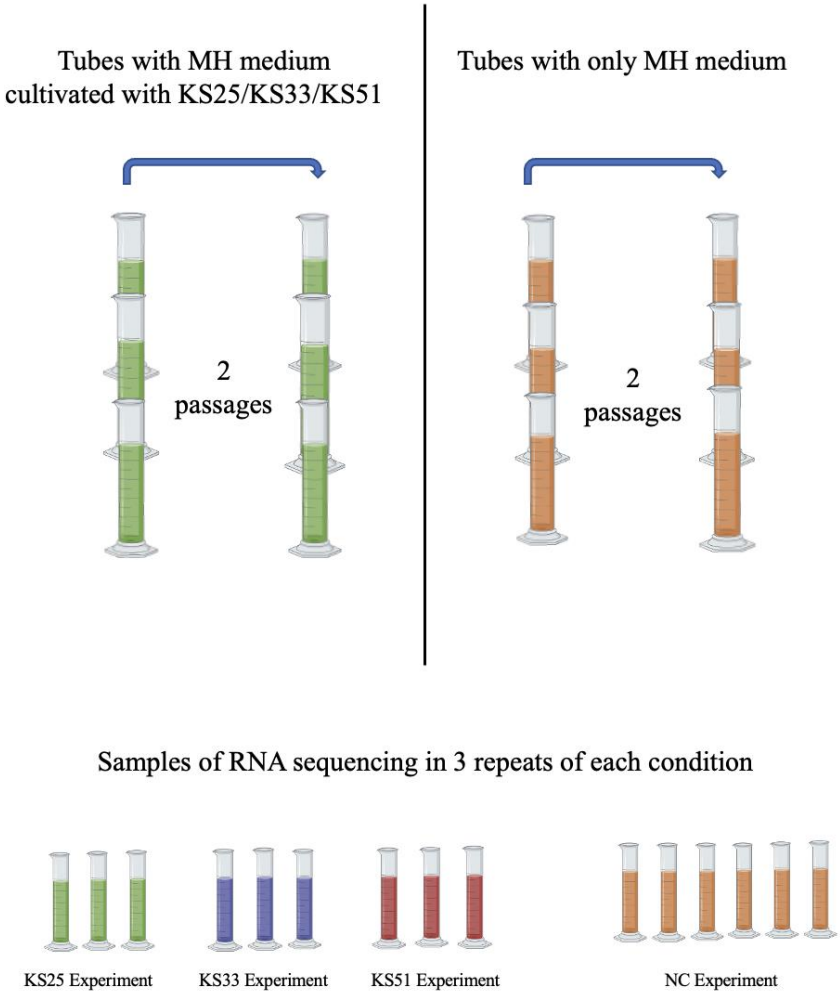

Figure 6. General schematic diagram of the experiment.

2.2.3 RNA extraction and sequencing

The isolation and extraction of total RNA samples from the negative control cultures and KS25/KS33/KS51-treated cultures was performed using the RiboPure Bacteria Kit (Ambion, Lithuania) as per the guidelines. The quality and quantity of the extracted RNA were determined by using a NanoDrop 2000c spectrophotometer (Thermo Scientific, USA) at optical wavelengths 260 and 280 nm. Purification of the total RNA from 16S and 23S ribosomal RNA was carried out using the MICROBExpress Bacterial mRNA Purification Kit (Ambion, Lithuania), as per the developer's instructions. Thereafter, the effectiveness of sample purification was determined on the Bioanalyzer 2100 (Agilent, Germany) with the RNA 6000 Nano LabChip Kit (Agilent Technologies, Lithuania). The library preparation from the extracted RNA samples included an enzymatic fragmentation step with the use of the Ion Total

RNA Seq kit V2 (Life Technologies, USA). Ion Xpress RNA-Seq Barcode 01-16 Kit was then used for RNA fragment barcoding. RNA sequencing was performed using the Ion 318 Chip Kit V2 on the Ion Torrent PGM sequencer (Life Technologies, USA). The quality of the generated RNA sequences were then evaluated using the standard RNA quality control pipeline implemented in UGENE v.36 (Okonechnikov *et al*., 2012). Trimmomatic version 0.40 (Bolger *et al*., 2014) was then used to remove short reads smaller than 30 bp and those with an average base call quality values below 21.

2.2.4 Gene Expression Analysis

Gene expression information was captured using RNA sequencing (RNA-seq) technologies, yielding RNA short reads fragments in fastq format. The effects of KS25, KS33 and KS51 on *E. coli* ATCC BAA-196 and *S. aureus* ATCC BAA-39 were assessed by measuring whether genes are differentially expressed in the experimental condition compared to the negative control. The trimmed RNA FASTQ sequences from the experimental and control conditions samples were mapped to genome using fasta and gff annotation files in R version 3.4.4. The alignment of reads was performed using the RSubread package, which generates normalised counts of reads aligned against orthologous features (*i.e.,* CDS) in 3 times repeated KS25/KS33/KS51 and NC samples. The generated normalized counts were combined into a joint table with different control and experiment samples in columns and feature counts in rows. DESeq2, a R-packaged pipeline combining GenomicFeatures and ggplots2 algorithms was used to estimate the statistics of differential gene regulation in the experimental compared to the control samples in csv file format. The csv file includes statistics on base mean, Log_2(fold-change) (Log_2FC), standard error (IfcSE) values, adjusted p-value and the p-value. A gene expression in-house Python tool was then used to generate volcano expression plots and txt document using; the generated csv files and source genome file (respective reference genome in gff (generic feature format) format). The output text documents include information on the upregulated and downregulated genes, with information including; Log_2FC, p-value, gene name and annotation. Gene expression analysis allows one to locate where genes can be found in various biochemical pathways by determining how these genes are regulated under various conditions.

2.2.5 Statistical evaluations

All RNA sequencing experiments were performed in several repetitions as shown in (Table 4). Genes showing 2-fold or greater expression difference with calculated p-value equal or smaller 0.05 were considered as significantly regulated.

2.2.6 Networks of Coregulated Genes Analysis

Networks of regulated genes were constructed using Web based tool PheNetic (http://bioinformatics.intec.ugent.be/phenetic/index.html#/index) (De Maeyer *et al*., 2013) based on the regulation network designed for *E. coli* K12 [NC_000913. 2], available on the PheNetic Web site. The input required by Phenetic consists of an interaction network of the organism under study (which can be downloaded from the web server), the differential expression data and a gene list. The web server calculates from the interaction network, based on the provided expression data set, what is most likely differentially activated or inactivated between the compared conditions (Maeyer *et al*., 2015). The web-based tool does this by calculating the upstream regulatory mechanisms that are causal to the observed differential expression phenotype or downstream with default settings by finding pathways/protein complexes that are activated or inactivated by the differentially expressed genes (Maeyer *et al*.,2015). To identify the pairs of homologous genes between *E. coli* K12 [NC_000913. 2] and *E. coli* ATCC BAA-196 GET_HOMOLOGUES with default parameters (Contreras-Moreira & Vinuesa, 2013) was used. Homologous genes shared by *S. aureus* BAA-39 and *E. coli* BAA-196 were determined using the same program with the parameters set to default (Contreras-Moreira & Vinuesa, 2013). Large, admixed clusters of homologous phage-related integrases and transposases were considered as strain-specific genes and excluded from the transcription comparison.

2.2.7 Gene Ontology Analysis

To perform over-representation analysis on sets of genes, the gene lists predicted by DESeq2 and the in-house Gene expression python tool, in response to each treatments was used. The lists containing statistically significant genes (≥2-log foldchange FC, P-value<0.05) from *E. coli* ATCC BAA-196 and *S. aureus* ATCC BAA-39, from each treatment were queried against

ShinyGO v0.66 (http://bioinformatics.sdstate.edu/go/) (Ge SX *et al*., 2020) using species *E. coli* K12, strain MG1655 STRINGdb and *S. aureus* STRINGdb with p-value cut-off of 0.05. Gene Ontology Analysis allows for the classification of genes that are over-represented in the data, and are classified according to their molecular function, the biological process they are involved in, and their cellular location.

2.2.8 Metabolic Pathway Analysis

The effects of the iodine-containing nanomolecular structures on the metabolic pathways of *E. coli* ATCC BAA-196 and *S. aureus* ATCC BAA-39 were determined using Pathway Tools software version 24.0, smartTables feature (https://www.genome.jp/kegg/) (Karp *et al*., 2016). Pathway Tools predicts metabolic pathways in sequenced and annotated genomes using Biocyc and MetaCyc PGDB as the reference metabolic pathway database and using *E. coli* K-12 substr. MG1655 and *S. aureus LAC* reference genomes, displaying the results in tabular format. The database contains biological known pathways including gene names and information on species-specific pathways (Kanehisa *et al*., 2006). To use Pathway Tools and create smartTools, you must have an account and be logged in.

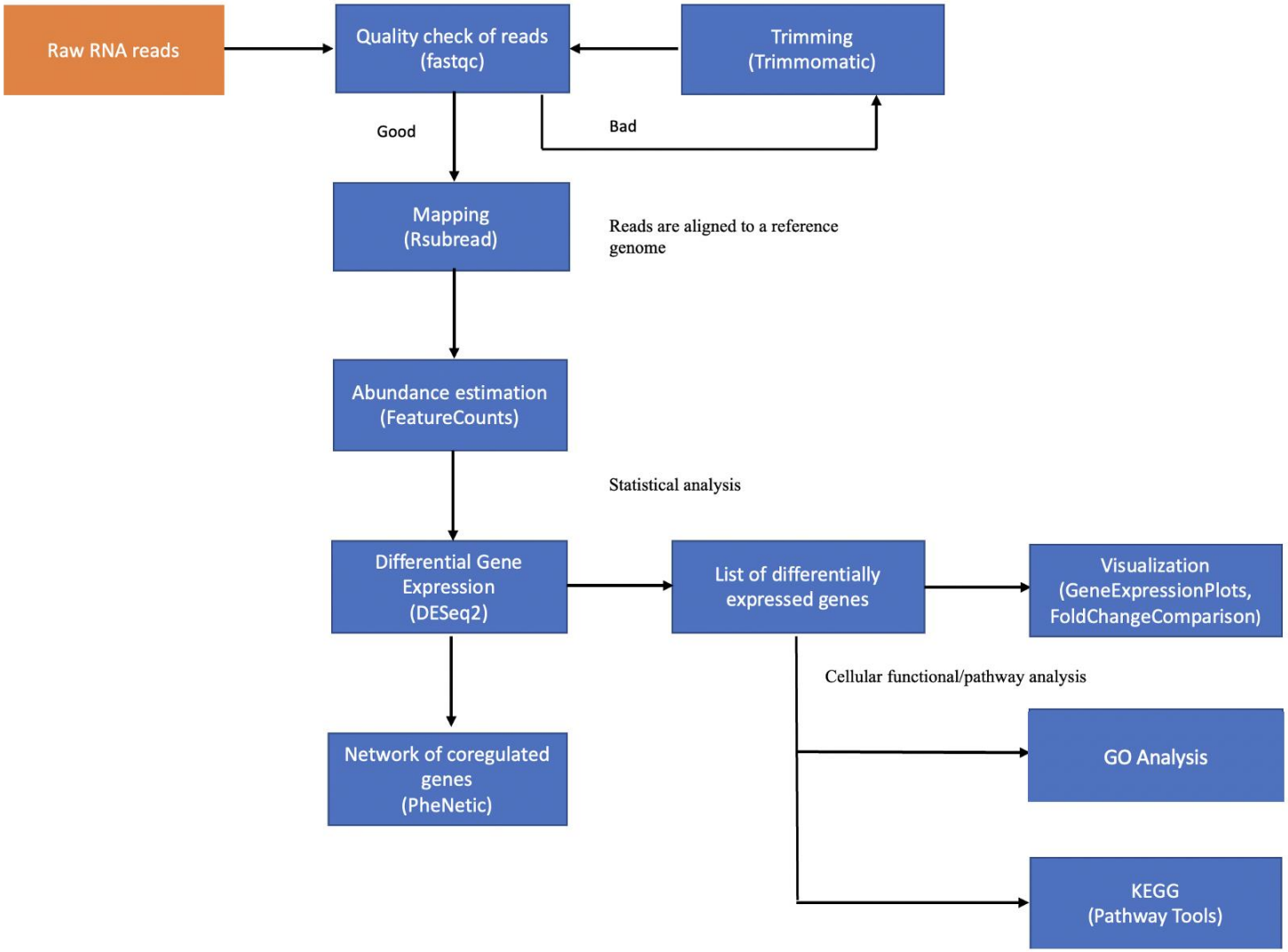

Figure 7. An RNA-Seq workflow for Gene Expression and Metabolic Pathway Analysis.

2.3 Results

2.3.1 RNA reads sequenced data

Three sets of the RNA sequence data treated with the complex drugs and 6 sets of RNA sequenced data not treated with the complex drugs, during the lag and log growth phase were provided by SCAID, see (Table 4). Trimmomatic version 0.40 was used to trim the short reads that were smaller than 30bp, with an average base call quality value below 21, returning fastq files.

Table 5. Sets of RNA extracted and sequenced data.

Strain	Growth phase	KS25	KS33	KS51	NC
***E. coli* BAA-196**	Lag	3	3	3	6
	Log	3	3	3	6
***S. aureus* BAA-39**	Lag	3	3	3	6
	Log	3	3	3	6

2.3.2 Characterization of the iodine-containing nanomolecular complex KS25, KS33 and KS51

The iodine-containing nanomolecular complexes denoted as KS25, KS33 and KS51 were synthesized and provided by SCAID. The complexes were entrapped and synthesized with iodine, amino acids and metal ions. The structure, characteristics and morphology of the nanomolecular complexes were confirmed and resolved by X-ray crystallography, Infra-red, ultra-violet spectra and Discovery Studio modelling, described in (Fig. 8 and Table 6). Complex KS25 contains two molecules of glycine bound by coordination bonds with one three-iodine molecule and three K^+ ions. Complex KS33 contains three alanine molecules bound with one three-iodine molecule and three Li^+ ion. Complex KS51 contains two molecules of isoleucine associated with an iodine ion.

The concentration of molecular iodine per 1,000 g of the complexes was measured:

$$\text{Conc. of. } I_2 = {}^{V1.K1.12{,}69}/_{m} \qquad \text{Eq. 2}$$

where V1 is the volume of 0.05M sodium thiosulfate spend for complete titration, K1 is the correction on sodium thiosulfate concentration in the buffer, for 0.05M solution K1 = 0.5 and m is the weight of the complex in g.

The concentration of KI was measured as:

$$\text{Conc. of. KI} = {}^{(V2.K2 - V1.K1).16{,}60}/_{m} \qquad \text{Eq. 3}$$

where V1 is the volume of 0.05M sodium thiosulfate spent for complete titration, V2 is the volume of 0.05M AgNO3 spent for complete titration; K1 = K2 = 0.5 and m is weight of the complex in g.

The concentration of LiI was measured as:

$$\text{Conc. of. LiI} = {}^{(V2.K2 - V1.K1).133{,}85}/_{m} \qquad \text{Eq. 4}$$

where V1 is the volume of 0.05M sodium thiosulfate spent for complete titration, V2 is the volume of 0.05M AgNO3 spent for complete titration; K1 = K2 = 0.5 and m is weight of the complex in g.

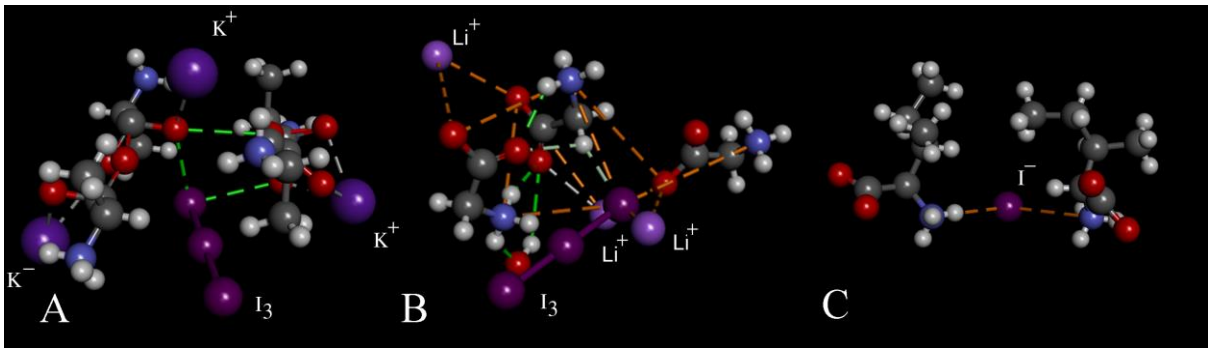

Figure 8. Iodine-containing nanomolecular complexes described as A) KS25, B) KS33 and C) KS51. Carbon atoms are represented by grey balls; oxygen atoms – red balls; nitrogen atoms – blue balls; and hydrogen atoms – white balls. Covalent bonds are shown as sticks. Predicted hydrogenic, electrostatic and metal ion coordination bonds are depicted by dashed green, orange and white lines, respectively. Structure A, represents complex KS25 (I_2 + KI + alanine); structure B, represents complex KS33 (I_2 + LiI + glycine); structure C, represents complex KS51 (I_2 + LiI + isoleucine).

Table 6. The composition of designed iodine-containing nanomolecular complexes.

Complex	Amino acid	Iodine source	Solvent	Form of Iodine in compound	Nanomolecular charge	Hydrophobicity
K25	Glycine	I_2 + KI	Ethanol	I^- + I_3	+1	0
K33	Alanine	I_2 + LiI	Ethanol	I^- + I_3	+1	0
K51	Isoleucine	I_2 + LiI	Water	I^-	0	2

2.3.3 Differential Gene Regulation

In this study, gene regulation effects of iodine-containing nanomolecular complexes denoted as KS25, KS33 and KS51 were analysed on model microorganisms *E. coli* ATCC BAA-196 and *S. aureus* ATCC BAA-39. This was evaluated by measuring differentially expressed genes in the experimental conditions compared to the control conditions during the lag and exponential growth phases. The trimmed RNA FASTQ sequences from the experimental and control conditions samples, during the lag and log phase, were mapped to their respective reference sequences. The alignment of reads was performed using the RSubread package, which generates normalised counts of reads aligned against orthologous features (*i.e*., CDS) in 3 repeats from (KS25, KS33, KS51) and negative control samples. DESeq2, an R-packaged pipeline combining genomicFeatures and ggplots2 algorithms was used to estimate the statistically reliability of differential gene regulation in the experimental compared to the control in csv file format. Gene expression differences equal to or greater than 2-folds with a p-value equal or lower than 0.05 were only considered. Overall, in *E. coli* ATCC BAA-196, 122 DEG (50 upregulated, 72 downregulated) between KS25 and the control group were identified, 138 DEG (85 upregulated, 53 downregulated) between KS33 and the control group, and 184 DEG (69 upregulated, 115 downregulated) between KS51 and the control group with 17 non-ribosomal transcribed RNA (nrRNA) all together. In *S. aureus* ATCC BAA-39 we identified 244 DEG (154 upregulated, 90 downregulated) between KS25 and the control group, 111 DEG (81 upregulated, 30 downregulated) between KS33 and the control group, 184 DEG (84 upregulated, 100 downregulated) between KS51 and the control group, illustrated in (Table 7). Several DEG were of unknown function including conserved genes and hypothetical genes. Some genes were highly activated (≥ 5-fold up-regulation), indicating that they might have had a significant role in the adaption mechanisms of both model microorganisms. The shared DEG are represented in (Fig 9), with (Fig. 9A) comparing upregulated genes within KS25, KS33 and KS51 in *E. coli* ATCC BAA-196, (Fig. 9B) comparing downregulated genes in within KS25, KS33 and KS51 in *E. coli* ATCC BAA-196 (Fig. 9C) comparing upregulated genes in within KS25, KS33 and KS51 in *S. aureus* ATCC BAA-39 and (Fig. 9D) comparing downregulated genes in within KS25, KS33 and KS51 in *S. aureus* ATCC BAA-39. The names and annotations of the shared genes amongst the nanomolecular complexes are detailed in Supplementary Table 1 (Table S1) and Supplementary Table 2 (Table S2). The size of this response is subject to the statistical and expression filters that were applied to the data. Genes that had a regulation less than 2 fold were excluded and regarded to have very low regulation

levels. In addition, the data was subject to confidence level testing to determine and obtain the results that were statistically reliable by selecting DEG that had a p-value of 0.05 or less. Subsequently, a network of coregulated genes analysis was conducted using PheNetic (Fig. 14-19) on *E. coli* ATCC BAA-196 and homologous genes shared between *E. coli* K-12 [NC_000913.2] and *S. aureus* ATCC BAA-196 (see Supplementary Table S1). The pairs of homologous genes shared by these two genomes were identified using the program GET-HOMOLOGOUS. In total, 725 pairs of homologous genes were found, of which only those that were affected by the treatments, are shown in Supplementary Table 5.

Table 7. Numbers of differentially expressed genes in model microorganisms *E. coli* ATCC BAA-196 and *S. aureus* ATCC BAA-39 treated with KS25, KS33 and KS51 in the Lag and Log growth phases with parameters (≥2-log_2FC; P< 0.05).

Bacterial strain	**Growth Phase**	**KS25**		**KS33**		**KS51**	
		Up-regulated	**Down-regulated**	**Up-regulated**	**Down-regulated**	**Up-regulated**	**Down-regulated**
***E. coli* ATCC BAA-196**	Lag	22	23	40	26	34	70
	Log	28	49	45	27	35	45
***S. aureus* ATCC BAA-39**	Lag	99	56	52	15	43	64
	Log	55	34	29	15	41	36

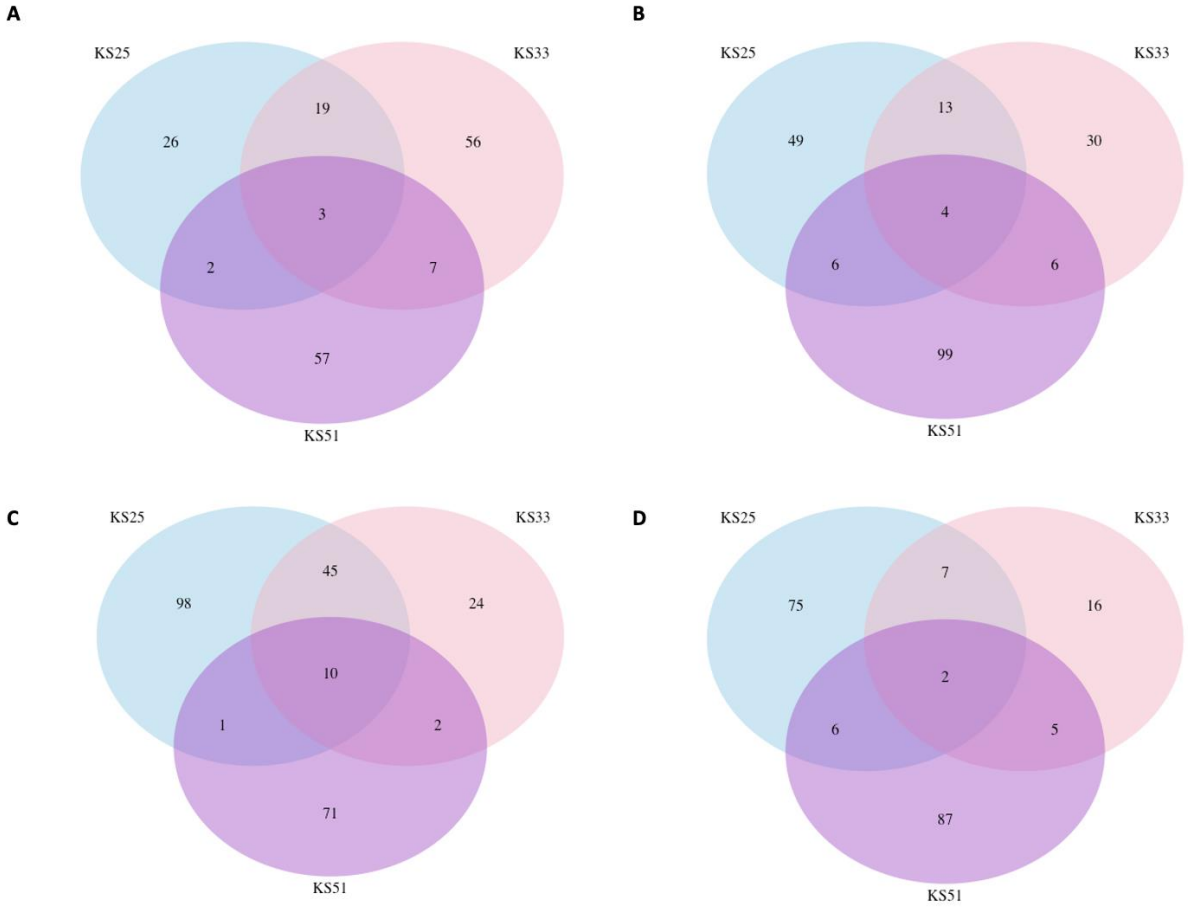

Figure 9. Venn diagram of the number of differentially expressed genes shared between the treatment groups KS25, KS33 and KS51. Three comparison were made: **A** compares upregulated genes within KS25, KS33 and KS51 in *E. coli* ATCC BAA-196 and **B** compares downregulated genes in within KS25, KS33 and KS51 in *E. coli* ATCC BAA-196. **C** compares upregulated genes in within KS25, KS33 and KS51 in *S. aureus* ATCC BAA-39 and **D** compares downregulated genes in within KS25, KS33 and KS51 in *S. aureus* ATCC BAA-39.

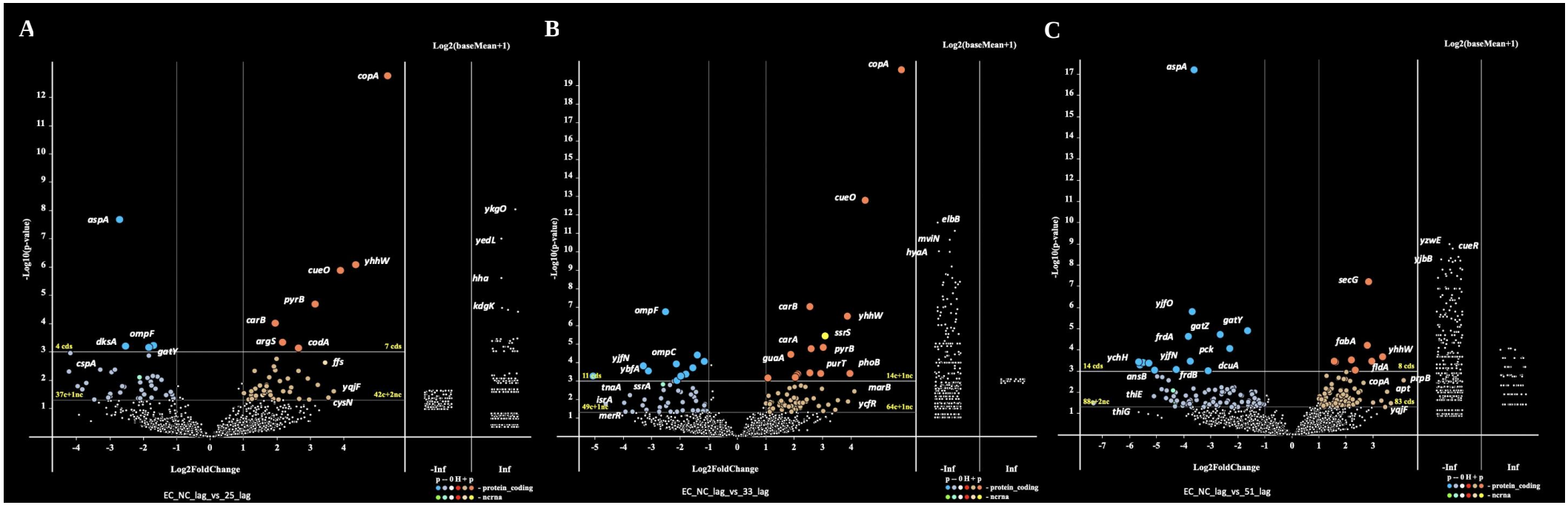

Figure 10. Volcano plot of differentially expressed genes identified between KS25, KS33 and KS51 treated variants of *E. coli* ATCC BAA-196 and control group, during the lag growth phase. A) Represents gene regulation in KS25 treated variant of *E. coli* versus the negative control, B) Represents gene regulation in KS33 treated variant of *E. coli* versus the negative control C) Represents gene regulation in KS51 treated variant of *E. coli* versus the negative control. Circles on the plot represent protein coding genes (CDS) plotted according to their negative (blue circles) and positive (orange circles) Log_2FC values calculated in the Lag-experiment. The strongest regulated genes are labelled by their gene names. The thin vertical and horizontal lines within the plots separate genes with 1-fold or higher regulation. The panels denoted as -Inf and Inf represent genes that were only expressed in NC (-Inf) and only in treated samples (Inf), respectively.

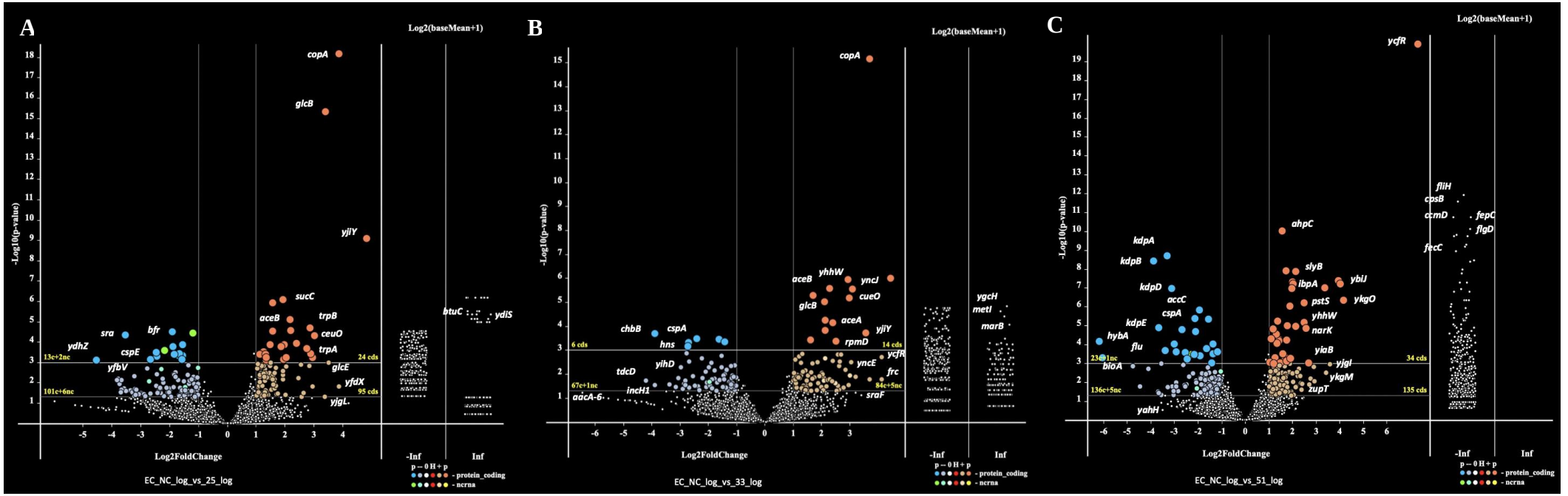

Figure 11. Volcano plot of differentially expressed genes identified between KS25, KS33 and KS51 treated variants of *E. coli* ATCC BAA-196 and control group, during the log growth phase. A) Represents gene regulation in KS25 treated variant of *E. coli* versus the negative control, B) Represents gene regulation in KS33 treated variant of *E. coli* versus the negative control C) Represents gene regulation in KS51 treated variant of *E. coli* versus the negative control. Circles on the plot represent protein coding genes (CDS) plotted according to their negative (blue circles) and positive (orange circles) Log_2FC values calculated in the Log-experiment. The strongest regulated genes are labelled by their gene names. The thin vertical and horizontal lines within the plots separate genes with 1-fold or higher regulation. The panels denoted as -Inf and Inf represent genes that were only expressed in NC (-Inf) and only in treated samples (Inf), respectively.

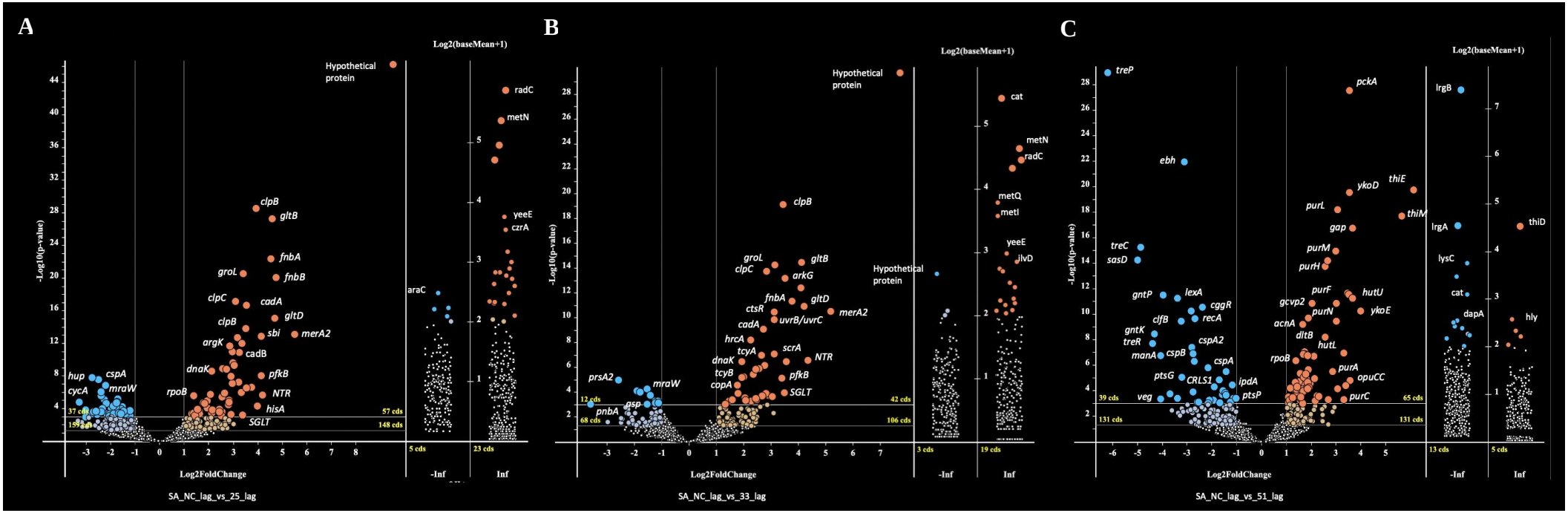

Figure 12. Volcano plot of differentially expressed genes identified between KS25, KS33 and KS51 treated variants of *S. aureus* ATCC BAA-39 and control group, during the lag growth phase. A) Represents gene regulation in KS25 treated variant of *S. aureus* versus the negative control, B) Represents gene regulation in KS33 treated variant of *S. aureus* versus the negative control C) Represents gene regulation in KS51 treated variant of *S. aureus* versus the negative control. Circles on the plot represent protein coding genes (CDS) plotted according to their negative (blue circles) and positive (orange circles) Log_2FC values calculated in the Lag-experiment. The strongest regulated genes are labelled by their gene names. The thin vertical and horizontal lines within the plots separate genes with 1-fold or higher regulation. The panels denoted as -Inf and Inf represent genes that were only expressed in NC (-Inf) and only in treated samples (Inf), respectively.

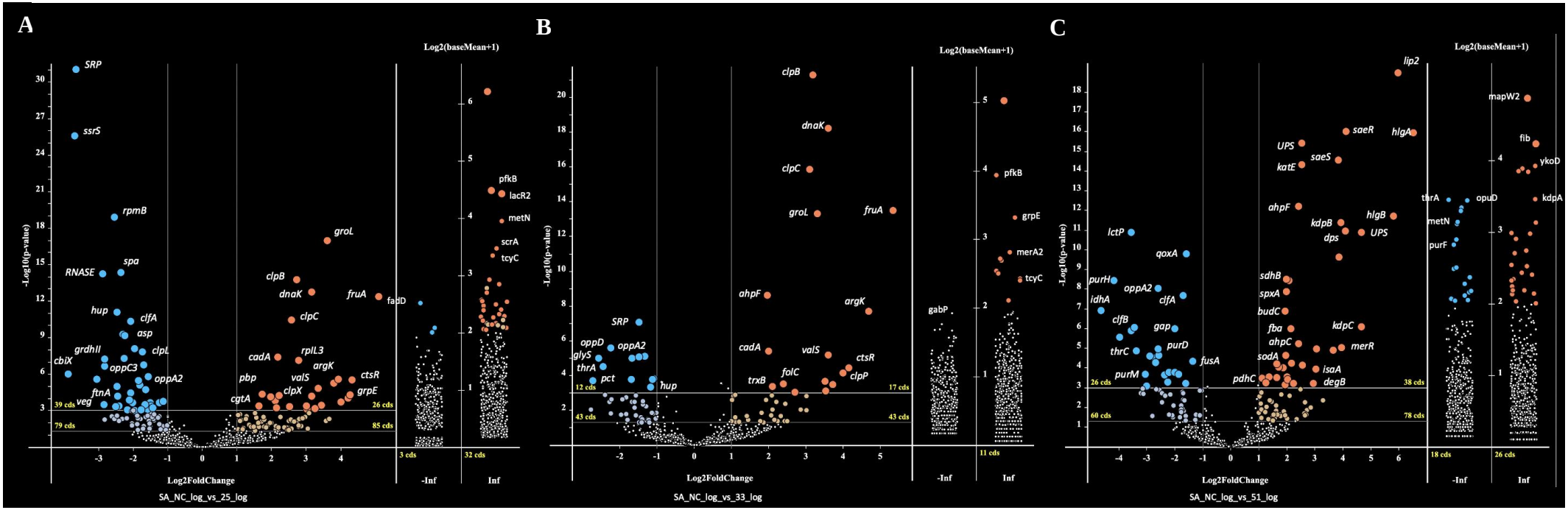

Figure 13. Volcano plot of differentially expressed genes identified between KS25, KS33 and KS51 treated variants of *S. aureus* ATCC BAA-39 and control group, during the log growth phase. A) Represents gene regulation in KS25 treated variant of *S. aureus* versus the negative control, B) Represents gene regulation in KS33 treated variant of *S. aureus* versus the negative control C) Represents gene regulation in KS51 treated variant of *S. aureus* versus the negative control. Circles on the plot represent protein coding genes (CDS) plotted according to their negative (blue circles) and positive (orange circles) Log_2FC values calculated in the Log-experiment. The strongest regulated genes are labelled by their gene names. The thin vertical and horizontal lines within the plots separate genes with 1-fold or higher regulation. The panels denoted as -Inf and Inf represent genes that were only expressed in NC (-Inf) and only in treated samples (Inf), respectively.

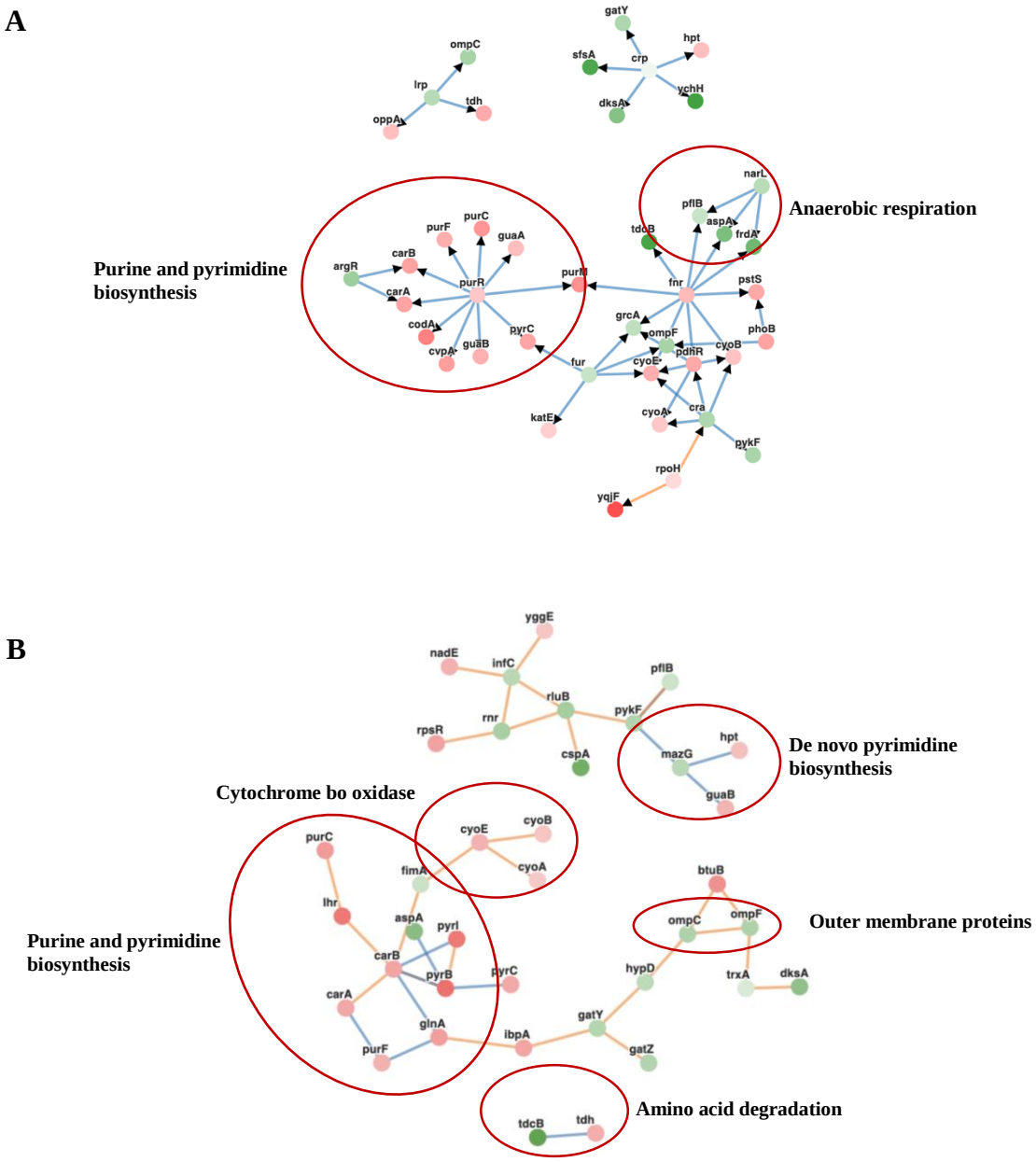

Figure 14. PheNetic networks of transcriptional regulation of differentially expressed genes of *E. coli* BAA-196 and *S. aureus* ATCC BAA-39 treated with KS25, during the lag phase, grouped by functional or regulatory interactions between genes using upstream (A) which identifies the regulatory mechanisms that induced the observed differential expression and downstream (B) which identifies activated pathways in response to the treatments. Upregulated genes are depicted by pink/red nodes and downregulated genes by green nodes (vertices). The colour intensity indicates the level of regulation. Green edges show activation relations, blue edges show activities of inhibition relations. Direct regulations by transcriptional regulators are indicated by arrowheads. The genes are grouped regulons that are controlled by transcriptional regulators including; *lrp*, *purR*, *crp*, *narL*, *fnr*, *fur*, *rpoH*, *cra*, *phoB* and *pdhR*.

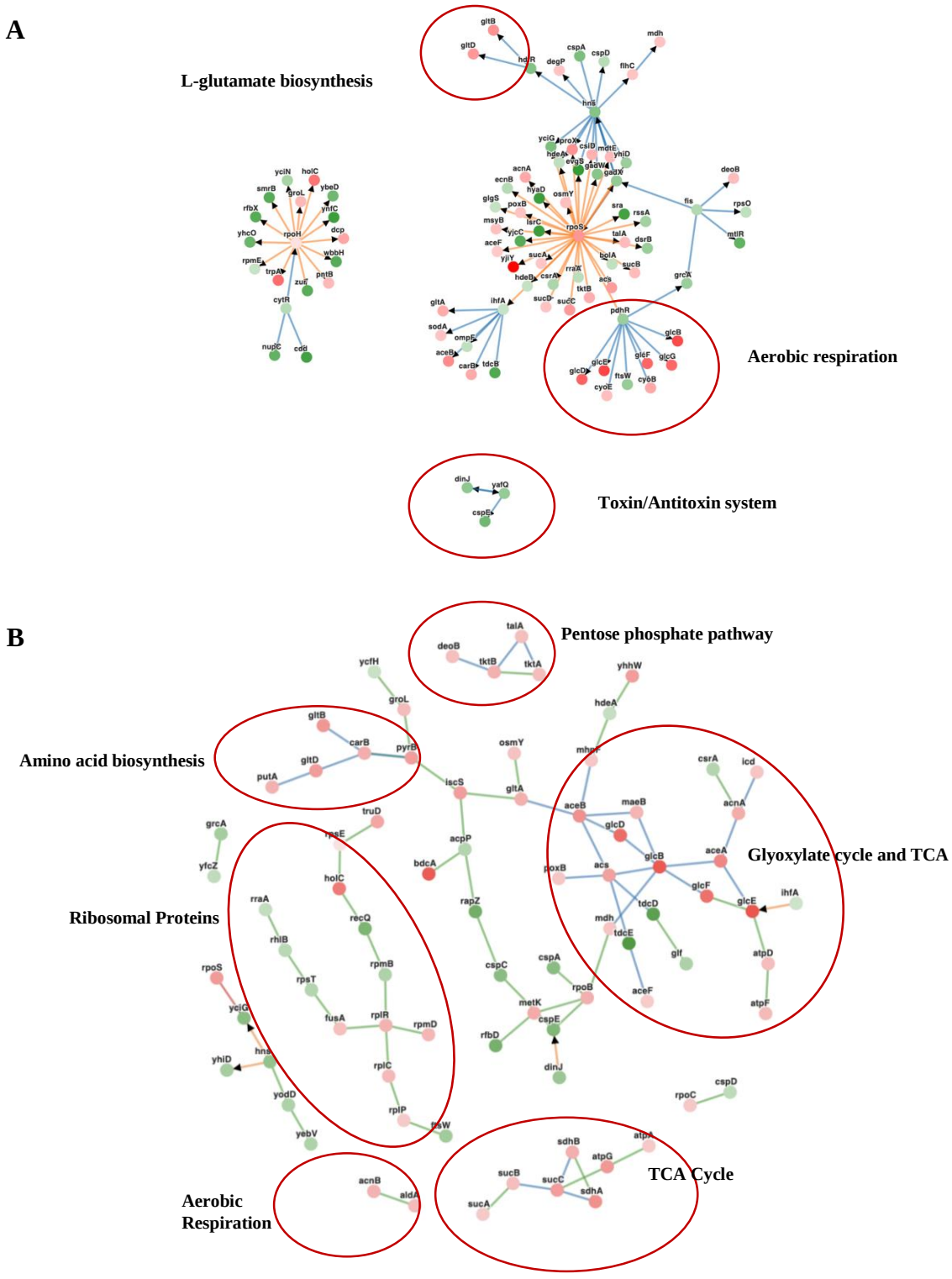

Figure 15. PheNetic network of transcriptional regulation of differentially expressed genes of *E. coli* BAA-196 and *S. aureus* ATCC BAA-39 treated with KS25, during the log phase, grouped by functional or regulatory interactions between genes using upstream (A) which identifies the regulatory mechanisms that induced the observed differential expression and downstream (B) which identifies activated pathways in response to the treatments. Upregulated genes are depicted by pink/red nodes and downregulated genes by green nodes (vertices). The colour intensity indicates the level of regulation. Green edges show activation relations, blue edges show activities of inhibition relations. Direct regulations by transcriptional regulators are indicated by arrowheads. The genes are grouped regulons that are controlled by transcriptional regulators including; *rpoHS*, *ifhA*, *pdhR*, *fis*, *cytR*, *hns*, *hdfR*, *fihC*, *yafQ* and *dinJ*.

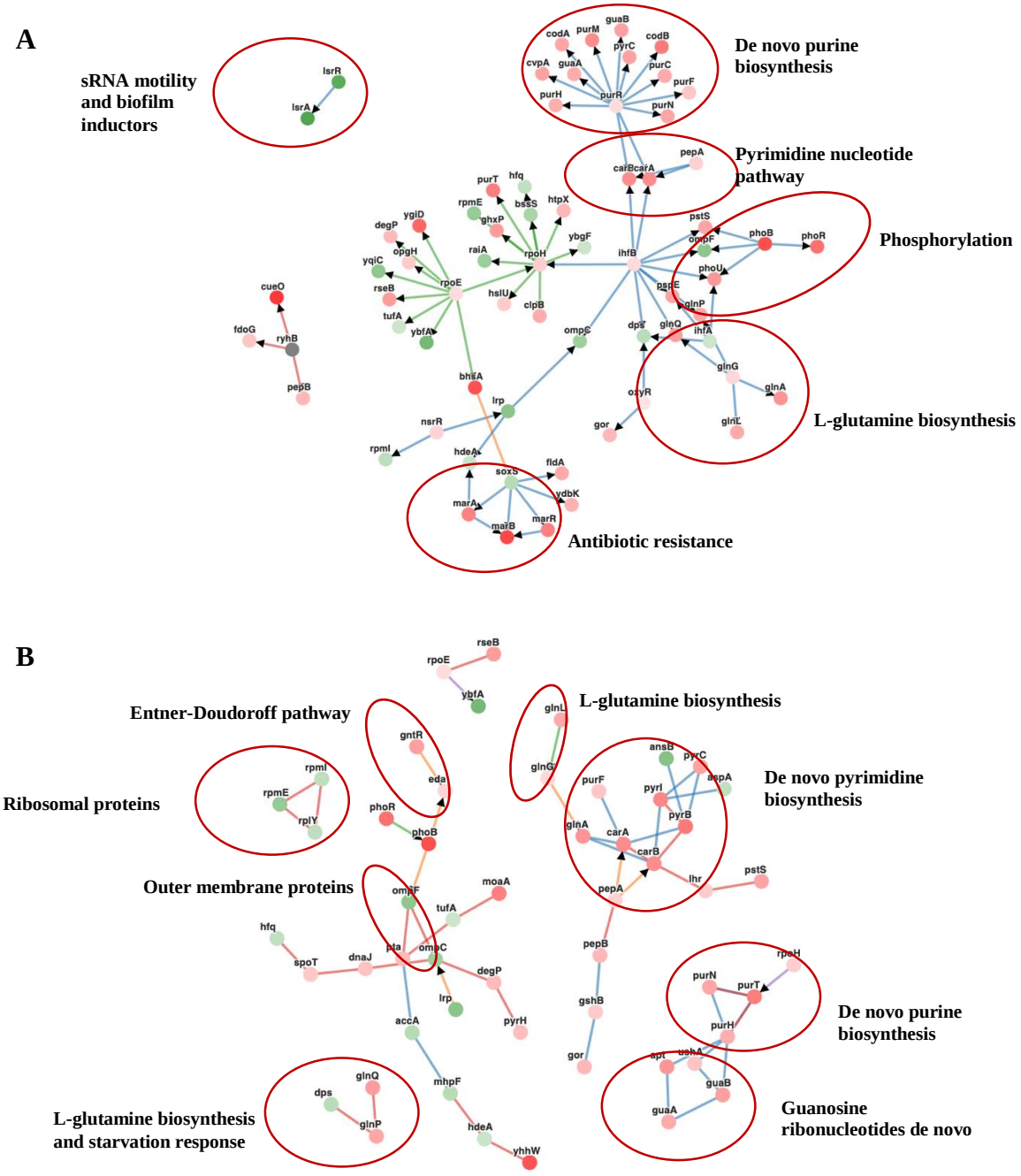

Figure 16. PheNetic network of transcriptional regulation of differentially expressed genes of *E. coli* BAA-196 and *S. aureus* ATCC BAA-39 treated with KS33, during the lag phase, grouped by functional or regulatory interactions between genes using upstream (A) which identifies the regulatory mechanisms that induced the observed differential expression and downstream (B) which identifies activated pathways in response to the treatments. Upregulated genes are depicted by pink/red nodes and downregulated genes by green nodes (vertices). The colour intensity indicates the level of regulation. Green edges show activation relations, blue edges show activities of inhibition relations. Direct regulations by transcriptional regulators are indicated by arrowheads. The genes are grouped regulons that are controlled by transcriptional regulators including; *isrR*, *purR*, *marAB*, *pepA*, *ryhB*, *rpoEH*, *ihfB*, *phoB*, *lrp*, *nsrR*, *soxS*, *oxyR* and *glnG*.

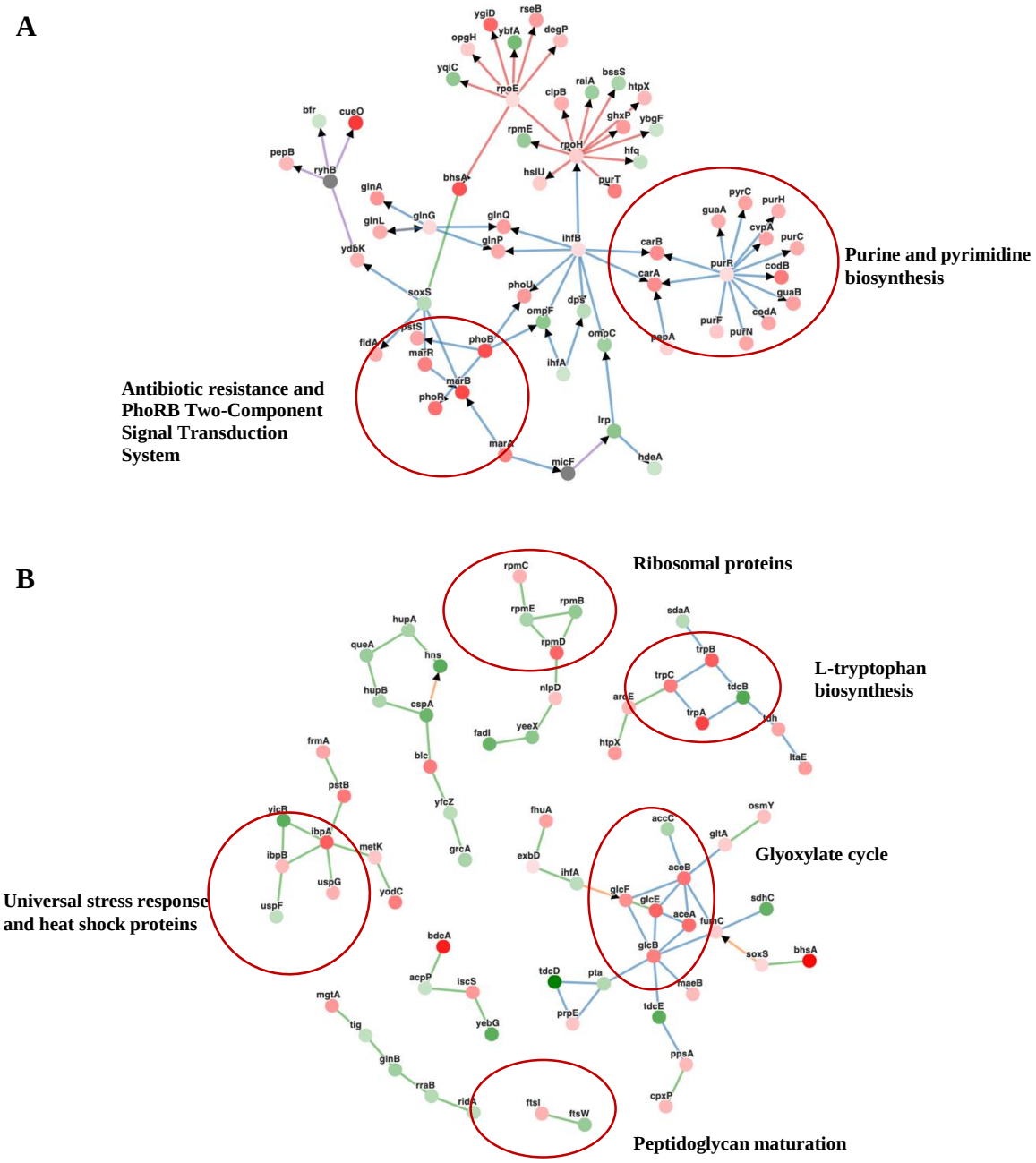

Figure 17. PheNetic network of transcriptional regulation of differentially expressed genes of *E. coli* BAA-196 and *S. aureus* ATCC BAA-39 treated with KS33, during the log phase, grouped by functional or regulatory interactions between genes using upstream (A) which identifies the regulatory mechanisms that induced the observed differential expression and downstream (B) which identifies activated pathways in response to the treatments. Upregulated genes are depicted by pink/red nodes and downregulated genes by green nodes (vertices). The colour intensity indicates the level of regulation. Green edges show activation relations, blue edges show activities of inhibition relations. Direct regulations by transcriptional regulators are indicated by arrowheads. The genes are grouped regulons that are controlled by transcriptional regulators including; *rpoEH*, *ryhB*, *glnG*, *soxS*, *ihfB*, *purR*, *micF*, *marAB* and *phoB*.

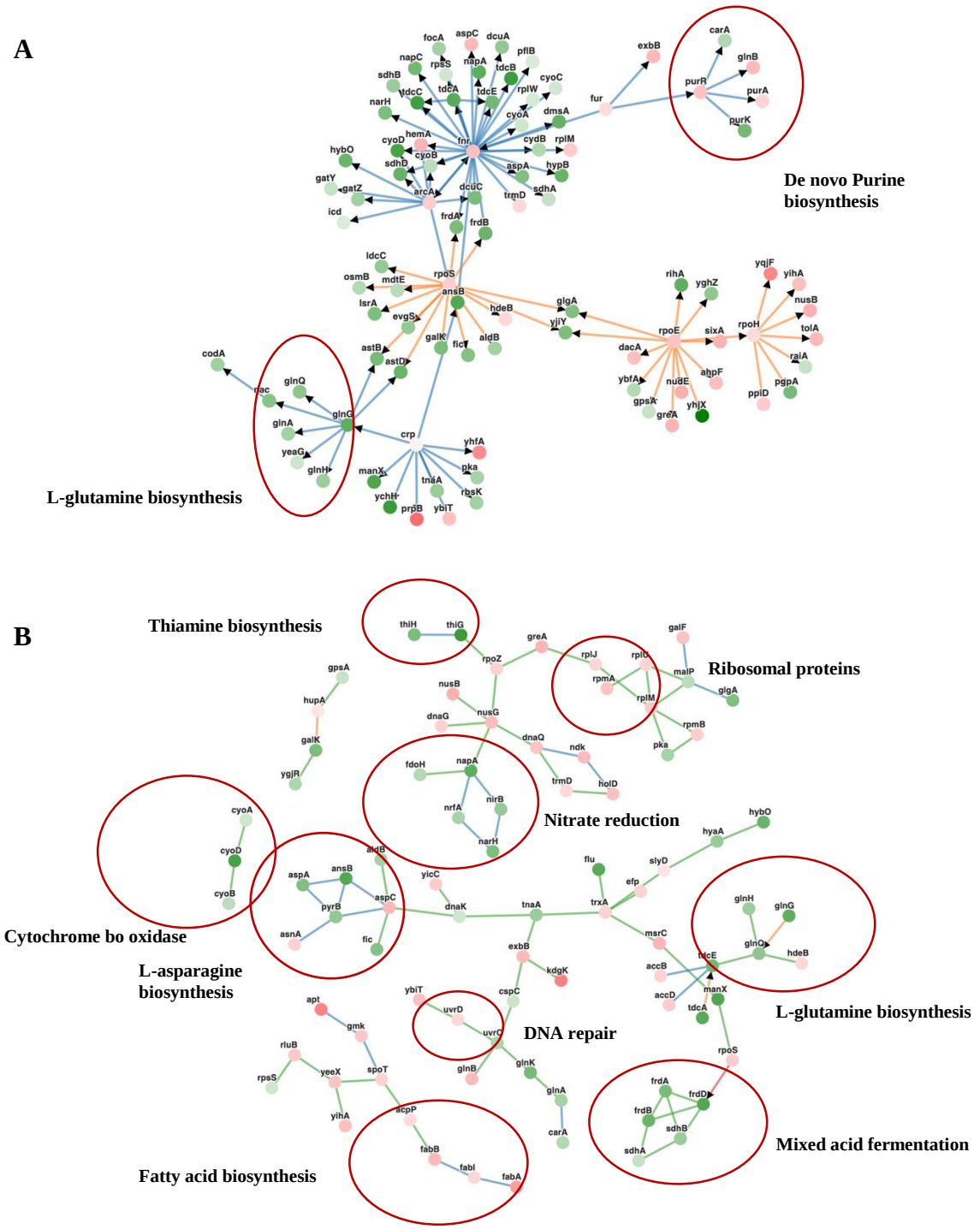

Figure 18. PheNetic network of transcriptional regulation of differentially expressed genes of *E. coli* BAA-196 and *S. aureus* ATCC BAA-39 treated with KS51, during the lag phase, grouped by functional or regulatory interactions between genes using upstream (A) which identifies the regulatory mechanisms that induced the observed differential expression and downstream (B) which identifies activated pathways in response to the treatments. Upregulated genes are depicted by pink/red nodes and downregulated genes by green nodes (vertices). The colour intensity indicates the level of regulation. Green edges show activation relations, blue edges show activities of inhibition relations. Direct regulations by transcriptional regulators are indicated by arrowheads. The genes are grouped regulons that are controlled by transcriptional regulators including; *purR*, *fur*, *rpoEHS*, *fnr*, *arcA*, *glnG* and *crp*.

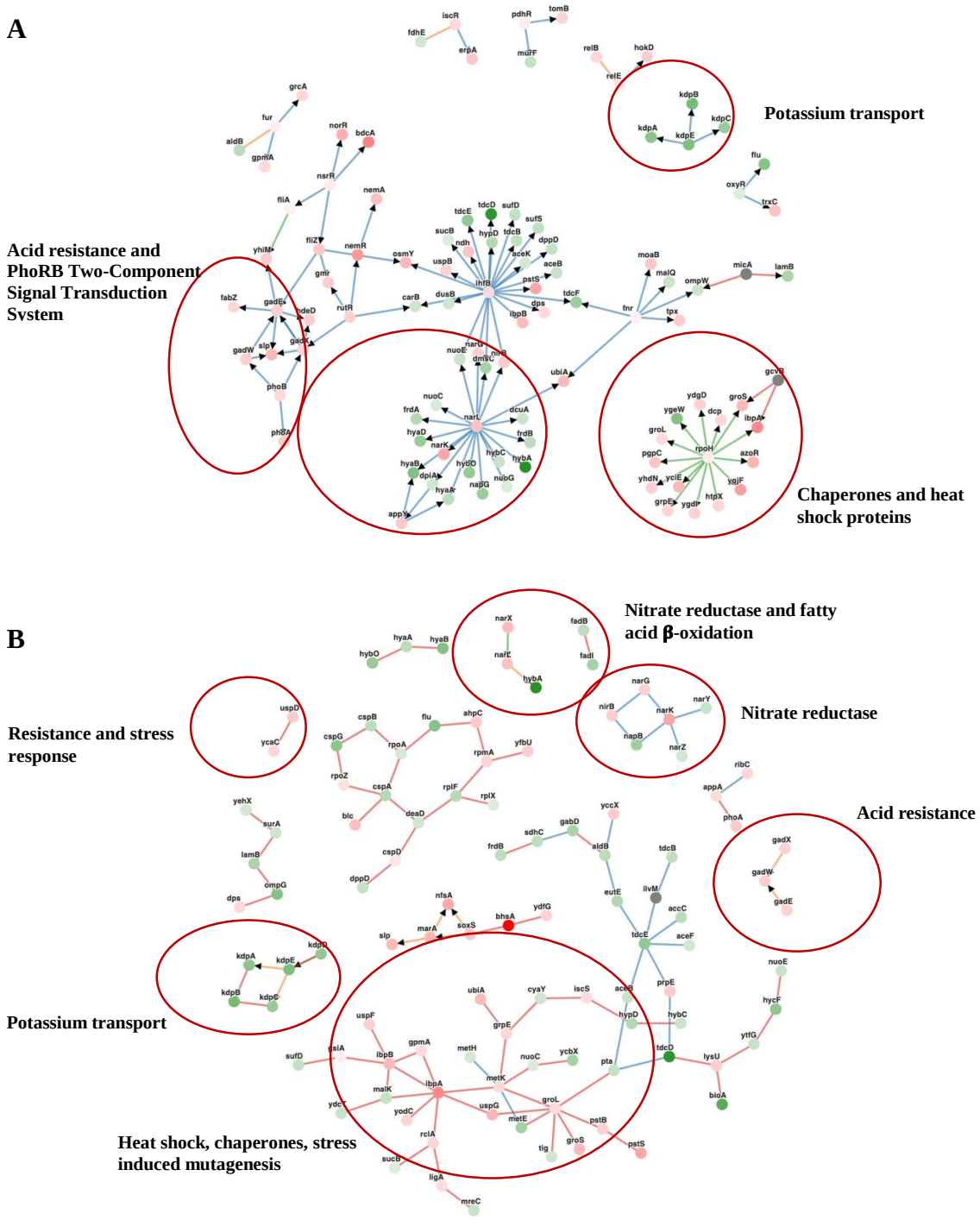

Figure 19. PheNetic network of transcriptional regulation of differentially expressed genes of *E. coli* BAA-196 and *S. aureus* ATCC BAA-39 treated with KS51, during the log phase, grouped by functional or regulatory interactions between genes using upstream (A) which identifies the regulatory mechanisms that induced the observed differential expression and downstream (B) which identifies activated pathways in response to the treatments. Upregulated genes are depicted by pink/red nodes and downregulated genes by green nodes (vertices). The colour intensity indicates the level of regulation. Green edges show activation relations, blue edges show activities of inhibition relations. Direct regulations by transcriptional regulators are indicated by arrowheads. The genes are grouped regulons that are controlled by transcriptional regulators including; *fnr*, *micA*, *fur*, *nsrR*, *nemR*, *gadEWX*, *phoB*, *appY*, *narL*, *ihfB*, *rpoH*, *gcvB*, *oxyR*, *kdpE*, *relE* and *pdhR*.

2.3.4 Gene Ontology and Pathway Analysis

Biological information was evaluated and interpreted from the filtered gene lists, from *E. coli* and *S. aureus* treated with all three treatments, by searching for gene ontology (GO) biological process terms, that were significantly over-expressed in the data. The results are shown in (Fig. 20) for *E. coli* and (Fig. 21) for *S. aureus*. All treatments were found to affect several proteins involved in biosynthesis, metabolism, regulation, cellular respiration, detoxification, cellular and metabolic processes, transport, signalling and stress. To investigate the regulatory pathways altered by KS25, KS33 and KS51, Pathway Tools using the smart tables feature was used, illustrated in (Table 8) for *E. coli* and (Table 9) for *S. aureus*.

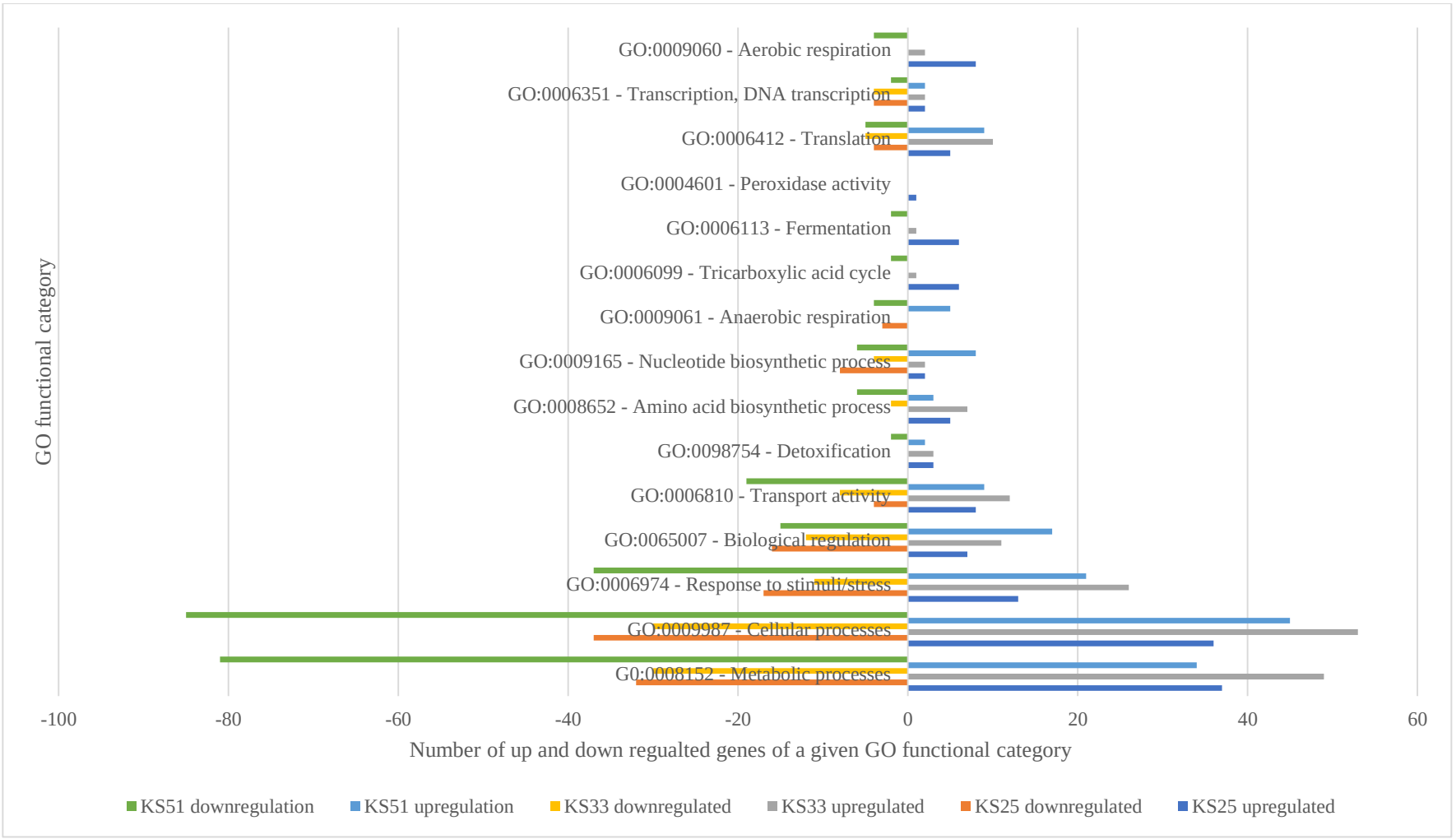

Figure 20. GO functional categories of genes upregulated and downregulated, from RNA-seq, organized based on GO biological, metabolic and cellular process terms, during the lag and log phase (≥2 Log_2FC, p-value 0.05) in *E. coli* strain ATCC BAA-196 in response to KS25, KS33 and KS51. The number of genes for each functional category are listed. The x-axis represents the number of genes. Positive values indicate upregulation of genes and negative values indicate downregulation of genes.

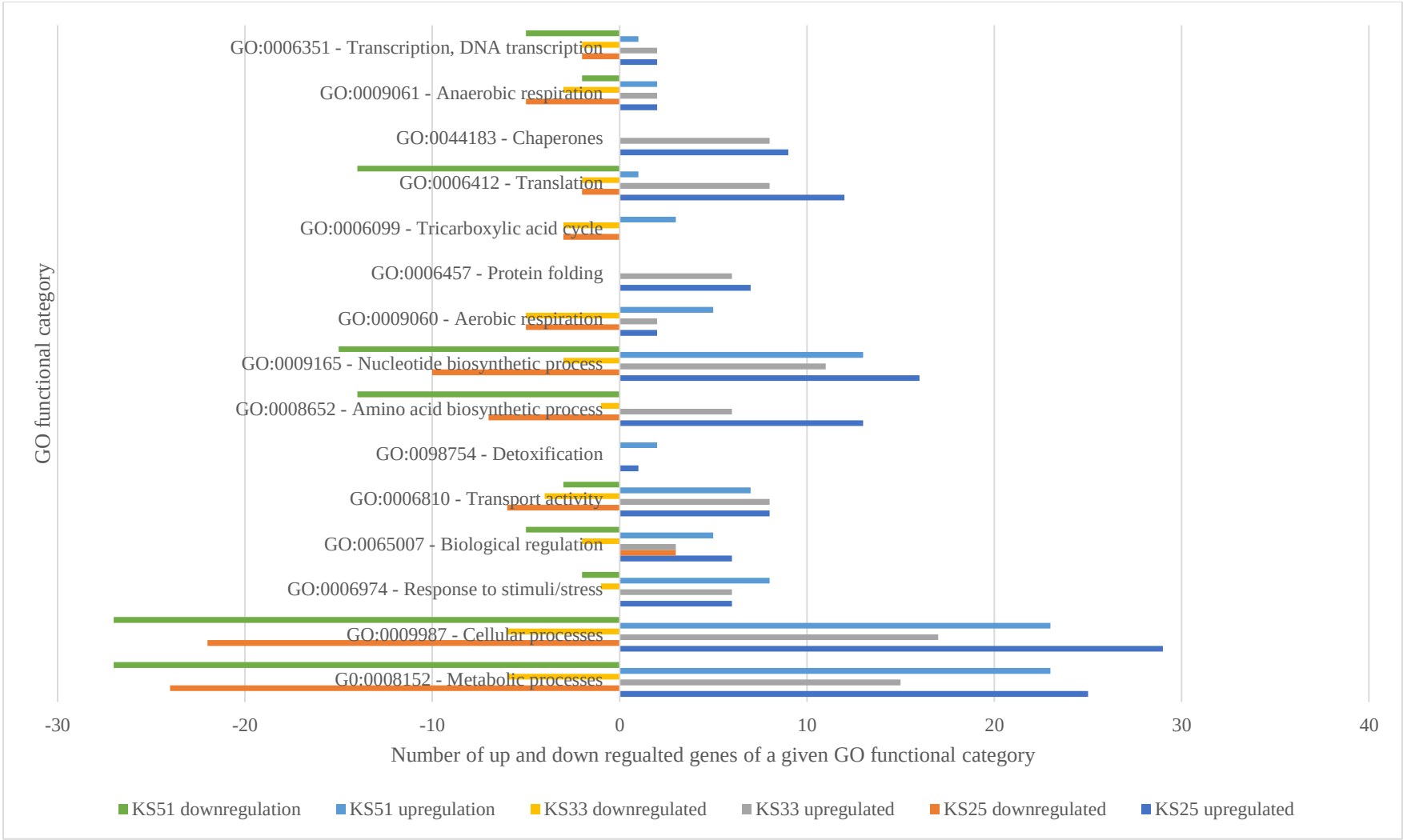

Figure 21. GO functional categories of genes upregulated and downregulated, from RNA-seq, organized based on GO biological, metabolic and cellular process terms, during the lag and log phase (≥2 Log_2FC, p-value 0.05) in *S. aureus* strain ATCC BAA-39 in response to KS25, KS33 and KS51. The number of genes for each functional category are listed. The x-axis represents the number of genes. Positive values indicate upregulation of genes and negative values indicate downregulation of genes.

Table 8. Pathways and biological processes of genes expressed during the lag and log phase (≥2 Log_2FC, p-value 0.05) in *E. coli* strain ATCC BAA-196 in response to KS25, KS33 and KS51.

	KS25		KS33		KS51	
Pathways/ Biological processes	Upregulated genes	Downregulated genes	Upregulated genes	Downregulated genes	Upregulated genes	Downregulated genes
Protein biosynthesis						
RNA maturation/processing		X			X	
tRNA charging	X				X	
Ribosomal proteins/assembly	X	X	X	X	X	X
Methyltransferase activity	X		X			
tRNA modification/processing					X	X
Protein folding and maturation						
tRNA modification			X		X	X
Translation initiation/activation		X		X		
Transcription elongation					X	
Translation termination/inhibition						
Transcription antitermination					X	
Transcription termination					X	
tRNA-dihydrouridine synthase		X				
Trans-translation mechanisms		X				
tRNA-uridine 2-thiolation selenation	X		X	X		
Amino acid biosynthesis/Degradation						
L-tyrosine biosynthesis						
L-asparagine biosynthesis	X			X	X	X
L-tryptophan biosynthesis	X		X			X
L-glutamine biosynthesis	X		X		X	X
L-methionine biosynthesis				X	X	X
L-threonine degradation		X	X	X		X
L-glutamate degradation		X			X	X
L-arginine degradation						X
L-lysine degradation						X
Aminopropylcadaverine biosynthesis						X
L-tryptophan degradation				X		X
L-glutamate biosynthesis	X		X			
Modulation of ribosome activity				X		
L-aspartate degradation	X	X	X			
L-alanine biosynthesis	X					
L-serine degradation		X		X		
L-glutamine degradation			X			X
L-arginine biosynthesis			X			X

Amino acid degradation			X				
L-leucine biosynthesis					X		
L-cysteine degradation					X		
Amino acid salvage							X
L-lysine degradation							X
Cofactor, secondary metabolite							
Molybdenum cofactor biosynthesis			X	X			
Iron-sulfur clusters/Iron uptake	X			X		X	
Riboflavin biosynthesis							
Protoporphyrin-IX biosynthesis						X	
Porphyrin-containing compound metabolism						X	
Ubiquinone and cofactor biosynthesis							
Thiamine diphosphate and cofactor biosynthesis						X	
Hydrogenase maturation pathway							X
Biotin and cofactor biosynthesis						X	X
Ethanolamine degradation							X
Cobalamin (vitamin 12) transport	X						
Transport of β-D-cellobiose + chitobiose			X				
Pyridoxal 5'-phosphate biosynthesis cofactor (Vitamin B6)				X			
Transport of iron(III)-enterobactin complex						X	
Methylerythritol phosphate pathway						X	
Fatty acid, lipids, membranes and Peptidoglycan biosynthesis			X				X
Murein precursor, activator and maturation			X		X	X	X
Membrane biogenesis/maintenance			X				
Fatty acid biosynthesis						X	X
Fatty acid beta-oxidation/degradation			X		X		X
Phosphatidylglycerol biosynthesis							X
Phospholipid biosynthesis			X				
Cell wall/peptidoglycan biosynthesis			X		X	X	
DNA and nucleotide biosynthesis							
Cytochrome c biogenesis	X					X	
Pyrimidine and purine biosynthesis/ metabolism	X			X			
Pyrimidine salvage pathway	X			X			
Purine salvage and metabolism			X	X		X	X
Replication and cell division	X		X			X	X
de novo UMP biosynthesis	X		X	X			X
5-aminoimidazole ribonucleotide				X			
Cell division inhibitor	X						
UMP biosynthesis l	X			X			
Guanosine nucleotide biosynthesis				X			
4-aminobenzoate biosynthesis I (folate synthesis)				X			

Purine catabolic pathway						X
Response to stimuli and repair						
General stress	X	X	X	X	X	
Recovery from glucose phosphate stress		X		X	X	
Cold/Heat/phage shock/peroxidase		X	X		X	X
Methylglyoxal degradation lll	X		X		X	
Copper/zinc/lead/mercury transport	X	X	X		X	
Acidity/ acid tolerance			X	X	X	
General/DNA repair/SOS			X	X		X
Phage degradation						X
Thiol-oxidative stress	X				X	
Glycine betaine transport	X					
Toxin-antitoxin systems		X				X
Two-Component Signal Transduction System		X				
Detoxification of toxic formaldehyde			X			
Carbon starvation induced regulation			X			X
Ubiquinone biosynthesis					X	
Energy and Cellular respiration						
Glyoxylate cycle bypass, and glycolate dehydrogenase activity	X		X			
Glycolysis						X
Gluconeogenesis	X		X			X
Carbohydrate/ pyruvate metabolism		X			X	X
Pentose phosphate pathway						X
Carbohydrate degradation		X		X		X
ATP biosynthesis	X					
Entner-doudoroff pathway catabolism			X			
Glycogen biosynthesis pathway						X
CMP-3-deoxy-D-manno-octulosonate biosynthesis						X
Formate-independent degradation						X
Acetate and pyruvate metabolism						X
Propionate metabolism: 2-methylcitrate cycle I					X	
Anaerobic-associated processes						X
Nitrate reduction pathway					*X*	X
Nitrogen metabolism					*X*	
Threonine degradation						X
C4-dicarboxylate transporter						X
Anaerobic metabolism						X
Anaerobic respiration/ Mixed Fermentation		*X*				X
Propionate metabolism					*X*	
Isoprenoid biosynthesis					*X*	X

Aerobic-associated processes						X
The citric acid cycle (TCA)	X		X			X
Oxidative phosphorylation	X		X			
Cytochrome bo oxidase electron transfer						X
Sulfur metabolism	X		X			
Sulfur degradation				X		
Resistance-associated genes						
Antimicrobial/multi-drug resistance		X	X	X	X	X
Efflux pump/transporter	X		X		X	X
Inner/outer membrane proteins	X	X	X	X	X	X
Toxin/Antitoxin		X	X		X	
Plasmid/Transposase						X
Degradation of toxins	X		X			
Detoxification of alcohols and aldehydes						X
Virulence-associated genes						
Biofilm formation	X	X	X	X	X	X
Motility		X				
Virulent toxins	X		X	X		
Plasmids/Transposase						X
Adhesion		X				
Transport						
Formate transporter						X
Phosphate transporter/uptake			X		X	
MFS superfamily transporter					X	
Carbohydrate/Sugar transport system		X		X		X
Nitrate/Nitrite transporter					X	
Zinc uptake						
Hexose phosphate transporter						X
L-cysteine sodium transporter					X	
Potassium transport						X
Glutamate and aspartate transporter			X			X
Cobalamin (vitamin B12) transporter	X					
Nucleoside transporter		X	X			
Periplasmic and amino acid transport		X			X	
ABC organic solvent transporter			X			
Outer membrane transport mediation				X		
Autoinducers and quorum sensing		X		X		X
Signalling/sensory proteins					X	
Transcriptional regulators	X	X	X	X	X	X
Transcriptional activators		X	X	X		
Transcriptional repressor		X	X	X	X	

Table 9. Pathways and biological processes of genes expressed during the lag and log phase (≥2 Log_2FC, p-value 0.05) in *S. aureus* strain ATCC BAA-39 in response to KS25, KS33 and KS51.

	KS25		KS33		KS51	
Pathways/ Biological processes	Upregulated genes	Downregulated genes	Upregulated genes	Downregulated genes	Upregulated genes	Downregulated genes
Protein biosynthesis						
RNA synthesis/maturation	X					X
Aminoacyl-tRNA synthetases	X	X	X	X		
Ribosomal protein/maturation	X	X			X	X
Transcription		X				X
mRNA/ tRNA processing/binding	X	X				
Protein catabolism	X		X			
Transcription termination						
Translation termination/inhibition		X				X
Aminotransferase	X					
tRNA Methyltransferase	X					
tRNA wobble base modification						
Amino acid biosynthesis/Degradation						
Amino acid catabolism/degradation	X	X				
L-lysine biosynthesis				X		
L-arginine biosynthesis	X		X			X
L-glutamate biosynthesis	X	X	X			X
L-threonine degradation	X	X				
L-glycine biosynthesis	X	X				
Glycine degradation	X		X		X	
Amino transferases	X		X			
Isoleucine biosynthesis	X		X			
Valine biosynthesis	X		X			
Threonine synthesis						X
L-leucine biosynthesis	X		X			
Amino acid-proton transporter		X		X		
L-serine, glycine, threonine metabolism		X				
Valine, leucine, isoleucine degradation	X			X		X
L-glutamine synthesis		X				
Protein synthesis inhibition		X				
L-alanine catabolism		X				
L-Histidine biosynthesis	X		X	X		
Histidine catabolism		X			X	
Arginine and proline metabolism						X
Serine/glutamate/threonine degradation		X				

Amino acid salvage	X					
L-cysteine biosynthesis	X					
L-glycine biosynthesis	X		X			
L-methionine biosynthesis	X					
Fatty acid, lipids, membranes and Peptidoglycan biosynthesis						
Peptidoglycan hydrolyses						X
Lipoteichoic acid biosynthesis					X	
Aerobic fatty acid beta oxidation		X			X	
Fatty acid biosynthesis						
Cell wall/Peptidoglycan biosynthesis		X				X
Lipid catabolic process		X			X	
DNA and nucleotide biosynthesis						
Pyrimidine and purine biosynthesis		X		X	X	X
Pyrimidine nucleobases salvage		X				
Purine salvage/metabolism						X
Guanosine nucleotide de novo biosynthesis		X			X	
Folate biosynthesis	X		X			
Uptake of purine bases						
DNA/Nucleic acid binding	X					X
Nucleotide-sugar biosynthesis		X				X
Cell division and DNA replication	X	X		X		X
Adenosine ribonucleotides de novo biosynthesis					X	X
5-aminoimidazole ribonucleotide biosynthesis I					X	X
Inosine-5'-phosphate biosynthesis I					X	X
UMP biosynthesis					X	
Response to stimuli and repair						
General stress	X		X		X	X
Cold/Heat shock/ Chaperones	X		X		X	X
Oxidative stress caused by reactive oxygen species	X	X		X	X	
Copper/zinc ion transport/homeostasis	X		X			
Cadmium ion transport	X		X			
Zinc ion or cobalt transport/homeostasis	X		X		X	
Alkaline shock protein/tolerance		X	X	X		
Chaperone/Protein folding	X		X			
General/DNA repair	X	X	X	X		X
DNA Protection during starvation	X		X		X	
Defence against phagocytosis	X		X			
Immunogenic protein	X					

Defence against neutrophil killing						X
Plasmid	X					
Protection against thiol-specific stress	X					
Phosphate starvation	X					
Thioredoxin pathway			X			
Energy and cellular respiration						
Glyoxylate cycle		X				
Fructose and mannose metabolism	X		X			
Pyruvate generation		X				
D-gluconate degradation		X				X
Pentose phosphate pathway					X	
Sugar/carbohydrate metabolism	X	X				X
Nitrate reduction/nitrogen metabolism		X				
Gluconeogenesis	X	X	X		X	X
Methylglyoxal degradation					X	
Glycolysis	X				X	X
Electron transport chain						X
Trehalose degradation						X
Acetate and pyruvate metabolism	X		X		X	
Embden-Meyerhof-Parnas	X		X			
Anaerobic-associated processes						
Nitro-reductase family proteins		X	X			X
Mixed fermentation	X		X		X	X
NADH dehydrogenases						X
Aerobic-associated processes						
The citric acid cycle (TCA)	X	X	X	X	X	
Glycerol uptake/degradation		X	X		X	X
Cytochrome bo oxidase electron transfer	X					X
NADH dehydrogenases						X
Sulfur transport/metabolism	X					
Degradation of aromatic compounds					X	
Resistance-associated genes						
Antimicrobial resistance	X		X	X	X	
Efflux pump/transporter	X					
Copper, zinc efflux	X		X		X	
Acid resistance/tolerance						X
Carotenoid biosynthesis		X		X		X
Cadmium stress proteins	X		X			
Virulence-associated genes						
Biofilm formation	X		X		X	
IgG-binding protein	X		X		X	
Invasion	X		X		X	

Adhesion	X	X			X	X
Surface colonization	X		X		X	
Secreted proteins/toxins	X		X		X	X
Autolysis	X	X				
Transport						
L-cysteine transport	X		X			
Sodium transporter	X		X			
Sugar/carbohydrate transport system	X	X	X	X		X
Methionine transport	X		X			
Histidine permease ABC transporter	X		X			
Glutamine transport	X		X			
Maltodextrin ABC transporter				X		
Uracil symporter				X		
D-serine/D-alanine/glycine transporter		X				
Manganese ABC transporter	X	X				X
Oligopeptide/Choline ABC transporter	X	X	X	X	X	X
Nucleotide transporter						X
Nitrate ABC transporter		X				
Glutamate symporter		X				
Amino acid transporter	X					X
Zinc ion transporter	X		X		X	
Potassium transport					X	
Translocase pathway						X
L-lysine transporter						X
ABC transporter	X		X			X
Thiamine ABC transporter		X			X	
Spermidine/putrescine transporter				X	X	
L-lactate transmembrane transporter						X
Gluconate transporter						X
Secondary metabolites and co-factors						
Dephospho-CoA kinase	X					
Thiamine biosynthesis		X			X	
Molybdenum cofactor	X				X	X
Tetrahydrofolate and cofactor biosynthesis (vitamin B6)	X					
Shikimate pathway		X				
Thiamine salvage pathway		X				
Pyridoxine biosynthesis (vitamin B6)	X					
Iron clusters assembly/storage/uptake		X	X			
Signalling proteins		X		X	X	
Transcriptional regulators	X		X		X	
Transcriptional repressor	X		X			X

- Lag and log refer to the lag and log growth phases in both Table 8 and 9. The X sign represents the biological processes or pathways that were affected in response to the respective treatment. The complete list of the up- and downregulated genes can be found in Table S3 in the supplemental material, with their respective log2 fold change in Table S1 and S2.

2.3 Discussion

Exposure of nanomolecular complexes induced the upregulation of genes involved in heavy metal transport and efflux systems in *E. coli* and *S. aureus* in response to KS25,33 and 51

Several genes involved in copper, lead, cadmium, zinc and mercury homeostasis were upregulated in response to all treatments in *E. coli*, including; *copA* except in treatment KS51 during the log growth phase, *yobA* in the KS25 treatment, *cueO* in all treatments except for treatment KS51 in both phases and *zupT* in the KS51 treatment. In *S. aureus copA* and *cadABC* were upregulated in all treatments except in the KS51 treatment. Additionally, Zn(II) and Co(II) transmembrane diffusion facilitator *zitB*, zinc transport system *zntA* and *czrA* were upregulated in treatments; KS25 during the lag growth phase, KS33 during the log growth phase and KS51 during the lag growth phase with potassium transport and uptake *kdpBC* upregulated in treatment KS51, whereas downregulated in *E. coli* treatment KS51 regulated by transcriptional activator *kdpE*, as illustrated in (Fig. 19). Manganese transporter genes *sitAB* were downregulated in both KS25 and KS51 treatments, with *mntH* upregulated in KS25 in *S. aureus*. Tellurium resistance cAMP binding protein *terE* was found to be upregulated in *E. coli* treated with KS51, during the log growth phase. Detoxification genes *ahpCF*, *katE* and *yhcN* were found to be induced in *S. aureus* treated with KS51. Trace metal ions play an essential role in many reactions in bacteria. Some metal ions, in excess, can however be toxic to the cell through the generation of ROS via the Fenton reaction ($Fe^{2+}+H_2O_2 \rightarrow Fe^{3+}+\bullet OH+{}^{-}OH$), causing oxidative stress, often controlled by *soxSR*. For this reason, bacteria respond to metal ion excess by inducing the expression of specific genes involved in either detoxification or metal ion uptake and transport to either enhance survival or efflux systems, typically controlled by metal-sensing transcription factors to promote resistance while maintaining adequate levels necessary for growth.

Copper homeostasis is primarily maintained by Cu(I)-translocating P-type ATPase *copA*, which is responsible for copper resistance by removing excess Cu(I) from the cytoplasm in *E. coli* and *S. aureus* (Bondarczuk *et al*., 2013) and multi-copper oxidase *cueO* which appears to be involved in copper tolerance under aerobic conditions (Djoko *et al*., 2010). Out of all the genes, the highest regulation in both model microorganisms observed was copper efflux and detoxification gene *copA* in treatment KS25 and KS33, in both model strains. The upregulation of Cu(I)-translocating P-type ATPase *copA* and *cueO* may indicate excessive copper.

Excessive copper and cadmium are extremely toxic due to their ability to easily interact with free radicals that cause oxidative damage (Chudobova *et al*., 2015). Furthermore, copper has been linked to the degradation of Fe–S clusters by the displacement of iron, subsequently inducing the Fenton reaction, causing oxidative damage (Macomber and Imlay, 2009).

Zinc homeostasis is maintained by *zitB*, plasmid encoded *cadCA* transporter and chromosomally encoded *czrA* transporter, regulated by *zur,* that bind to Zn/Zn^{2+} and decreases affinity to their relative promoter when in excess. In excess, zinc has been reported to block an essential pathway that causes starvation in the bacteria (University of Adelaide, 2013). Zinc transporters have also shown to be involved in biofilm formation in *S. aureus* and increased fitness in the host cell (Conrady *et al*.,2008). Additionally, zinc has been shown to be involved in the synthesis of antioxidant enzymes thus reducing oxidative stress (Olechnowics *et al*., 2018). Like zinc, manganese is a cofactor in bacteria that has also been shown to contribute to virulency in *S. aureus* and act as an antioxidant (Coady *et al*., 2015). Potassium ion homeostasis is maintained by kdp high-affinity transporter, and is induced when there is very low external potassium concentration in *E. coli* (Epstein, 2003). Furthermore, the activation of a potassium transporter in *S. aureus* has been shown to contribute to its virulency (Gründling, 2013).

A proposed hypothesis for the overall metal ion efflux, uptake and transport upregulation may be that the primary target of the iodine ions from the iodine-containing nanomolecular complexes were the cell wall and membrane, leading to an increase in the penetrability within the bacterial cell wall and membrane. Iodine ions have been shown to decomposes and disturb the cell wall structures through oxidation thus increasing the permeability of affected cells to surrounding metal ions and other toxins from the surrounding environment. The increased penetrability may have resulted in an influx of metal ions from the extracellular environment. The penetrability was further enhanced due to the attraction potential between cations and negatively charged barriers of the bacterial cell. Teichoic acids in *S. aureus* and lipopolysaccharides in *E. coli* attract cations such as copper, zinc and cadmium (Marquis *et al*,. 1976). Furthermore, *S. aureus* may have induced detoxifying proteins *ahpCF, katE* and *yhcN* and uptake and transport systems of potassium and manganese in efforts to help the bacterium cope with stress and increase survival by possibly forming biofilms, after exposure to all treatments.

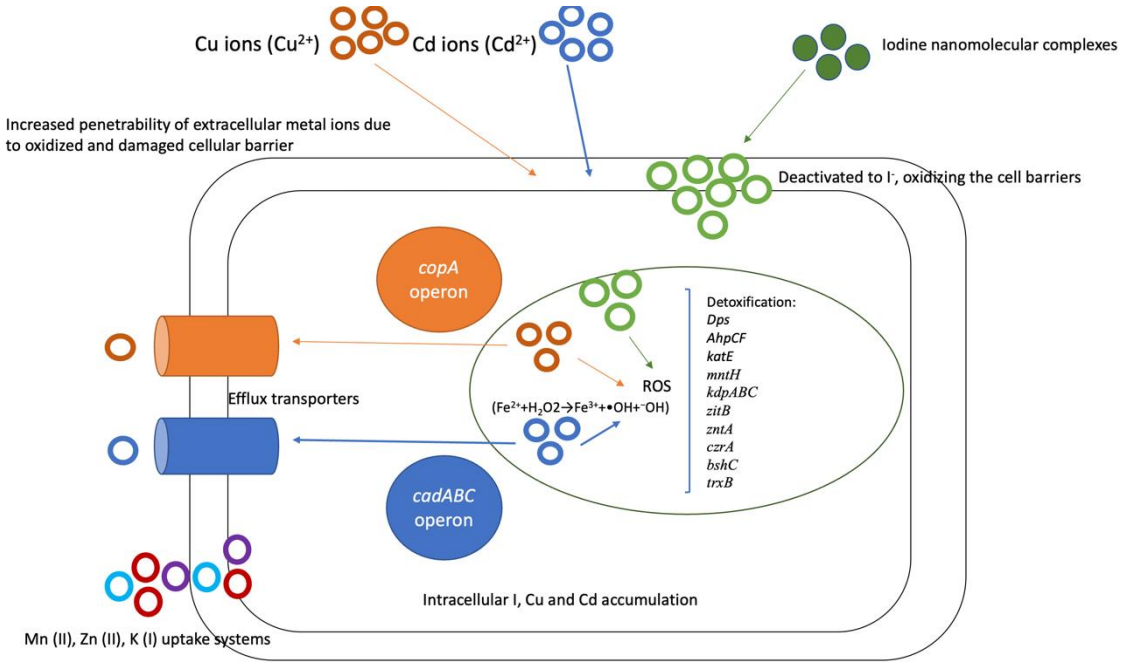

Figure 22. Schematic drawing of iodine, copper and cadmium ion uptake from the nanomolecular complexes and environment into bacterial cytoplasm. The Foldchange regulation of *Dps* are highlighted for KS25, KS33 and KS51, respectively and *AhpCF* for KS51.

Exposure to nanomolecular complexes induced pathways governing DNA protection and repair and general oxidative stress KS25, KS33 and KS51

The chromosomal DNA of bacteria is constantly exposed and prone to DNA damage and repair. During normal growth conditions, genes involved in SOS response are expressed at basal level and only increase distinctly upon DNA damage. Various endogenous and exogenous factors like oxidative compounds, antibiotics and chemicals trigger the SOS response system in bacteria, which then facilitates pathways governing DNA repair, protection, and mutagenesis (Žgur-Bertok *et al*., 2013). In *E. coli* and *S. aureus*, the first featured genes to detect, verify and excise damaged DNA are *uvr* genes, responsible for the excision of damaged DNA/nucleotides. Nucleotide excision repair protein, with *uvrB/uvrC* motif were found to be upregulated in *S. aureus* treated with KS25 and KS33 in both phases, however downregulated in KS51. Additionally, error-prone repair DNA polymerase IV *dinB*, controlled by sigma *rpoS* was upregulated in treatment KS25, in *S. aureus*. It was further observed that nucleotide excision repair protein, with *uvrD* motif was upregulated in the lag phase, as illustrated in (Fig 18). Excinuclease ABC subunit C *uvrC* was additionally found to be downregulated in *E. coli* treated with KS51, during the lag growth phase and not activated in the other treatments. During the process of *uvrABC* excision of damaged DNA, the *uvrAB* complex moves along

DNA, looking for possible damage. When DNA damage is found, the complex stops on the site, bends the DNA and releases itself, for *uvrC*, to attach (see Figure 23). Two proteins may also be involved in the initial steps of the repair pathway: *lexA*, a repressor gene and *recA*, a gene activator. During normal growth conditions, *lexA* binds to the promoter region of several SOS genes thus inhibiting their expression levels (Žgur-Bertok *et al*.,2013). Upon DNA damage, *recA* is induced by binding to single-stranded DNA (ssDNA), facilitating the self-cleavage reaction of *lexA* and decreasing its expression levels (Žgur-Bertok *et al*.,2013). *RecA* and *yeeS* are involved in recombinational repair in *E. coli* and *S. aureus*. Both *recAQ* and *lexA* were, however, found to be downregulated in *S. aureus* in treatment KS51 during the log growth phase and not affected in other treatments including *E. coli*. Additionally, DNA repair, crossover junction endodeoxyribonuclease *ruvC* was found to be upregulated in KS33 during the log growth phase in *E. coli*, which in addition, is involved in the late step of *RecE* and *RecF* recombinational repair pathway (Iwasaki *et al*., 1991).

Several genes involved in general stress response were highly upregulated after exposure to the nanomolecular complexes. Universal stress proteins (Usp) were induced in both *E. coli* and *S. aureus*, treatment KS51. In *S. aureus*, defence against phagocytosis protein *hlgB* was upregulated in treatment KS25 and KS33. In *E. coli* exposed to KS25, multiple stress resistance protein *yqhD* was upregulated during the log growth phase. In *E. coli* exposed to KS33, *yqhD* was upregulated in the lag growth phase, acid tolerance protein *frc* and multiple stress resistance protein *ycfR* were upregulated during the log phase. In *E. coli* exposed to KS51 multiple stress response proteins *yciF, ycfR, uspG* and *osmY* were upregulated in the log growth phase. Detoxifying and DNA protection genes were activated in certain treatments including; FMN-dependent NADH-azoreductase *azoR* in treatment KS25 and KS51 in *E. coli* and KS25 in *S. aureus*. In *S. aureus*, *ahpCF*, *katE* and *yhcN* in KS51 during the log growth phase, *dps* in all treatments, *bshC* in treatment KS25 and *trxB* in treatment KS33 during the log growth phase were induced in efforts to protect the cell against oxidative stress by detoxifying sub-lethal ROS generated by alkyl hydroperoxides and hydrogen peroxide.

The overall SOS and stress regulation may suggest that the multiple stress response proteins induced in *E. coli*, in all treatments, most likely, protected the cell against heat, shock and oxidative stress, thus protecting the bacterial cell from DNA damage. In *S. aureus* however, DNA excision proteins and error-prone repair DNA polymerase IV were activated in KS25 and KS33. This regulation in *S. aureus* thus, may suggest that treatment KS25 and KS33

succumbed to DNA damage, most likely, caused by oxidative damage. ROS attack the base and sugar moieties producing single and double breaks in the backbone, potentially blocking DNA replication. Error-prone repair DNA polymerase IV is induced only when there is extensive, persistent DNA damage (Henrikus *et al*., 2018), this may however have allowed for DNA replication across persistent DNA lesions that block DNA polymerase III, thus promoting elevated mutation rate, continuous replication and cell survival (Courcelle *et al*., 2001; Henrikus *et al*., 2018). In addition, on the account of the upregulation of genes involved in the protection against alkyl hydroperoxides, hydrogen peroxide and other oxidants in *S. aureus* treated with KS51, iodide atoms may have induced the generation of reactive oxygen species (ROS) like H_2O_2, through the Fenton reaction, activating oxidative stress and thus inducing the stress and detoxifying proteins to protect the *S. aureus* strain treated with KS51 from significant biological damage. Furthermore, glucosaminyl-malate:cysteine ligase *bshC* is involved in producing antioxidant glutathione and thioredoxin reductase *trxB*, both of which, neutralizes or reduces thiols/oxidants and thus reduces oxidative stress.

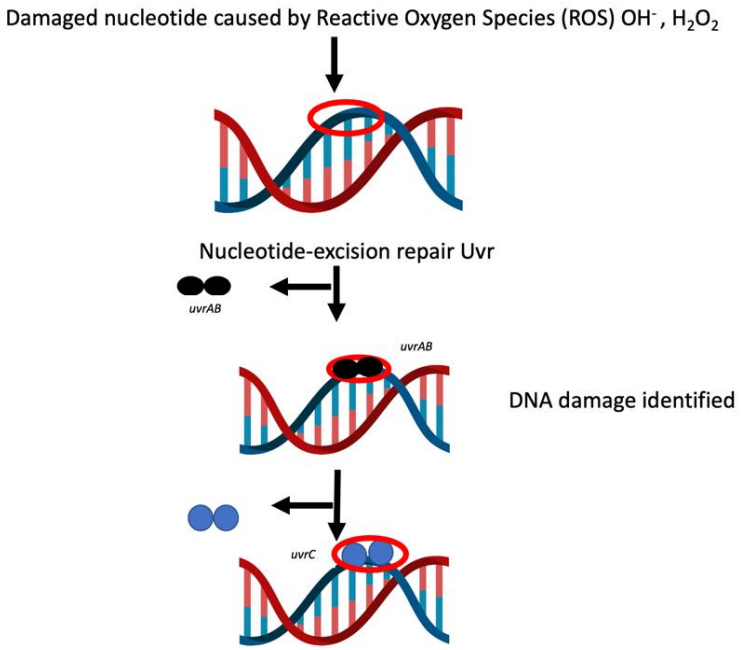

Figure 23. Schematic representation of nucleotide excision repair in response to DNA damage caused by ROS in *S. aureus*.

Exposure of nanomolecular complexes induced the upregulation of chaperones, proteases that stabilize, heat shock, protein folding and amino acid degradation genes in treatment KS25 and KS33 during both growth phases in *S. aureus* and in KS51 treatment in *E. coli*, indicating possible protein damage

Exposure of *S. aureus* to the nanomolecular complex KS25 and KS33 induced the upregulation of cochaperonins; heat shock proteins *groLS*, HSP70 systems; *dnaJK*, *grpE* and HSP100; *clpBCPX* and *hslO, hrcA* in both growth phases. Cochaperonins heat shock proteins *groS* and *ibpAB* also appeared to be upregulated in *E. coli*, treatment KS51 during the log growth phase. Furthermore, treatment KS51 induced universal stress proteins (Usp) in both *E. coli* and *S. aureus*. Chaperone proteins are abundant in *E. coli* and *S. aureus*. They are often induced and undergo changes in levels of expression in response to environmental changes (temperature, salinity, pH, exposure to reactive oxygen species and metal ions/extreme stress) in efforts to either refold misfolded proteins, prevent aggregation or remove aggregated denatured proteins. The activation of these chaperones have been previously reported to be an early response to stress, followed by other protective adaptations like metal transport proteins, efflux system and biofilm formation (Pereira *et al*., 2020). Chaperones and heat shock proteins are often positively regulated by a rapid increase in cytosolic concentration of the σ32 subunit of RNA polymerase from the *rpoH* gene. Therefore, σ32 levels are controlled by chaperones and heat shock proteins (Lund *et al*., 2001). Exposure of proteins to ROS causing oxidative stress can lead to carbonylated proteins and the disruption of protein interactions, leading to loss of secondary and tertiary structure (denaturation) and eventually protein unfolding, misfolded proteins, and loss of function (Schramm *et al*., 2020). When there is an accumulation of denatured, unfolded and misfolded proteins, they can interact with one another and co-aggregate, leading to protein aggregation (Schramm *et al*., 2020). Denatured proteins are prone to undergo protein aggregation due to their exposed hydrophobic groups. Induced chaperonins therefore, function in folding proteins and preventing aggregation. HSP70 assists in protein folding and unfolding, regulating heat shock response and targeting certain substrates for degradation and HSP100 is involved in unfolding, proteolysis and thermotolerance (Saibil, 2013).

The transcriptional analysis indicated that, after the exposure of *E. coli* to iodine ions from KS51 and *S. aureus* from KS25 and KS33, heat shock proteins *groLS* and *ibpAB* were induced and worked together to possibly refold, stabilize or disaggregate the aggregated and repair misfolded damaged proteins. Furthermore, if the denatured proteins have accumulated to the

point that they have overburdened heat shock protein mechanisms, then *clpB* and *dnaK* disintegrate or breakdown the damaged or denatured proteins, as illustrated in (Fig. 20). The regulation of genes involved in disintegration and proteolysis may suggest that some proteins within the cell were carbonylated, such as L-threonine, which may have lead to the upregulation of *tcyA* in *S. aureus*, treated with KS25, which is involved in L-threonine degradation. Several studies have indicated that carbonylated proteins are more prone to degradation than their non-oxidized counterparts (Maisonneuve *et al*., 2008). Additionally, genes involved in amino acid degradation were induced in *E. coli* in treatment KS51 and *S. aureus* treated with KS25 and KS33. As discussed, protein unfolding due to oxidative damage often exposes amino acid structures, leading to the interaction with other similar unfolded amino acids, subsequently forming non-functional proteins. The faulty or non-functional proteins are then recognized and degraded, eliminating the chances of mistakes that may occur during protein synthesis. Furthermore, the upregulation of multiple stress proteins *uspAB* in *S. aureus* has been shown to be induced simultaneously with chaperones after being exposed to hydrogen peroxide in efforts to protect cells from protein damage (Siegele, 2005). In addition, the induction of cadmium stress/tolerance genes *cadABC* has been shown to be a common regulation with induced chaperones involved in the removal of denatured proteins. This is because Cd^{2+} from the surrounding environment, has a high affinity for sulfur-containing compounds in cell-like thiol groups of cysteine residues thus causing protein damage in sulfur-containing proteins (Helbig *et al*., 2008).

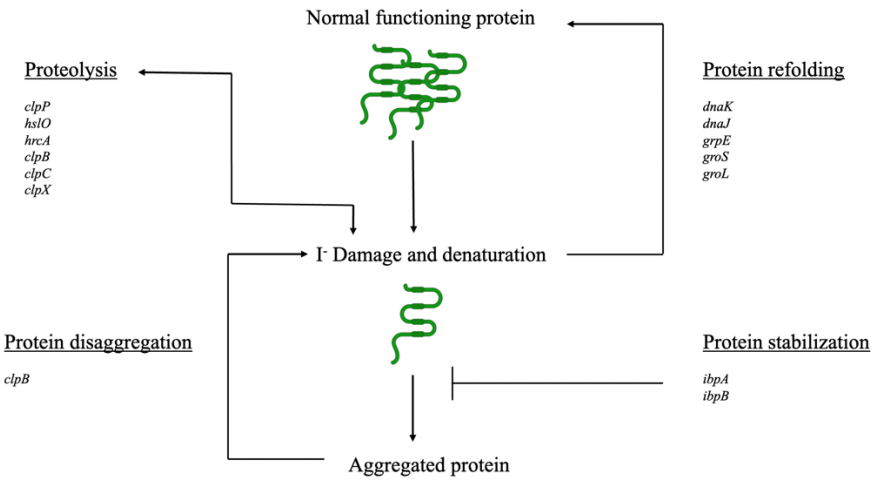

Figure 24. Schematic drawing of the iodide induced gene expression for inducing chaperones and removing denatured proteins.

Nanomolecular complexes KS25, KS33 and KS51 induced the upregulation of genes involved in Fe-S clusters biosynthesis, iron uptake and sulfur metabolism in *E. coli* whilst thioredoxins (Trxs) and glutaredoxins (Grxs) systems were upregulated in *S. aureus* possibly indicating that I^- acts on proteins, causing protein damage

Iron-sulfur clusters (Fe-S) are cofactors that are made of iron and sulfur atoms, found and incorporated in proteins posttranslationally (Ayala-Castro *et al*., 2008). They are involved in several biological processes, including DNA replication and repair, electron transfer (respiration pathways), nucleotide and amino acid metabolism (Beinert *et al*., 1997; Xu and Møller, 2011). Well over 80 proteins containing Fe-S clusters have been identified in *E. coli* (Py and Barras, 2010). In treatment KS25, *E. coli* responded to the iodine ions and metail ions by upregulating Fe-S cluster assembly apparatus; cysteine desulfurase protein *iscS* during the log growth phase in KS25 and tRNA modifying, folate-Dependent protein *ygfZ* in KS51, during the lag growth phase. Cysteine desulfurase *iscS* is a [2Fe-2S] cluster that provides the sulfur in *de novo* Fe-S cluster biosynthesis (Schwartz *et al*., 2000). Folate-dependent protein *ygfZ* participates in the synthesis and repair of oxidatively damaged Fe-S clusters and replenishes damaged proteins (Walker *et al*., 2020). This regulation may indicate that the iodide ions and some of the metal ions induced ROS which targeted and altered proteins containing Fe-S clusters. In addition to this upregulation, iron uptake/transport proteins; enterobactin synthase component B *entB* and iron catecholate outer membrane transporter *fiu* were upregulated in KS25 and KS33, respectively, with TonB-ExbBD energy transducing system, subunit *exbB* upregulated in KS51, in both phases. Additionally, sulphate assimilation proteins *cysN*, *cysD* were also upregulated in *E. coli* in treatment KS33 during the lag phase. Enterobactin synthase enzymes are responsible for enterobactin biosynthesis in the cytosol, which are essentially iron-siderophores complexes. Iron-siderophores complexes are often synthesized in response to low levels of iron in which the TonB-ExbBD systems mediate the transport of the complexes (Noinaj *et al*., 2010).

This regulation may, further, indicated that iron uptake/transport proteins could be playing a role in acquiring the raw materials for Fe-S cluster biosynthesis and thus protein biosynthesis. Additionally, studies have been reported that histidines, methionines and cysteines are very sensitive to oxidation by ROS due to their high reaction susceptibility of their sulfur group (Zhang *et al.*,2013). The expression of the sulphate assimilation proteins may, also, be playing a role in converting inorganic sulphate to sulphide, providing raw materials for Fe-S cluster

biosynthesis and additionally incorporating sulfide into the carbon skeletons of sulfur-containing amino acids L-cysteine and L-methionine. Furthermore, glucosaminyl-malate:cysteine ligase *bshC* was upregulated in *S. aureus* in treatment KS25, during the log growth phase. Azoreductase *azoR* was upregulated in treatment KS25, KS51 in *E. coli* and KS25 in *S. aureus* and thioredoxin reductase *trxB* and *trxC* were upregulated in treatment KS33 during the log phase in *S. aureus* and KS51 in *E. coli*. Glucosaminyl-malate:cysteine ligase is involved in the first steps of bacillithol and glutathione biosynthesis (Gaballa *et al*., 2010). Thioredoxin reductase *trxBC* is an antioxidant that protects against oxidative stress and involved in renaturation of some unfolded proteins (Ding *et al*., 2005; Kern *et al*., 2003). Studies have reported that glutathione and bacillithol are involved in reducing oxidative stress caused by ROS and regulates thiol in *S. aureus* (Gaballa *et al*., 2010), subsequently, protecting proteins from oxidation (Ezraty *et al*., 2017) and FMN-dependent NADH-azoreductase *azoR* is involved in protecting against thiol stress, indicating possible protein damage and repair.

Exposure to nanomolecular complexes affected pathways governing deoxyribonucleotides, fatty acid and amino acid biosynthesis, transport and translation inhibition in *E. coli* and *S. aureus*

Fatty acid biosynthesis pathway in *E.coli* was generally activated in KS51 however inhibited in KS25 and KS33 during the lag phase. This included proteins responsible for the elongation of short-chain unsaturated acyl-ACP *fabAB*, which play a role in maintaining the hydrophobicity of phospholipids, thus, maintaining a protective membrane barrier (Cronan *et al*., 2009). Lipids are primary targets during oxidative stress because free radicals directly attack polyunsaturated fatty acids located in the membrane, initiating lipid peroxidation (Kashmiri and Mankar., 2014). Genes involved in cell wall/peptidoglycan and lipoteichoic acid biosynthesis, responsible for the protection against uptake of harmful molecules were however generally downregulated in KS25 and KS33 but upregulated in KS51 including; *mltD, ftsN* in *E. coli* during the lag phase and *dltBD* upregulated in KS51 *S. aureus*, during the both phase. Genes involved in nucleotide biosynthesis were generally activated in all treatments, controlled by DNA-binding transcriptional repressor *PurR*, as illustrated in (Fig. 14, 16, 17), however downregulated in *S. aureus*, in all treatments. Genes involved in the synthesis of amino acid biosynthesis were generally activated in all experiments except for treatment KS51 in *E. coli* and *S. aureus*, where these biosynthetic pathways were mostly inhibited. Some ribosomal proteins were downregulated in *E. coli* treated with KS25 and KS33 and *S. aureus* treated with KS51. Additionally, translation initiation gene *infA* and *yhbJ* were downregulated in *E. coli* in

treatment KS25 and KS33. Genes that code for the specific transport of amino acids were also generally upregulated in *S. aureus* treated with KS25 and KS33, including transport of methionine, cysteine, aspartate and glutamine associated genes *glnAPQ* regulated by transcription regulator *glnG* (see Fig. 16), carbamoyl-phosphate synthetase *carA*, regulated by transcriptional repressor *pepA* (see Fig. 16) and aspartate carbamoyltransferase *pyrBI*, required for the flux of glutamine for pyrimidine synthesis.

Amino acids and nucleotides play an important role in the growth, survival of bacteria, serve as energy donors for cellular processes and modulate protein/nucleotide homeostasis. The downregulation of nucleotide biosynthesis in *S. aureus* may be due to sub-lethal concentration of ROS possibly generated by free radicals affecting nucleotide synthesis and growth in the bacterial strain. A study by Buvelot *et al*., 2021 reported that the exposure of sub-lethal concentration H_2O_2 to *S. aureus*, downregulated genes involved in pyrimidine biosynthesis pathway and the downregulation was caused by a decrease in DNA replication, which affects growth. The downregulation of genes involved in translation (ribosomal proteins, translation initiation) in *E. coli* treated with KS25, KS33 and *S. aureus* could primarily be due to the oxidative inactivation or disruption of translation related macromolecules, decreasing their activity. Several macromolecules involved in translation in bacteria are specific targets of oxidation in *in vivo* and *in vitro* experiments, including; ribosomal proteins, aminoacyl-tRNA synthetases and protein factors involved in the initiation, elongation, and termination of translation, thus inhibiting translation (Katz and Orellana, 2012). Additionally, the oxidation of machinery involved in translation may increase the translation error rate thus increasing the susceptibility to ROS within the cell (Dukan *et al*., 2000).

Nanomolecular complexes KS25, KS33 and KS51 induced the upregulation of genes involved general resistance response and virulency

Stressful environments may often modulate bacterial resistance and virulence (Fang *et al*., 2016). A few genes belonging to antibiotic resistance, multidrug and metal ion efflux functional groups and resistance to infections were differentially expressed. DNA-binding transcriptional dual activator of multiple antibiotic resistance protein *marA* was found to be upregulated in KS51, during the log growth phase and *marB* in KS33, during the lag growth phase, in *E. coli*. In *S. aureus*, *marR* was upregulated in both KS25 and KS33, regulated by *soxS* (see Fig. 16 and 17). Methicillin resistant protein *mecA* and *fmtB1* were upregulated in KS51 and KS25, respectively in *S. aureus*. Several universal stress proteins were upregulated in treatment KS51

in both *E. coli* and *S. aureus* and outer membrane proteins *ompCF* were downregulated in *E. coli* in treatment KS25 and KS33, during the lag growth phase. Transposase for insertion sequence element IS5 *insH-3* was found to be transcriptionally silenced in *E. coli*, treatment KS51, during the log phase. As mentioned, several metal ion efflux and transport genes were upregulated in both model microorganisms. D-alanyl transfer proteins *dltBD* were found to be upregulated in *S. aureus* in both growth phases. Virulence-associated genes involved in biofilm, adhesion and toxicity were generally upregulated in *S. aureus* in all treatments including *mcsB, sbi, fnbAB, sraP, lysM, lysR, hlgAB, sarV* and kdp systems with some biofilm-associated genes upregulated and some downregulated in *E. coli*.

A proposed hypothesis for the upregulation of metal ion efflux like *copA* and uptake transport systems like *mntH* and kdp systems may be that the activation was a mechanism to resist oxidative damage and stress by removing excess metal ions from the cell *i.e.* metal resistance or detoxifying oxidants. Furthermore, cross resistance has become a major concern in hospitals and scientific research. Exposure to certain drugs, ions or biocides can induce the upregulation of antibiotic resistant or metal ion efflux pump genes that can potentially select for bacteria with high tolerance (Guo *et al*., 2021) and thus potentially select for bacteria with high tolerance against iodide ions. The expression of multidrug resistance proteins may also be induced by agents that cause oxidative stress in efforts to ameliorate the effects of the stress. The upregulation of *dltBD* was also observed in *S. aureus*. In some pathogens such as *S. aureus*, *dltBD* proteins which are involved in modifying teichoic acids, have been shown to reduce the net negative charge of cell envelopes and increase resistance (McBride and Sonenshein, 2011). Outer membrane porins *ompCF* were found to be upregulated in *E. coli* treated with KS25 and KS33. Porins are pore-like proteins positioned in the outer membrane of Gram-negative bacteria, responsible for mediating the diffusion of hydrophilic molecules and antibiotics, thus contributing to antibiotic resistance (Umji and Chang-Ro, 2019). Studies have reported that the presence of ROS can lead to a decrease in porins proteins and thus also contribute to the resistance to NPs (Niño-Martínez *et al*., 2019). The observed induced virulent genes may therefore be due to the excess of metal ions such as manganese, potassium and zinc within the cell, promoting biofilm associated genes in *S. aureus*.

Exposure to nanomolecular complexes induced the upregulation of carbohydrate metabolism, fermentation and a switch in respiration pathway, inducing anaerobiosis in *E. coli* treated with KS51 and *S. aureus* treated with KS25 and KS33

Carbohydrate metabolism and transport genes were generally upregulated in most treatments except KS51 in both model microorganisms. *E. coli* treated with KS25 and KS33 activated gluconeogenesis genes *pck* and *pps*. The TCA glyoxylate cycle genes *sucC* regulated by *rpoS* (see Fig. 15), *sdhAB* regulated by *fnr* (see Fig. 18), *glcBCGFE*, *aceAB* and cytochrome bo oxidase *cyoABE* regulated by *pdhR* (see Fig. 15), were also induced, activating aerobic respiration via either succinate dehydrogenase or cytochrome bo(3) oxidase. Mixed fermentation was also upregulated in KS25 and KS33 in *E. coli* through formate to nitrite and glycerol/fumarate to hydrogen electron transfer. In *E. coli* treated with KS51, during the log growth phase, glycolysis and gluconeogenesis genes *pckA* and *gapA* were downregulated, aerobic participating pathways; TCA, glyoxylate cycle genes *sdhBD* and cytochrome bo oxidase genes *cyoD*, *cydB* were downregulated, anaerobically induced genes nitrate reductase *napAC* and *narHK* regulated by *narL*, *tdcC*, dimethyl sulfoxide reductase *dmsA*, c4-dicarboxylate *dcuC* and fumurate reductase *frdAB*, regulated by *rpoS* (see Fig. 18) were downregulated. Mixed fermentation genes *tdcE* and *frdAB* were also downregulated. In *S. aureus*, treated with KS25 and KS33, aerobic associated genes *sucABCD* and anaerobic respiration pathways associated genes *narHK*, *nirB* were inhibited while gluconeogenesis genes *pfkB*, *gpmA*, *fpb* and the mixed fermentation *gmpA*, *pta* were activated. In *S. aureus* treated with KS51, EMP glycolysis genes *gap*, *fba*, TCA aerobic genes *sdhABC* via either succinate dehydrogenase and mixed fermentation genes *frdAB* were upregulated through fumarate to hydrogen electron transfer, (see Fig. 28).

Genes involved in fatty acid oxidation were mostly upregulated in *S. aureus* treated with KS51, including *fadAB*. In addition, lipid catabolism gene *lip2* was unregulated in *S. aureus* treated with KS51. For energy production, fats and triglycerides are broken down via hydrolysis into fatty acids, a process known as lipid catabolism (Parsons *et al*., 2013). The resulting fatty acids are then oxidized or degraded by β-oxidation genes *fadAB* into acetyl CoA via the beta-oxidation pathway. Acetyl-CoA is involved in the Krebs cycle and glyoxylate cycle, subsequently producing ATP by substrate-level phosphorylation for cell growth. A proposed hypothesis for this regulation is that the halogen oxidation from the iodine ions induced either an alternative respiration pathway or inhibited it completely. In treatment KS51, in *E. coli*, cytochrome bo terminal oxidase complexes were inhibited, indicating damage by oxidation

caused by iodine ions. Furthermore, the shutdown of aerobic respiration in treatment KS51 in *E. coli* and treatment KS25, KS33 in *S. aureus* may be that the model microorganism's stress mechanism was to possibly reduce ROS and oxidative stress. Studies have shown and reported that an increase in aerobic respiration often increases higher oxidative stress as it generates ROS as a by-products of oxidative phosphorylation (Kashmiri *et al*., 2014). Additionally, the shutdown of aerobic, anaerobic and mixed fermentation in *E. coli* treated with KS51 may suggest that the treatment arrested growth in this bacterial strain, prioritizing other metabolic pathways like repair of biological components.

The regulation of aerobic respiration in KS25 and KS33 may further suggest that the possible oxidative damage may not have had a major or impactful effect to induce a switch in cellular respiration. In analysing the overall regulation in both model microorganism, not only did treatments KS25 and KS33 in *E. coli* show very similar regulation in cellular respiration, it was observed that both treatments showed similar regulation patterns in DNA repair, biosynthesis pathways and protein damage repair, as compared to KS51. Similarly, treatment KS25 and KS33 in *S. aureus* showed very similar regulation as compared to KS51, thus approving the hypothesis. The antimicrobial activity of KS25 and KS33 seemed to have the overall most optimal effect on *S. aureus* whereas the antimicrobial activity of KS51 had the most optimal effect on *E. coli*. This may primarily be due to the different surfaces of the bacterial strain and the difference in hydrophobicity difference between KS25 and KS33 compared to KS51 and the surface of the bacterial strain.

2.4 References

1. Aggarwal P, Hall JB, McLeland CB, Dobrovolskaia MA, McNeil SE. Nanoparticle interaction with plasma proteins as it relates to particle biodistribution, biocompatibility and therapeutic efficacy. *Adv Drug Deliv Rev*. 2009;61(6):428–37.
2. Ayala-Castro C, Saini A, Outten FW. Fe-S cluster assembly pathways in bacteria. *Microbiol Mol Biol Rev*. 2008;72(1):110-125.
3. Badetti E, Calgaro L, Falchi L, Bonetto A, Bettiol C, Leonetti B, Ambrosi E, Zendri E, Marcomini A. Interaction between Copper Oxide Nanoparticles and Amino Acids: Influence on the Antibacterial Activity. *Nanomaterials*. 2019;9(5):792.
4. Beinert H, Holm RH, Münck E. Iron-sulfur clusters: Nature's modular, multipurpose structures. *Science* 1997 Aug 1;277(5326):653-9.
5. Blattner, FR, Plunkett G 3rd, Bloch CA, Perna NT, Burland V, Riley M, Collado-Vides J, Glasner JD, Rode CK, Mayhew GF, Gregor J, Davis NW, Kirkpatrick HA, Goeden MA, Rose DJ, Mau B, Shao Y. The Complete Genome Sequence of *Escherichia coli* K-12. *Science*. 1997. 277(5331): p. 1453-1462.
6. Block C, Robenshtok E, Simhon A, Shapiro M. Evaluation of chlorhexidine and povidone iodine activity against methicillin-resistant *Staphylococcus aureus* and vancomycin-resistant *Enterococcus faecalis* using a surface test. *J Hosp Infect* 2000;46:147–152.
7. Bolger AM, Lohse M, Usadel B. Trimmomatic: a flexible trimmer for Illumina sequence data. *Bioinformatics*. 2014 Aug 1;30(15):2114-20.
8. Bondarczuk K, Piotrowska-Seget Z. Molecular basis of active copper resistance mechanisms in Gram-negative bacteria. *Cell Biol Toxicol*. 2013;29(6):397-405. doi:10.1007/s10565-013-9262-1
9. Buvelot H, Roth M, Jaquet V, Lozkhin A, Renzoni A, Bonetti EJ, Gaia N, Laumay F, Mollin M, Stasia MJ, Schrenzel J, François P, Krause KH. Hydrogen Peroxide Affects Growth of *S. aureus* Through Downregulation of Genes Involved in Pyrimidine Biosynthesis. Front Immunol. 2021 Sep 7;12:673985.
10. Cassu-Corsi D, Martins WM, Nicoletti AG, Almeida LG, Vasconcelos AT, Gales AC. Characterisation of plasmid-mediated *rmtB-1* in Enterobacteriaceae clinical isolates from São Paulo, Brazil. *Mem. Inst. Oswaldo Cruz*. 113(2), e180392 (2018).
11. Chudobova D, Dostalova S, Ruttkay-Nedecky B, Guran R, Rodrigo MA, Tmejova K, Krizkova S, Zitka O, Adam V, Kizek R. The effect of metal ions on Staphylococcus aureus revealed by biochemical and mass spectrometric analyses. *Microbiol Res*. 2015 Jan;170:147-56.
12. Coady A, Xu M, Phung Q, Cheung TK, Bakalarski C, Alexander MK, Lehar SM, Kim J, Park S, Tan MW, Nishiyama M. The *Staphylococcus aureus* ABC-Type Manganese Transporter MntABC Is Critical for Reinitiation of Bacterial Replication Following Exposure to Phagocytic Oxidative Burst. *PLoS One*. 2015 Sep 17;10(9):e0138350.
13. Contreras-Moreira B, Vinuesa P. GET_HOMOLOGUES, a versatile software package for scalable and robust microbial pangenome analysis. *Appl. Environ. Microbiol*. 2013, 79: 7696-7701.

14. Courcelle J, Khodursky A, Peter B, Brown PO, Hanawalt PC. Comparative gene expression profiles following UV exposure in wild-type and SOS-deficient *Escherichia coli*. *Genetics.* 2001 May;158(1):41-64.
15. Cronan JE, Thomas J. Bacterial fatty acid synthesis and its relationships with polyketide synthetic pathways. *Methods Enzymol*. 2009;459:395-433.
16. Deschamps P, Zerrouk N, Nicolis I, Martens T, Curis E, Charlot MF, Girerd JJ, Prangé T, Bénazeth S, Chaumeil JC, *et al*. Copper(II)–l-glutamine complexation study in solid state and in aqueous solution. *Inorg. Chim*. Acta 2003, 353, 22–34.
17. De Maeyer D, Renkens J, Cloots L, De Raedt L, Marchal K. PheNetic: network-based interpretation of unstructured gene lists in *E. coli*. *Mol. Biosyst.* 2013, 9: 1594-1603. doi: 10.1039/c3mb25551d.
18. Ding H, Harrison K, Lu J. Thioredoxin reductase system mediates iron binding in *IscA* and iron delivery for the iron-sulfur cluster assembly in *IscU*. J Biol Chem. 2005 Aug 26;280(34):30432-7. doi:
19. Djoko KY, Chong LX, Wedd AG, Xiao Z. Reaction mechanisms of the multicopper oxidase *CueO* from *Escherichia coli* support its functional role as a cuprous oxidase. *J Am Chem Soc*. 2010 Feb 17;132(6):2005-15.
20. Dukan S, Farewell A, Ballesteros M, Taddei F, Radman M, Nyström T. Protein oxidation in response to increased transcriptional or translational errors. Proc Natl *Acad Sci U S* A. 2000;97(11):5746-5749.
21. Duval V, Lister IM. *MarA, SoxS* and Rob of *Escherichia coli*–Global regulators of multidrug resistance, virulence and stress response. *Int J B Wellness Ind*. 2013;2:101.
22. Edis Z, Haj Bloukh S, Abu Sara H, Bhakhoa H, Rhyman L, Ramasami P. "Smart" Triiodide Compounds: Does Halogen Bonding Influence Antimicrobial Activities?. *Pathogens*. 2019;8(4):182.
23. Epstein W. 2003. The roles and regulation of potassium in bacteria. Prog. *Nucleic Acid Res*. Mol. Biol. 75:293–320.
24. Ezraty B, Gennaris A, Barras F. *et al*. Oxidative stress, protein damage and repair in bacteria. *Nat Rev Microbiol* 15, 385–396 (2017).
25. Fang FC, Frawley ER, Tapscott T, Vázquez-Torres A. Bacterial Stress Responses during Host Infection. *Cell Host Microbe*. 2016;20(2):133-143.
26. Gaballa A, Newton GL, Antelmann H, *et al*. Biosynthesis and functions of bacillithiol, a major low-molecular-weight thiol in Bacilli. *Proc Natl Acad Sci U S A*. 2010;107(14):6482-6486.
27. Gao T, Fan H, Wang X, Gao Y, Liu W, Chen W, Dong A, Wang YJ. Povidone-Iodine-Based Polymeric Nanoparticles for Antibacterial Applications. *ACS Appl Mater Interfaces*. 2017 Aug 9;9(31):25738-25746.
28. Ge SX, Jung D, Yao R. ShinyGO: a graphical gene-set enrichment tool for animals and plants. *Bioinformatics*. 2020 Apr 15;36(8):2628-2629.
29. Gene Ontology Consortium. The Gene Ontology resource: enriching a GOld mine. Nucleic Acids Res. 2021 Jan 8;49(D1):D325-D334. doi: 10.1093/nar/gkaa1113.
30. Gründling A. Potassium uptake systems in *Staphylococcus aureus*: new stories about ancient systems. *mBio*. 2013 Oct 8;4(5):e00784-13.

31. Guo K, Zhao Y, Cui L, Cao Z, Zhang F, Wang X, Feng J, Dai M. The Influencing Factors of Bacterial Resistance Related to Livestock Farm: Sources and Mechanisms. *Frontiers in Animal Science*. doi=10.3389/fanim.2021.650347
32. Haley CE, Marling-Cason M, Smith JW, Luby JP, Mackowiak PA. 1985. Bactericidal activity of antiseptics against methicillin-resistant *Staphylococcus aureus*. J Clin Microbiol 21:991–992.
33. He C, Parrish DA, Shreeve JM. Alkyl ammonium cation stabilized biocidal polyiodides with adaptable high density and low pressure. *Chemistry. 2014 May 26; 20(22):6699-706.*
34. Helbig K, Grosse C, Nies DH. Cadmium toxicity in glutathione mutants of *Escherichia coli*. *J Bacteriol*. 2008;190(15):5439-5454.
35. Henrikus SS, van Oijen AM, Robinson A. Specialised DNA polymerases in *Escherichia coli*: roles within multiple pathways. *Curr Genet*. 2018 Dec;64(6):1189-1196.
36. Holden MT, Feil EJ, Lindsay JA, Peacock SJ, Day NP, Enright MC, Foster TJ, Moore CE, Hurst L, Atkin R, Barron A, Bason N, Bentley SD, Chillingworth C, Chillingworth T, Churcher C, Clark L, Corton C, Cronin A, Doggett J, Dowd L, Feltwell T, Hance Z, Harris B, Hauser H, Holroyd S, Jagels K, James KD, Lennard N, Line A, Mayes R, Moule S, Mungall K, Ormond D, Quail MA, Rabbinowitsch E, Rutherford K, Sanders M, Sharp S, Simmonds M, Stevens K, Whitehead S, Barrell BG, Spratt BG, Parkhill J. Complete genomes of two clinical *Staphylococcus aureus* strains: evidence for the rapid evolution of virulence and drug resistance. *Proc Natl Acad Sci U S A* 101:9786–9791
37. Holmgren A. Thioredoxin and glutaredoxin systems. J Biol Chem. 1989 Aug 25;264(24):13963-6.
38. Howden BP, Beaume M, Harrison PF, Hernandez D, Schrenzel J, Seemann T, Francois P, Stinear TP. Analysis of the small RNA transcriptional response in multidrug-resistant *Staphylococcus aureus* after antimicrobial exposure. *Antimicrob*. *Agents Chemother*. 2013, 57: 3864-3874.
39. Ilin AI, Kulmanov ME, Korotetskiy IS, Islamov RA, Akhmetova GK, Lankina MV, Reva ON. Genomic Insight into Mechanisms of Reversion of Antibiotic Resistance in Multidrug Resistant *Mycobacterium tuberculosis* Induced by a Nanomolecular Iodine-Containing Complex FS-1. *Front Cell Infect Microbiol*. 2017 May 8;7:151.
40. Iwasaki H, Takahagi M, Shiba T, Nakata A, Shinagawa H. *Escherichia coli* RuvC protein is an endonuclease that resolves the Holliday structure. *EMBO J*. 10, 4381-9, (1991).
41. Joubert M, Reva ON, Korotetskiy IS, Shvidko SV, Shilov SV, Jumagaziyeva AB, Kenesheva ST, Suldina NA, Ilin AI. Assembly of Complete Genome Sequences of Negative-Control and Experimental Strain Variants of *Staphylococcus aureus* ATCC BAA-39 Selected under the Effect of the Drug FS-1, Which Induces Antibiotic Resistance Reversion. *Microbiol Resour Announc*. 2019 Jul 25;8(30):e00579-19.
42. Kaczmarek A, Budzyńska A, Gospodarek E. Prevalence of genes encoding virulence factors among Escherichia coli with K1 antigen and non-K1 *E. coli* strains. *J M Microbiol*. 2012;61:1360–5.

43. Kanehisa M, Goto S, Hattori M, Aoki-Kinoshita KF, Itoh M, Kawashima S, Katayama T, Araki M, Hirakawa M. From genomics to chemical genomics: new developments in KEGG. *Nucleic Acids Res*. 2006 Jan 1;34(Database issue):D354-7.
44. Karp PD, Paley S, Romero P. The Pathway Tools software. Bioinformatics. 2002;18 Suppl 1:S225-32.
45. Kashmiri ZN, Mankar SA. Free radicals and oxidative stress in bacteria. *International journal of current Microbiology and Applied Sciences*. ISSN: 2319-7706 Volume 3 Number 9 (2014) pp.
46. Katz A, Orellana O. Protein Synthesis and the Stress Response. *IntechOpen*. DOI: 10.5772/50311
47. Kern R, Malki A, Holmgren A, Richarme G. Chaperone properties of *Escherichia coli* thioredoxin and thioredoxin reductase. *Biochem J*. 2003 May 1;371(Pt 3):965-72.
48. Kilstrup M, Hammer K, Jensen PR, Martinussen J. Nucleotide metabolism and its control in lactic acid bacteria. *FEMS Microbiology Reviews*, Volume 29, Issue 3, August 2005, Pages 555–590.
49. Kim ST, Saha K, Kim C, Rotello VM. The role of surface functionality in determining nanoparticle cytotoxicity. *Acc Chem Res*. 2013;46(3):681–91.
50. Korotetskiy LS, Joubert M, Taukobong S, Jumagaziyeva AB, Shilov SV, Shvidko SV, Suldina NA, Kenesheva ST, Yssel A, Reva ON, Ilin AL. 2019. Complete genome sequence of a multidrug resistant strain *Escherichia coli* ATCC BAA-196 as a model to study the induced antibiotic resistance reversion. *Microbiol Resour Announc* 8:e01118-19.
51. Korotetskiy IS, Jumagaziyeva AB, Shilov SV, Kuznetsova TV, Myrzabayeva AN, Iskakbayeva ZA, Ilin AI, Joubert M, Taukobong S and Reva ON. 2021. Transcriptomics and methylomics study on the effect of iodine-containing drug FS-1 on *Escherichia coli* ATCC BAA-196. *Future Microbiology* 2021 16:14, 1063-1085.
52. Kunisada T, Yamada K, Oda S, Hara O. Investigation on the efficacy of povidone-iodine against antiseptic-resistant species. Dermatology. 1997;195 Suppl 2:14-8.
53. Kuroda M, Ohta T, Uchiyama I, Baba T, Yuzawa H, Kobayashi I, Cui L, Oguchi A, Aoki K, Nagai Y, Lian J, Ito T, Kanamori M, Matsumaru H, Maruyama A, Murakami H, Hosoyama A, Mizutani-Ui Y, Takahashi NK, Sawano T, Inoue R, Kaito C, Sekimizu K, Hirakawa H, Kuhara S, Goto S, Yabuzaki J, Kanehisa M, Yamashita A, Oshima K, Furuya K, Yoshino C, Shiba T, Hattori M, Ogasawara N, Hayashi H, Hiramatsu K. Whole genome sequencing of meticillin-resistant *Staphylococcus aureus*. *Lancet*. 2001 Apr 21;357(9264):1225-40.
54. Lepelletier D, Maillard JY, Pozzetto B, Simon A. Povidone Iodine: Properties, Mechanisms of Action, and Role in Infection Control and *Staphylococcus aureus* Decolonization. Antimicrob Agents Chemother. 2020 Aug 20;64(9):e00682-20.
55. Lund PA. Microbial molecular chaperones. *Adv Microb Physiol*. 2001;44:93-140.
56. Macomber L, Imlay JA. The iron-sulfur clusters of dehydratases are primary intracellular targets of copper toxicity. *Proc Natl Acad Sci U S A*. 2009 May 19;106(20):8344-9.

57. Maisonneuve E, Fraysse L, Lignon S, Capron L, Dukan S. Carbonylated proteins are detectable only in a degradation-resistant aggregate state in *Escherichia coli*. *J Bacteriol*. 2008;190(20):6609-6614.
58. McBride SM, Sonenshein AL. The dlt operon confers resistance to cationic antimicrobial peptides in Clostridium difficile. *Microbiology (Reading).* 2011;157(Pt 5):1457-1465.
59. Nidya M, Umadevi M, Rajkumar BJM. Synthesis of Amino acid Capped Silver Nanoparticles, Characterization and Biological Application. *Exp. Nanosci*., 2015, 10, 167–180.
60. Niño-Martínez N, Salas Orozco MF, Martínez-Castañón GA, Torres Méndez F, Ruiz F. Molecular Mechanisms of Bacterial Resistance to Metal and Metal Oxide Nanoparticles. *Int J Mol Sci*. 2019 Jun 8;20(11):2808.
61. Noinaj N, Guillier M, Barnard TJ, Buchanan SK. TonB-dependent transporters: regulation, structure, and function. *Annu Rev Microbiol*. 2010;64:43-60.
62. Okonechnikov K, Golosova O, Fursov M; UGENE team. Unipro UGENE: a unified bioinformatics toolkit. *Bioinformatics*. 2012 Apr 15;28(8):1166-7.
63. Olechnowicz J, Tinkov A, Skalny A, Suliburska J. Zinc status is associated with inflammation, oxidative stress, lipid, and glucose metabolism. *J Physiol Sci*. 2018 Jan;68(1):19-31.
64. Parsons JB, Rock CO. Bacterial lipids: metabolism and membrane homeostasis. *Prog Lipid Res.* 2013;52(3):249-276.
65. Pereira BMP, Wang X, Tagkopoulos, I. Short- and Long-Term Transcriptomic Responses of *Escherichia coli* to Biocides: a Systems Analysis. *ASM* DOI: https://doi.org/10.1128/AEM.00708-20
66. Py, B. and F. Barras, Building Fe-S proteins: bacterial strategies. *Nat Rev Microbiol*, 2010. 8(6): p. 436-46.
67. Reva ON, Korotetskiy IS, Joubert M, Shilov SV, Jumagaziyeva AB, Suldina NA, Ilin AI. The Effect of Iodine-Containing Nano-Micelles, FS-1, on Antibiotic Resistance, Gene Expression and Epigenetic Modifications in the Genome of Multidrug Resistant MRSA Strain *Staphylococcus aureus* ATCC BAA-39. *Front Microbiol*. 2020 Oct 22;11:581660.
68. Saibil H. Chaperone machines for protein folding, unfolding and disaggregation. *Nat Rev Mol Cell Biol*. 2013;14(10):630-642.
69. Schramm FD, Schroeder K, Jonas K. Protein aggregation in bacteria, *FEMS Microbiology Reviews*, Volume 44, Issue 1, January 2020, Pages 54–72
70. Schwartz CJ, Djaman O, Imlay JA, Kiley PJ. The cysteine desulfurase, IscS, has a major role in in vivo Fe-S cluster formation in *Escherichia coli*. *Proceedings of the National Academy of Sciences* Aug 2000, 97 (16) 9009-9014.
71. Sharma R. Synthesis of Amino Acid Capped Silver Nanoparticles, Characterization, and Biological Application. *Orient J Chem* 2020;36(2).
72. Siegele DA. Universal stress proteins in *Escherichia coli*. *J Bacteriol*. 2005;187(18):6253-6254.
73. Sriwilaijaroen N, Wilairat P, Hiramatsu H, Takahashi T, Suzuki T, Ito M, Ito Y, Tashiro M, Suzuki Y. Mechanisms of the action of povidone-iodine against human and avian

influenza A viruses: its effects on hemagglutination and sialidase activities. *Virol J*. 2009 Aug 13;6:124.

74. Umji, C and Chang-Ro, L. Distinct Roles of Outer Membrane Porins in Antibiotic Resistance and Membrane Integrity in *Escherichia coli*. *Front Microbiol*. 2019 Apr 30;10:953.
75. Waller JC, Ellens KW, Hasnain G, Alvarez S, Rocca JR, Hanson AD. Evidence that the folate-dependent proteins YgfZ and MnmEG have opposing effects on growth and on activity of the iron-sulfur enzyme MiaB. *J Bacteriol*. 2012 Jan;194(2):362-7.
76. Xu XM, Møller SG. Iron-sulfur clusters: biogenesis, molecular mechanisms, and their functional significance. *Antioxid Redox Signal*. 2011 Jul 1;15(1):271-307.
77. University of Adelaide. "How zinc starves lethal bacteria to stop infection." *ScienceDaily*. ScienceDaily, 11 November 2013.
78. Žgur-Bertok D. DNA damage repair and bacterial pathogens. *PLoS Pathog*. 2013;9(11):e1003711.
79. Zhang W, Xiao S, Ahn DU. Protein oxidation: basic principles and implications for meat quality. *Crit Rev Food Sci Nutr*. 2013;53(11):1191-201.
80. Zhu M, Nie G, Meng H, Xia T, Nel A, Zhao Y. Physicochemical properties determine nanomaterial cellular uptake, transport, and fate. *Acc Chem Res*. 2013;46(3):622–31. pmid:22891796

Chapter 3: Gene expression comparison between Gram-negative *E. coli* and Gram-positive *S. aureus* treated with iodine-containing nanomolecular complexes KS25, KS33 and K51

3.1 Introduction

To understand and evaluate how NPs complexes interacts with Gram-negative *E. coli* compared to Gram-positive *S. aureus*, much of the focus needs to be on the bacterial cell envelope and the survival strategy employed by each bacterium. To survive harsh environmental conditions, bacteria have developed and evolved complex cell envelopes to selectively allow certain substances to come in and out of the cell. Moreover, specialized reactions also take place on the surface of the bacteria in efforts to enhance protection. The cell envelope comprises of the cell membranes and cell wall of the bacteria. Bacteria are divided into two classes, distinguished by their cell wall structure, namely; Gram-positive and Gram-negative bacteria, as illustrated in (Fig. 25). Gram-negative bacteria such as *E. coli* are characterised by three layers in their cell envelope, mainly; the inner membrane, outer membrane and a thin peptidoglycan cell wall (Silhavy *et al*., 2010). In the centre of the two membranes, lies a gel-like matrix termed the periplasm, which contains the peptidoglycan (Silhavy *et al*., 2010). The outer membrane is a lipid bilayer that serves as the first line of defence against harsh environmental conditions and is the distinguishing feature of Gram-negative bacteria (Bertani *et al*., 2018). It is made of phospholipids that are confined to the inner leaflet of the membrane and glycolipids lipopolysaccharides in the outer leaflet, consisting of lipid A, polysaccharides and O antigen (Kamio and Nikaido, 1976). Lipopolysaccharides (LPS) function in creating a permeability barrier against small, hydrophobic molecules for protection, secretes metabolic waste products and determines the initial, physical interaction with the nanomolecular complex drugs and attachment site (Nikaido, 2003; Galloway and Raetz, 1990). The lipid A component of the lipopolysaccharides (LPS) serve as an endotoxin, responsible for the toxicity of Gram-negative bacteria (Raetz and Whitfield, 2002). The outer membrane also consist of lipoproteins anchored to the periplasmic surface of the inner leaflet and β-barrel outer membrane proteins (OMPs) in the outer leaflet. *E. coli* has over 100 lipoproteins in the inner leaflet of the outer membrane with an unknown function wheras β-barrel OMPs are known as porins (Miyadai *et al*., 2004). The general *OmpACF* porins have been described to determine the permeability barrier of the cell, with

others meditating the uptake or entry of certain hydrophilic substrates of particular size and charge across the membrane. Porins *ompFC* have been implicated in promoting antimicrobial resistance by limiting antimicrobial uptake and have been shown and reported to be related to the resistance of β-Lactams (Jaffe *et al.*,1982).

The cell envelope of Gram-positive bacteria such as *S. aureus*, slightly differs to that of Gram-negative bacteria, as it lacks an outer membrane. As discussed, the outer membrane plays an important role in protecting Gram-negative bacteria from external environmental factors and toxins. To compensate for the absent outer membrane, Gram-positive bacteria have developed and evolved a much thicker layer of peptidoglycan as compared to Gram-negative bacteria, to protect themselves from harsh conditions. Additionally, because Gram-positive bacteria lack an outer membrane, they contain extracellular proteins and branched stem peptides which serve as attachment sites for proteins like low affinity PBPs to bind, allowing resistance to β-lactam antibiotics (Chambers, 2003; Rohrer and Berger-Bachi, 2003; Pratt, 2008; Sauvage *et al*., 2008). Studies have also shown that extracellular proteins in *S. aureus* can drastically change as a response to change in environmental cues, thus allowing the cell envelope to adapt and protect the bacterial cell in the new environment (Pollack and Neuhaus, 1994). Seeping through the peptidoglycan, lies anionic polymers called teichoic acids, which make up majority of the mass of the Gram-positive cell wall (Silhavy *et al*., 2010). Teichoic acids form part of two classes namely; wall teichoic acids, covalently bound to peptidoglycan and the lipoteichoic acids, anchored to the lipid membrane. Teichoic acids play a role in providing flexibility in the cell wall, often by attracting cations such as potassium and calcium (Marquis *et al*,. 1976).

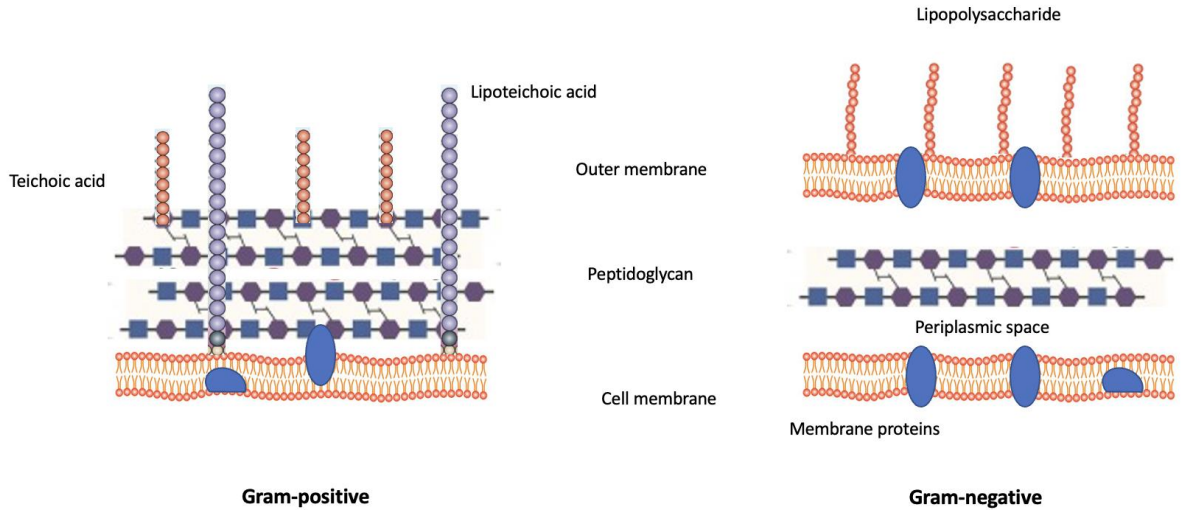

Figure 25. The structural differences between the cell envelope of Gram-positive (left) and Gram-negative (right) bacteria modified based on Clifton *et al*., 2013; Pajerski *et al*., 2019.

As discussed, Gram-positive and Gram-negative bacteria are classified based on their respective cell wall structure. Several studies have shown that some bacteria are more susceptible to NPs than others, owing to the nature of their cell wall composition and structure. Gram-positive bacteria have a thicker layer of peptidoglycan as compared to Gram-negative bacteria, which has a thinner layer of peptidoglycan containing an additional outer membrane, the lipopolysaccharide (Yael *et al*., 2017). *E. coli* has a peptidoglycan layer that is about 8 nm thick, with a layer of polysaccharide that is between 1-3 µm thick whereas *S. aureus* has a peptidoglycan layer that is 80nm thick (Slavin *et al*., 2017). Studies have reported that Gram-positive bacteria are more resistant to NPs whereas Gram-negative bacteria are more susceptible to NPs possibly owing to the thinner nature of their cell walls (Slavin *et al*., 2017). Additionally, Gram-positive and Gram-negative bacteria have negatively charged cell walls which influence the interactions between the cell walls of the bacteria and the NPs (Magnusson *et al*., 1982). The negatively charged cell wall has a high affinity towards the positive charges of NPs, therefore increasing the permeability and uptake of ions within the NPs, which then causes cell wall disruption and intracellular damage (Slavin *et al*., 2017). Gram-negative are however, known to be more negatively charged than Gram-positive bacteria owing to their lipopolysaccharides molecules thus making Gram-negative such as *E. coli* more prone and susceptible to the NPs as compared to Gram-positive like *S. aureus* (Slavin *et al*., 2017; Yael

et al., 2017). Gram-negative bacteria are however, more prone to cell wall destruction because they contain negatively charged lipopolysaccharide molecules (Slavin *et al*., 2017).

A novel hypothesis for this chapter and study, may, therefore be that, the mechanisms through which the iodine nanomolecular complex structures interact with bacteria is dependent on the bacterial cell envelope structure and the bacterial survival strategy. Owing to the thinner nature of Gram-negative *E. coli* ATCC BAA-196s peptidoglycan, it is hypothesized that the strain will likely be more susceptible to all the three treatments in comparison to Gram-positive *S. aureus* ATCC BAA-39. Furthermore, iodine-containing nanomolecular complexes KS25 and KS33 have positive charges whereas KS51 is uncharged, making Gram-negative *E. coli* even more susceptible to treatments KS25 and KS33. The objective for the work presented in this chapter, is to therefore, evaluate how the transcriptional effects of the iodine nanomolecular complexes of Gram-negative *E. coli* is similar or differs to that of Gram-positive *S. aureus* and then identify the factors influencing the biological activity of iodine in the differently synthesized complexes.

3.2 Methods

3.2.1 FoldChangeComparison between *E. coli* ATCC BAA-196 and *S. aureus* ATCC BAA-39

A FoldChangeComparison in-house Python tool was used to generate plots and a text document of coregulated- and counter-regulated genes between *E. coli* and *S. aureus* during the lag and log growth phase, with a set p-value cut-off of 0.05. This was done using the mapped reads that were counted and normalized by DESeq2, an R-package and a Cluster of Orthologous Genes (COG) text file that corresponds to the reference genomes of *E. coli* and *S. aureus*. The normalised count reads from each model microorganisms were compared to each other, during the same growth phases *i.e.* normalised count reads from *E. coli* treated with KS25 during the lag growth phase were compared to normalised count reads from *S. aureus* treated with KS25 during the lag. The same procedure was followed for treatment KS33 and KS51 during the lag and log growth phases.

3.3 Results

3.2.2 FoldChangeComparison between *E. coli* ATCC BAA-196 and *S. aureus* ATCC BAA-39 findings

Gene expression patterns comparison was carried out to determine commonly coregulated and counter-regulated genes in distantly related model microorganisms; *E. coli* and *S. aureus* under the effects of KS25, KS33 and KS51, illustrated in (Fig. 27, 28 and Table 10). Genes are ordered by clusters with similar patterns of expression. The specific shared genes and annotations are detailed in (Table S3). Genes that were significantly enriched (≥2-log FC, p-value 0.05) in the data, were only considered. Shared or similar genes that were upregulated in all treatments, in both *E. coli* and *S. aureus* were not observed, however lead, cadmium, zinc and mercury transporting ATPase *copA* was observed to be upregulated in *E. coli* and *S. aureus* exposed to KS25 and KS33 in both growth phases. In treatment KS25, only 5 protein coding genes were positively regulated in both model microorganisms during the lag growth phase and 3 during the log growth phase in KS25 versus NC treatment in both *E. coli* and *S. aureus*. These genes included; Nitroreductase *nfsA*, *ybhW*, Phosphoribosylformylglycinamidine cyclo-ligase *purM*, lead, copper, cadmium, zinc and mercury transporting ATPase *copA* and FMN-dependent NADH-azoreductase *azoR* in the lag growth phase and N-ethylmaleimide reductase *nemA*, *copA* and putative transporter subunit *yecS* in the log growth phase.

Solely in treatment KS33, only 2 protein coding genes were positively regulated during the lag growth phase and 2 during the log growth phase in KS25 versus NC treatment in both *E. coli* and *S. aureus*. These genes included; phosphoribosylformimino-5-aminoimidazole carboxamide *hisA* and *copA* in the lag phase and *nemA* and *copA* in the log growth phase. In the lag growth phase, only 3 genes were negatively coregulated and only 2 in the log growth phase, including; 4 D-ribose pyranase *rbsD*, cold shock protein *cspG*, Nitrate/nitrite transporter *narK* and only cold shock protein *cspE*, pyrimidine nucleoside transporter *nupC*, respectively. In treatment KS33, only 2 genes were positively regulated including; *hisA* and *copA* in the lag phase and 2 in the log phase, including *nemA* and *copA*. Only 3 genes were negatively coregulated in the lag phase including; maltodextrin transporter *msmX*, shikimate kinase II *aroL* and Nitrite reductase (NAD(P)H) large subunit *nirB*. In treatment KS51, only one gene was positively coregulated in the lag and log phase, including; 2-methylcitrate synthase *prpC* and Acyl carrier protein phosphodiesterase *azoR*, respectively. Six genes were negatively coregulated in the lag phase including; N-acetylglucosamine-specific IIC component *nagE*,

uncharacterized protein *phnB*, glycerate kinase II *glxK*, trehalose-6-P hydrolase *treC*, Maltose ABC transporter *malE* and cold shock protein *cspG* whilst 4 were negatively coregulated in the log phase including; ribosomal protein *rplF*, aspartate carbamoyltransferase catalytic subunit *pyrB*, acetyl-CoA:acetoacetyl-CoA transferase *ydiF* and cold shock protein *cspG*.

Genes that were upregulated in *E. coli*, however downregulated in *S. aureus* in both KS25 and KS33 included: nucleotide biosynthesis associated genes *carAB*, *purC* and *pyrB*, glutamate synthase *glnA*, and phosphate transport associated gene *phoB* in the lag growth phase whilst tryptophan synthesis genes *trpAB* were upregulated in the log growth phase. Genes solely upregulated in KS25 in *E. coli* and not *S. aureus*, included; translation and ribosomal-associated genes *argS* and *rpsR*, nucleotide associated gene *purC* and gluconate permease *yjhF* whilst ATP synthase gene *atpG* was upregulated in the log growth phase. Genes solely upregulated in KS33 in *E. coli* and not *S. aureus*, included; nucleotide biosynthesis genes *purMN*, *uraA* and *guaB*, phosphate transport associated gene *phoU* and molybdenum cofactor biosynthesis protein *moaA* whilst *moaBC* and ribosomal protein were upregulated in the log growth phase. Genes solely upregulated in KS51 in *E. coli* and not *S. aureus*, included; translation and ribosomal associated proteins *ykgM*, *yebR*, *cysS* and *hemA*, metal ion efflux gene *copA*, heat shock protein *groS*, nitrate reduction gene *narK* and nucleotide associated gene *apt*. Genes upregulated in *S. aureus*, however downregulated in *E. coli* included, in treatment KS25 included: translation associated gene *yhbJ* during the log phase. Genes upregulated in *S. aureus*, however downregulated in *E. coli* included, in treatment KS33 included; *yeeD*. Genes upregulated in *S. aureus*, however downregulated in *E. coli* included, in treatment KS51 included; *astC*, aldehyde dehydrogenase *B aldB*, amino salvage protein *ggt*, nucleotide biosynthesis genes *carA* and *purKN*, gluconeogenesis protein *pck*, thiamine biosynthesis *thiE*, glutamate synthase *glnA*, mixed fermentation gene *frdB* in the lag growth phase and *frdAB* and potassium transport genes *kdpBCE* in the log growth phase.

Genes downregulated in *E. coli*, however no regulation in *S. aureus* in all treatments included: *tcdB* in the log growth phase. In both KS25 and KS33; translation initiation factor IF-1 *infA* and in KS25 and KS51; fumarate reductase *frdA*. Solely in KS25; fumarate reductase (anaerobic), Fe-S subunit *frdB*, glycerol-3-phosphate dehydrogenase *gpsA*, exoribonuclease R, RNase R *rnr*, in the lag phase and *hisS*, putative RNA-binding protein *yhbY*, export of O-antigen protein *rfbX*, N,N'-diacetylchitobiose-specific enzyme *chbC*, stabilizing FstZ ring during cell division protein *ftsW* during the log growth phase. Solely in KS33; ribosomal

protein *rplm* and DNA excision and repair *mutY* in the lag phase. Solely in KS51; glutathione-dependent thiol reductase *yffB*, nucleotide biosynthesis *focA* and *pyrB*, DNA excision motif *uvrC*, cytochrome oxidase *cyoB*, pentose pathway gene *rbsK*, and aldehyde dehydrogenase B *aldB*, fatty acid biosynthesis *accC*, methionine metabolism gene *metE* during the log phase.

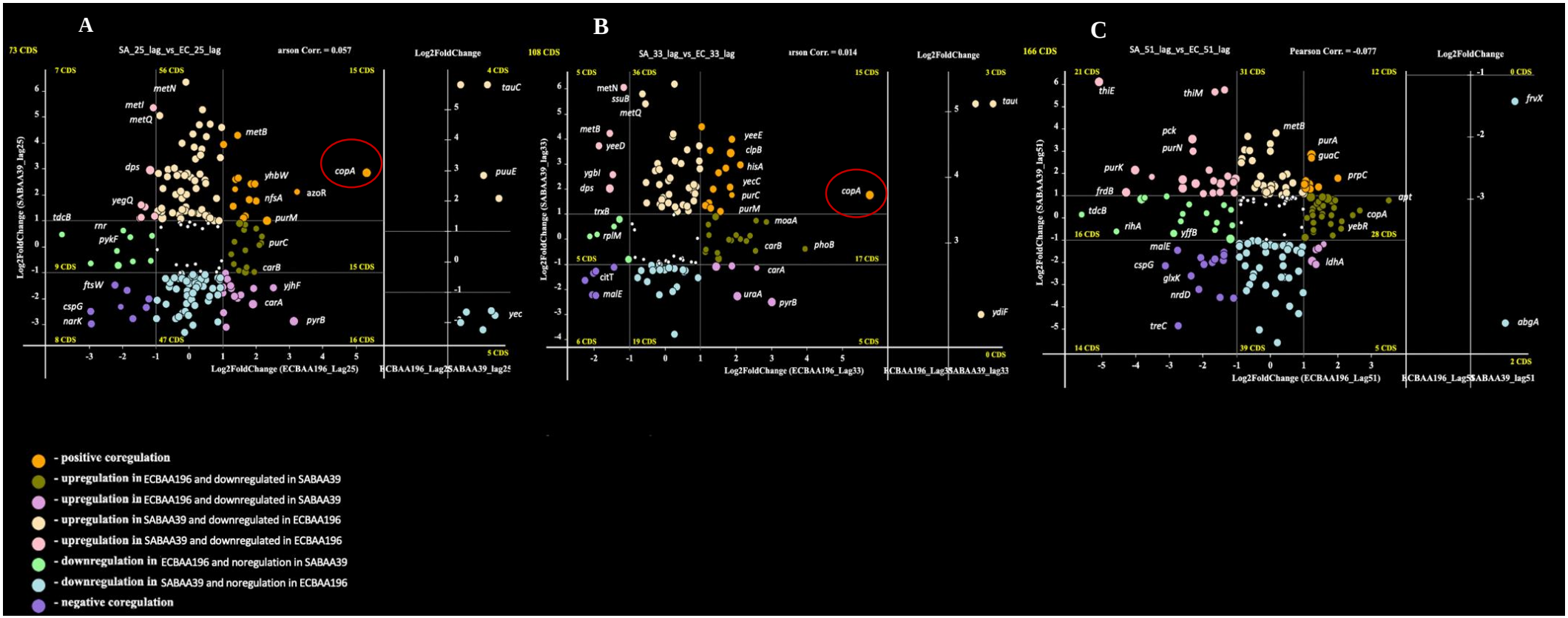

Figure 26. Plots of co-regulation of genes between *E. coli* BAA-196 and *S. aureus* ATCC BAA-39 in the Log experimental growth phases. A) *E. coli* BAA-196 vs *S. aureus* ATCC BAA-39 with both treated with KS25 compared with NC; B) *E. coli* BAA-196 vs *S. aureus* ATCC BAA-39 with both treated with KS33 compared with NC; and C) *E. coli* BAA-196 vs *S. aureus* ATCC BAA-39 with both treated with KS51 compared with NC. Circles represent protein coding genes (CDS) plotted according to their negative and positive Log_2FC values calculated in the *E. coli* ATCC BAA-196 (axis X) and *S. aureus* ATCC BAA-39 (axis Y). The outermost regulated genes are labelled by their names or CDS tag numbers. Thin vertical and horizontal lines within the plots separate genes with 1-fold or higher regulation and split the plots to sectors of genes of different categories depending on their coregulation. Numbers of CDS falling to different sectors are shown. Up- and down- coregulated genes, oppositely regulated genes and the genes regulated only in one experiment are depicted by different colours as depicted in the legends. The outermost co-regulated genes are labelled according to respective gene names. The color codes are represented in the key below.

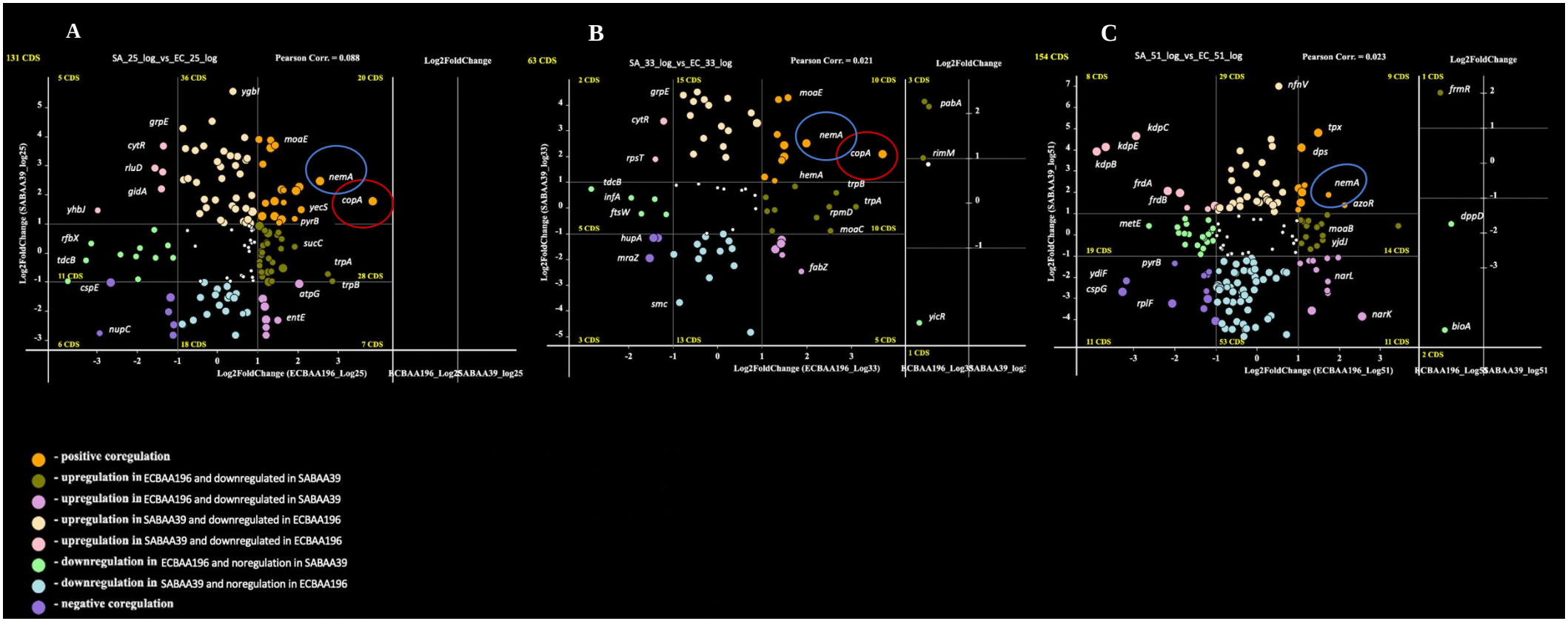

Figure 27. Plots of co-regulation of genes between *E. coli* BAA-196 and *S. aureus* ATCC BAA-39 in the Log experimental growth phases. A) *E. coli* BAA-196 vs *S. aureus* ATCC BAA-39 with both treated with KS25 compared with NC; B) *E. coli* BAA-196 vs *S. aureus* ATCC BAA-39 with both treated with KS33 compared with NC; and C) *E. coli* BAA-196 vs *S. aureus* ATCC BAA-39 with both treated with KS51 compared with NC. Circles represent protein coding genes (CDS) plotted according to their negative and positive Log_2FC values calculated in the *E. coli* ATCC BAA-196 (axis X) and *S. aureus* ATCC BAA-39 (axis Y). The outermost regulated genes are labelled by their names or CDS tag numbers. Thin vertical and horizontal lines within the plots separate genes with 1-fold or higher regulation and split the plots to sectors of genes of different categories depending on their coregulation. Numbers of CDS falling to different sectors are shown. Up- and down- coregulated genes, oppositely regulated genes and the genes regulated only in one experiment are depicted by different colours as depicted in the legends. The outermost co-regulated genes are labelled according to respective gene names. The color codes are represented in the key below.

Table 10. Specific pathways and processes of genes regulated in both *E. coli* ATCC BAA-196 and *S. aureus* ATCC BAA-39 during the lag and log growth phase in treatments KS25, KS33 and KS51 (≥2 Log_2FC, p-value 0.05).

	KS25		**KS33**		**KS51**	
Pathway/ Biological processes	Upregulated genes	Downregulated genes	Upregulated genes	Downregulated genes	Upregulated genes	Downregulated genes
Nucleotide biosynthesis	X	O	X	O		O
Detoxifying proteins	XO		XO			XO
Copper ATPase	XO		XO			
Zinc, cadmium, potassium transport systems	O		O		O	
The citric acid cycle (TCA)	X	O	X	O	O	
Outer membrane porins		X		X		
Nucleotide excision repair protein	O		O			XO
Chaperones, heat, cold shock proteins	O		O			
Thiol-oxidative stress	XO					
Mixed fermentation	O		O		O	X
Cell wall/peptidoglycan, fatty and lipoteichoic acid biosynthesis		X		X	XO	

- Lag and log refer to the lag and log growth phase. The capital letter X represents regulation in *E. coli* and the capital letter O represents regulation in *S. aureus*. Letters XO represents similar regulation in *E. coli* and *S. aureus*. The complete list of the up- and downregulated genes can be found in Table S5 in the supplemental material, including their respective log2 fold change values.

3.3 Discussion

Gene expression results in which *E. coli* ATCC BAA-196 and *S. aureus* ATCC BAA-39 showed similar regulation

The most common and highest regulation observed in *E. coli* and *S. aureus* was the activation of copper ATPase *copA* in response to treatment KS25 and KS33, in both growth phases, illustrated in (Fig. 27 and 28), circled in red. Additionally, detoxifying gene nitroreductase *nfsA* was activated in response to all the treatments during the log growth phase with *nemA* activated in KS25 and KS33. As discussed, the activation of copper efflux systems and resistance may suggest that I^- and Cu^{2+} may have caused the generation of ROS and further caused oxidative damage in both model microorganisms. The detoxifying and efflux transport system mechanisms were therefore deployed to reduce stress and damage.

The gene expression results in which *E. coli* ATCC BAA-196 and *S. aureus* ATCC BAA-39 showed a difference in gene regulation

Several upregulated genes were observed in *E. coli* but downregulated in *S. aureus* in response to each treatment. Nucleotide biosynthesis related genes *carB, purCMN, pyrB, uraA* and *guaB* were found to be upregulated in *E. coli*, however downregulated in *S. aureus*. The downregulation of nucleotide biosynthesis in *S. aureus* may, as mentioned, be due to sub-lethal concentration of ROS possibly generated by free radicals that interfere with nucleotide synthesis and subsequently affecting the growth in *S. aureus*, suggesting that cell growth was most likely arrested in *S. aureus* as compared to *E. coli*. Several gene regulations were observed in *S. aureus* however not observed in *E. coli* in response to each treatment. These included zinc efflux pumps *zitB* and *czrA*, and cadmium resistant proteins *cadABC*. This regulation suggests that a larger influx of metal ions were observed in *S. aureus* as compared to *E. coli*, further suggesting that the iodine ions increased penetrability through halogen oxidation and caused significantly more damage to the cells membrane and cell wall in *S. aureus*. Furthermore, metal ions such as cadmium ions and iodine ions play a significant role in oxidizing biological systems, this therefore may suggest that in addition to the damage caused by the iodine ions, the cadmium ions caused additional intracellular damage in *S. aureus*. Outer membrane proteins *ompCF* were found to be downregulated in *E. coli* treated with KS25 and KS33. This regulation provided increased protection reducing extracellular uptake of metal ions unlike in *S. aureus*.

Genes involved in cell wall/peptidoglycan and lipoteichoic acid biosynthesis were activated in *S. aureus* and less in *E. coli*. This regulation may suggest that there was significantly more barrier damage in *S. aureus* than in *E. coli*, thus inducing genes involved in cell wall/peptidoglycan and lipoteichoic acid biosynthesis. Genes involved in DNA repair and protection were mostly observed in *S. aureus* compared to *E. coli*. Nucleotide excision repair protein, with *uvrB/uvrC* motif were activated in *S. aureus* treated with KS25 and KS33 in both phases, with *uvrC* downregulated in *E. coli*. Additionally, error-prone repair DNA polymerase IV *dinB*, controlled by sigma *rpoS* was upregulated in treatment KS25 in *S. aureus* whereas DNA repair proteins *recAQ* and *lexA* were downregulated. This regulation suggests that the halogenation by iodine directly affected DNA in *S. aureus*, therefore, there was more significant DNA damage in *S. aureus* but hardly any in *E. coli*. The exposure of *S. aureus* to the nanomolecular complex KS25 and KS33 induced the activation of cochaperonins; heat shock proteins *groL*, HSP70 systems; *dnaJK, grpE* and HSP100; *clpBCPX* and *hslO, hrcA* in both growth phases, however not in *E. coli*. This regulation may suggest that there was significant protein damage that induced the activation of chaperones and protein folding genes, in efforts to either refold or remove aggregated, damaged proteins.

A slightly different regulation was observed in *E. coli* in terms of protein damage. Genes involved in Fe-S cluster biosynthesis and repair were activated suggesting that the iodine ions may have directly attacked proteins containing Fe-S clusters. In *S. aureus*, thioredoxins and glutaredoxins were found to be upregulated. This regulation in contrast to *E. coli*, may have played a role in protecting *S. aureus* against significant protein damage in Fe-S clustered proteins. The regulation of cellular respiration in both model microorganisms was also slightly different and may have been influenced by the nanomolecular complexes themselves. A similar regulation of induced aerobic respiration was observed in *S. aureus* treated with KS51 and *E. coli* treated with KS25 and KS33. Mixed fermentation was induced in all treatments in *S. aureus* whereas aerobic, anaerobic and mixed fermentation was inhibited in *E. coli* treated with KS51. The proposed action of the iodine ions and metals ions are illustrated in (Fig. 28), which is an extension of Fig. 22.

Upon evaluating of the results, the differences in gene regulation between *E. coli* and *S. aureus* confirmed that *S. aureus* was more susceptible to all three treatments compared to *E. coli*, thus disproving the hypothesis. This finding correlates with the findings by Korotetskiy *et al*., 2021, which showed that *S. aureus* ATCC BAA-39 was more susceptible to iodine-containing

micelle FS-1 compared to *E. coli* ATCC BAA-196. A more plausible explanation for the susceptibility of *S. aureus* as compared to *E. coli* is that the thick peptidoglycan layer of Gram-positive *S. aureus* is highly porous thus allowing greater access and easy penetrability within the cell by ions. Additionally, Gram-negative *E. coli* has an additional layer, the outer membrane, which regulates the passage of ions. It was also observed that *E. coli* was extremely affected by treatment KS51, most likely due to the hydrophobicity and interaction between the nanomolecular complex and the cell wall.

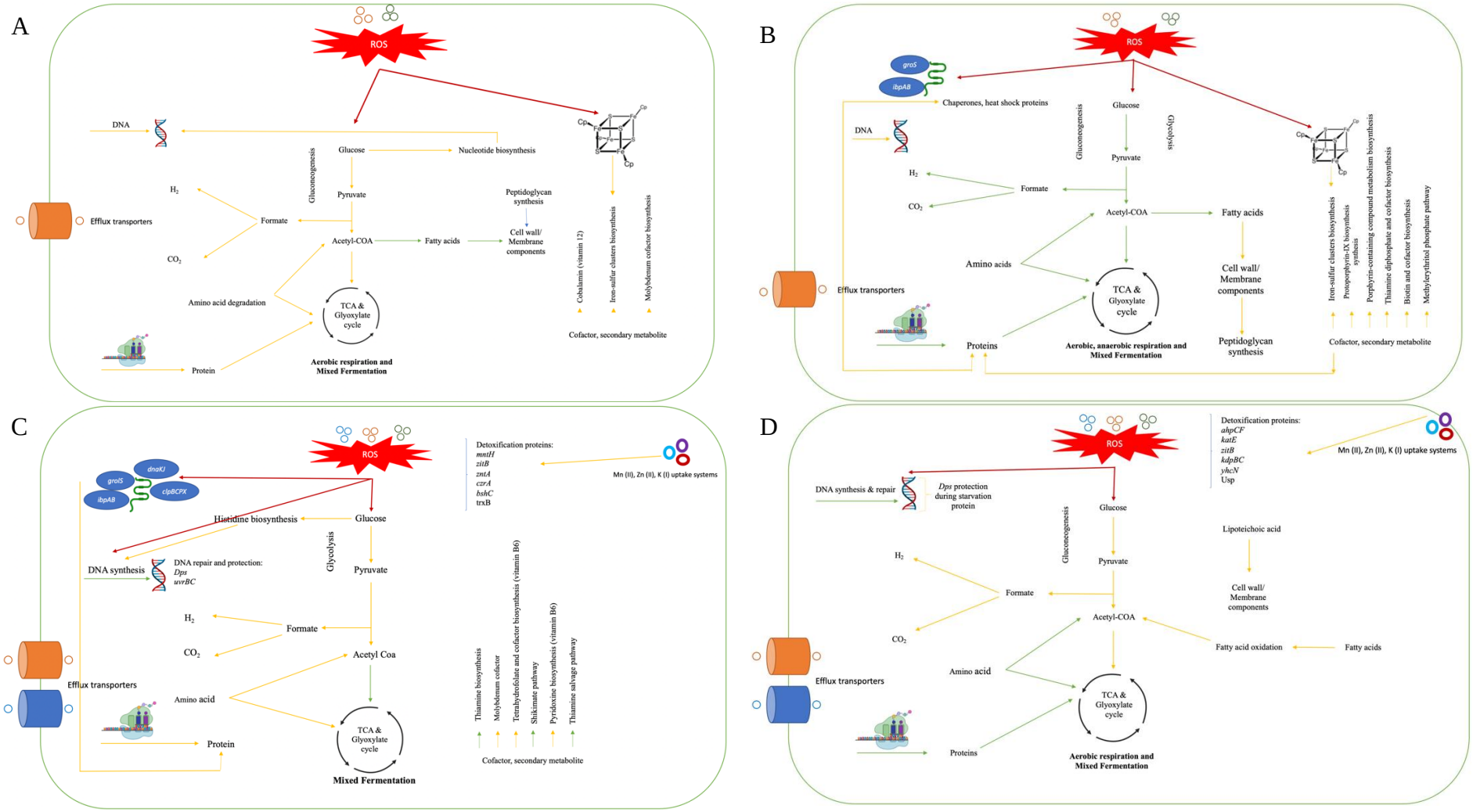

Figure 28. Metabolic pathways affected each treatment and extracellular metal ions on the model microorganisms. A) Affected pathways in *E. coli* BAA-196 treated with KS25 and KS33; B) Affected pathways in *E. coli* BAA-196 treated with KS51; C) Affected pathways in *S. aureus* BAA-39 treated with KS25 and KS33; and D) Affected pathways in *S. aureus* BAA-39 treated with KS51. Up- and down-regulation of pathways are depicted respectively by arrows of yellow and green colours, respectively.

3.4 References

1. Bertani B, Ruiz N. Function and Biogenesis of Lipopolysaccharides. *EcoSal Plus*. 2018;8(1):10.1128/ecosalplus.ESP-0001-2018.
2. Chambers HF. 2003. Solving *staphylococcal* resistance to beta-lactams. *Trends Microbiol*. 2003 Apr; 11(4):145-8.
3. Clifton LA, Skoda MWA, Daulton EL, Hughes AV, le Brun AP, Lakey JH, Holt SA. Asymmetric phospholipid: lipopolysaccharide bilayers; a gram-negative bacterial outer membrane mimic. *J R Soc Interface*. 2013.10:20130810.
4. Galloway SM and Raetz CR. A mutant of *Escherichia coli* defective in the first step of endotoxin biosynthesis. *J Biol Chem*. 1990 Apr 15; 265(11):6394-402.
5. Jaffe A, Chabbert YA, Semonin O. Role of porin proteins *ompF* and *ompC* in the permeation of beta-lactams. *Antimicrob Agents Chemother*. 1982;22(6):942-948.
6. Kamio Y, Nikaido H. Outer membrane of *Salmonella typhimurium*: accessibility of phospholipid head groups to phospholipase c and cyanogen bromide activated dextran in the external medium. *Biochemistry.* 1976 Jun 15; 15(12):2561-70.
7. Marquis RE, Mayzel K, Carstensen EL. Cation exchange in cell walls of gram-positive bacteria. *Can J Microbiol*. 1976 Jul; 22(7):975-82.
8. Miyadai H, Tanaka-Masuda K, Matsuyama S, Tokuda H. Effects of lipoprotein overproduction on the induction of DegP (HtrA) involved in quality control in the *Escherichia coli* periplasm. *J Biol Chem*. 2004 Sep 17; 279(38):39807-13.
9. Nikaido H. 2003. Molecular basis of bacterial outer membrane permeability revisited. Microbiol *Mol Biol Rev*. 2003 Dec; 67(4):593-656.
10. Raetz CR, Whitfield C. Lipopolysaccharide endotoxins. *Annu Rev Biochem*. 2002; 71():635-700.
11. Rohrer S, Berger-Bächi B. FemABX peptidyl transferases: a link between branched-chain cell wall peptide formation and beta-lactam resistance in gram-positive cocci. *Antimicrob Agents Chemother*. 2003 Mar; 47(3):837-46.
12. Pajerski W, Ochonska D, Brzychczy-Wloch M. *et al*. Attachment efficiency of gold nanoparticles by Gram-positive and Gram-negative bacterial strains governed by surface charges. *J Nanopart Res* 21, 186 (2019).
13. Pollack JH and Neuhaus FC. Changes in wall teichoic acid during the rod-sphere transition of *Bacillus subtilis* 168. *Pollack JH, Neuhaus FCJ Bacteriol*. 1994 Dec; 176(23):7252-9.
14. Pratt RF. Substrate specificity of bacterial DD-peptidases (penicillin-binding proteins). *Cell Mol Life Sci*. 2008 Jul; 65(14):2138-55.
15. Sauvage E, Kerff F, Terrak M, Ayala JA, Charlier P. The penicillin-binding proteins: structure and role in peptidoglycan biosynthesis. *FEMS Microbiol Rev*. 2008 Mar; 32(2):234-58.
16. Slavin YN, Asnis J, Häfeli UO, Bach H. Metal nanoparticles: understanding the mechanisms behind antibacterial activity. *J Nanobiotechnology*. 2017;15(1):65.
17. Silhavy TJ, Kahne D, Walker S. The bacterial cell envelope. *Cold Spring Harb Perspect Biol*. 2010;2(5):a000414.

Chapter 4: Concluding remarks and Future works

4.1 Concluding remarks

The evolution of antibiotic resistance in bacteria has presented significant challenges in medicine. The emergence has led to limited treatment options resulting in longer lasting hospital visits and increased mortality. The solution to resistance will require a pool of strategies including drug discovery, resistance monitoring, and combinations of innovative methods to select for and reverse antibiotic resistance. The use of nano-technology in antimicrobial resistance reversion studies have been showing promising results. Caster *et al*., (2016) reported that although few nanomedicines have been FDA approved, there are numerous projects that are currently in progress in terms of clinical trials suggesting many new nanotechnology-based drugs will soon be available to the market (Patra *et al*,.2018). The use of NPs and or nanomolecular complexes as antimicrobial agents has thus shown to be an option that could solve issues relating to resistance. Iodine has been a considered candidate for nano-therapy against multi-drug resistant and pathogenic bacteria due to its broad spectrum antimicrobial activity and no reported resistance.

In this study, we accomplished transcriptome investigation to analyse the short (lag phase) and long term (log phase) effects of KS25, KS33 and KS51 on *E. coli* ATCC BAA-196, supplemented with ceftazidime and *S. aureus* ATCC BAA-39, following treatment. The gene expression analysis of 444 genes (≥ 2-log FC) in *E. coli* ATCC BAA-196 and 539 genes ((≥ 2-log FC) in *S. aureus* ATCC BAA-39 treated with KS25, KS33 and KS51 which were differentially expressed as compared to untreated control ($P < 0.05$) were observed. The treatment of iodine-containing complexes KS25, KS33 and KS51 on *E. coli* and *S. aureus* induced a series of metal ion efflux and transport systems indicating possible barrier disruption of and entry within the cell wall and membrane by iodine ions and possibly the surrounding ions, interacting with the nanomolecular complexes. This regulation indicates an excess of metal ions and iodine ions, most likely, interacted with free radicals and induced oxidative damage and stress on the surface and within the cell. This regulation further, induced the protection against oxidants, induced virulency and biofilm formation of the bacterial cells for enhanced protection and cross resistance, possibly selecting against iodine. The interaction of free radicals possibly caused by iodide and the metal ions like copper further caused DNA damage in *S. aureus*, protein damage in both model microorganisms, inhibition in translation

machinery and nucleotide damage in *S. aureus* and arrested growth in *S. aureus* treated with KS25, KS33 and *E. coli* treated with KS51. Several studies have reported that the mechanism of action of many NPs is often due to the induction of (ROS) (Kaczmarek *et al*,2012), which are able to penetrate bacterial cells and cause significant oxidative damage to all kinds of cellular components, including nucleic acids, proteins and alteration of cellular respiration decreasing the activity of many metabolic pathways. Bacteria have the ability to adjust their metabolism in response to environmental changes by linking extracellular stimuli to the regulation of genes by means of transcription factors and in most cases, transcription regulators which control genes and operons that belong to different metabolic pathways (Duval *et al*,2013). *E. coli* activates sigma factor *rpoS* transcriptional regulator which positively or negatively controls the expression of several hundred genes, mainly involved in metabolism, transport, regulation and stress management. Several genes were positively and negatively regulated by *rpoS* in all three treatments in *E. coli*, as shown in (Fig. 16 and 18). In addition, other transcriptional activators and repressors were initiated in response to the different treatments activating genes involved in DNA repair, cellular respiration pathways, transport and efflux systems. Upon stress, the bacterial strains resort to slowing down or altering cellular and metabolic processes related to cell growth and increase the functionality of processes that aid in repair and overcome the stress (Katz *et al*,2012).

Furthermore, X-ray crystallography revealed that Complex KS25 contains two molecules of glycine bound by coordination bonds with one three-iodine molecule and three K^+ ions. Complex KS33 contains three alanine molecules bound with one three-iodine molecule and three Li^+ ion. Complex KS51 contains two molecules of isoleucine associated with an iodine ion. It was observed that treatment KS25 and KS33 had similar gene expression patterns as compared to treatment KS51 in both model microorganisms. This could primarily be due the R-group or side chains of the amino acids used in the synthesis process. Alanine and glycine have fewer hydrocarbon bonds (Hydrophobicity of 0) on their side chains as compared to isoleucine (Hydrophobicity of 2). This explains the similarities in gene expression regulation between KS25 and KS33, whereas the gene expression regulation of KS51 was different, in both model microorganisms. These results therefore, support the hypothesis that the R-group or side chain of the amino acid interacting with the iodine-containing nanomolecular complex may be a factor influencing the overall bioactivity. Furthermore, the antimicrobial activity of KS25 and KS33 seemed to have the overall most optimal effect on *S. aureus* whereas the bioactivity KS51 had the most optimal effect on *E. coli*. This may be primary due to, again, the

interactions between the amino acid side chain and the nanomolecular complexes and the difference in surface of the bacterial strains *i.e.,* the cell envelope of Gram-negative *E. coli* and Gram-positive *S. aureus*. The growth phase at which the iodine-containing nanomolecular complexes were applied at somewhat affected the gene expression response. Most pathways were induced in both growth phases however cellular respiration or genes involved in aerobic/anaerobic respiration/mixed fermentation, TCA and glyoxylate cycle were found to be primarily induced after long term exposure or during the exponential growth phase in both model microorganisms. Metal efflux pumps, metal ion transport proteins, chaperones and heat shock proteins were found to be primarily induced in the lag growth phase. Fatty acid biosynthesis in *S. aureus* treated with KS51 was also found to be induced during the exponential growth phase. Interestingly however, the overall regulation observed in this study was slightly different to that of *E. coli* ATCC BAA-196 and *S. aureus* ATCC BAA-39 treated with iodine-containing micelle FS-1, thus regurgitating the way in which NPs are synthesized is an essential step in order to identify bioactivity factors and gain knowledge on NPs with the most optimal antimicrobial results. Additionally, *E. coli* ATCC BAA-196 was treated with ceftazidime alongside the nanomolecular complexes. The resulting gene regulation could not, however, highlight or differentiate the role the antibiotic played. Chapter 2's findings, therefore illustrated that both model microorganisms showed significant changes in metabolism and pathways in response to the three treatments. Furthermore, it evaluated and addressed the factors influencing the bioactivity of the three differently synthesized iodine-containing complexes.

Chapter 3 presented findings on the broad spectrum activity of the iodine-containing complexes and illustrated how the complexes affected model microorganisms Gram-negative *E. coli* ATCC BAA-196 and *S. aureus* ATCC BAA-39, compared to each other. The findings showed that *S. aureus* ATCC BAA-39 was more susceptible to all three treatments despite *E. coli* being additionally supplemented with antibiotic ceftazidime. The iodine ions released by the nanomolecular complexes acted on *S. aureus* by targeting the cell wall/membrane, DNA, proteins, and cellular respiration, inhibiting nucleotide synthesis, translation and causing a switch in cellular respiration. In *E. coli* however, possible significant damage was observed during treatment KS51, with Fe-S clustered proteins and cellular respiration being mostly affected. The findings from this chapter therefore disproved the stated hypothesis, shared light on how the iodine containing complexes affect distantly related model microorganisms *i.e.,* Gram-positive bacteria compared to Gram-negative. This study is the first to provide evidence on the factors affecting the bioactivity of iodine when synthesized with the used amino acids

therefore further proving iodine to be a viable option in nano-based therapy against pathogenic and drug resistant microorganism.

4.2 Future Works

This study is a continuation of previous studies on antibiotic resistance reversions effects of iodine-containing micelle FS-1 in combination with antibiotics on model microorganisms: *S. aureus* ATCC BAA-39 and *E. coli* ATCC BAA-196 to induce antibiotic sensitivity to once resistant bacteria, thus reversing antibiotic resistance. This approach has been shown to be viable in multi-drug resistant *M. tuberculosis* SCAID 187.0, *S. aureus* ATCC BAA-39 and *E. coli* ATCC BAA-196 and *A. baumannii* ATCC BAA-1790. In this study, we used model microorganisms *S. aureus* ATCC BAA-39 and *E. coli* ATCC BAA-196 to evaluate the bioactivity of three iodine-containing nanomolecular complexes denoted as KS25, KS33 and KS51. This study however, did not take into account the gene regulation effects of antibiotic ceftazidime. Therefore, future work may include, a negative control sample, a sample in which *E. coli* is treated with ceftazidime without the iodine-containing complexes and lastly a sample in which *E. coli* is treated with ceftazidime and the iodine-containing complexes. This will thus, give a solid indication of the effects of complexes in combination with antibiotics compared to their activity when administrated separately. Additionally, *S. aureus* is a well preferred model microorganism to study antibacterial nano-therapy. Gram-positive bacteria in general however, have different peptidoglycan structure, thus may differ in the way that they respond to different nanomolecular complexes. Therefore, *S. aureus* may not be a sufficient model microorganism for studying how the iodine-containing complexes affect Gram-positive bacteria as a whole. Future work may therefore, look into adding more Gram-positive model microorganisms. Future work may also include evaluating the long-lasting effects of each treatment on gene regulation by profiling epigenetic modifications in both model microorganisms. Moreover, the majority of studies that have shown the potential of NPs in combination with antibiotics have been performed only *in vitro* and *in silico*. Human and animal systems are, however, more complex due to factors such as; how drugs are metabolized (Roberts *et al*., 2014) and the role of the immune system in selecting for resistant bacteria (Brandl *et al*., 2008). In addition to this, most *in vitro* and *in silico* studies have been performed using non-fastidious bacteria like *E. coli*, *B. subtilis*, *P. aeruginosa* and *S. aureus* as model

microorganisms due to extensive research being done on these species and them being cultured. This could potentially poses a challenge for the treatment of other infection-causing bacteria.

4.3 Research outputs and publications

This study is a continuation of previous studies on antibiotic resistance reversions effects of iodine-containing micelle FS-1 on model microorganisms: *S. aureus* ATCC BAA-39 and *E. coli* ATCC BAA-196. The final listed publication has been submitted to submitted to journal Antibiotics for review, for this specific study.

- Korotetskiy LS, Joubert M, **Taukobong S**, Jumagaziyeva AB, Shilov SV, Shvidko SV, Suldina NA, Kenesheva ST, Yssel A, Reva ON, Ilin AL. 2019. Complete genome sequence of a multidrug resistant strain *Escherichia coli* ATCC BAA-196 as a model to study the induced antibiotic resistance reversion. Microbiol Resour Announc 8:e01118-19. https://doi.org/10.1128/MRA.01118-109.

- Korotetskiy IS, Shilov SV, Kuznetsova T, Ilin A, Joubert M, **Taukobong S**, Reva ON. 2020. Comparison of transcriptional responses and metabolic alterations in three multidrug resistant model microorganisms, *Staphylococcus aureus* ATCC BAA-39, *Escherichia coli* ATCC BAA-196 and *Acinetobacter baumannii* ATCC BAA-1790, on exposure to iodine-containing nano-micelle drug FS-1. Microbiol Resour Announc. DOI: 10.1128/mSystems.01293-20

- Korotetskiy IS, Jumagaziyeva AB, Shilov SV, Kuznetsova TV, Myrzabayeva AN, Iskakbayeva ZA, Ilin AI, Joubert M, **Taukobong S** and Reva ON. 2021. Transcriptomics and methylomics study on the effect of iodine-containing drug FS-1 on *Escherichia coli* ATCC BAA-196. Future Microbiology 2021 16:14, 1063-1085.

- Kenesheva ST, **Taukobong S**, Shilov SV, Kuznetsova TV, Karpenyuk TA, Reva ON, Ilin AI. 2021. The effect of complexes of iodine with amino acids on gene expression of model antibiotic resistant micro-microorganisms *Escherichia coli* ATCC BAA-196 and *Staphylococcus aureus* ATCC BAA-39. Status: Submitted to American Society for Microbiology.

Supplementary Data

Table S1. Upregulated and downregulated genes in *E. coli* ATCC BAA-196 (BAA196NC) in response to treatments; KS25, KS33 and KS51 during the lag growth phase. Upregulated genes are represented in positive values and downregulated genes are represented in negative values. Statistically reliable changes of gene expressing (≥2 Log_2FC; p-value ≤ 0.05) are highlighted by yellow (upregulation) or green (downregulation) shading. Genes are ordered by clusters with similar patterns of expression.

Locus tag	Gene	Compounds and growth phases						Annotation
		KS25		KS33		KS51		
		Lag	Log	Lag	Log	Lag	Log	
BAA196NC_3269	*copA*	5.32	3.86	5.77	3.71	2.65	0.98	Copper transporter
BAA196NC_3615	*cueO*	3.90	3.01	4.49	2.99	0.76	1.06	Multicopper oxidase (laccase)
BAA196NC_0281	*yhhW*	4.36	1.93	3.86	2.94	3.35	2.48	Quercetin 2,3-dioxygenase
BAA196NC_0960	*cysN*	3.55	1.10	1.89	1.75	0.85	0.95	Sulfate adenylyltransferase subunit 1
BAA196NC_2291	*azoR*	3.22	1.47	0.45	1.28	1.78	2.13	Acyl carrier protein phosphodiesterase
BAA196NC_3356	*phoB*	1.92	-0.17	3.95	0.74	1.60	1.10	DNA-binding response regulator in two-component regulatory system with PhoR (or CreC)
BAA196NC_0675	*zupT*	2.98	2.93	3.44	2.32	1.93	2.92	Predicted dioxygenase
BAA196NC_3355	*phoR*	1.82	0.32	3.19	0.55	1.16	0.82	Sensory histidine kinase in two-component regulatory system with PhoB
BAA196NC_4210	*sbp*	0.40	1.48	3.01	2.38	2.23	1.77	Sulfate transporter subunit
BAA196NC_4387	*phoU*	-1.12	2.20	2.30	2.20	1.54	1.63	Negative regulator of PhoR/PhoB two-component regulator
BAA196NC_1133	*pdxJ*	2.24	1.18	1.54	2.09	1.97	1.25	Pyridoxal phosphate biosynthetic protein
BAA196NC_3342	*ybaD*	2.54	0.95	3.11	0.79	1.38	0.06	Hypothetical protein
BAA196NC_0959	*cysD*	2.73	0.83	3.52	0.47	-1.55	0.28	Sulfate adenylyltransferase subunit 2
BAA196NC_2850	*nfsA*	2.01	2.18	1.43	3.22	1.55	2.47	Nitroreductase A, NADPH-dependent, FMN-dependent
BAA196NC_3925	*ytfE*	1.85	0.57	1.74	1.75	1.62	1.56	Predicted regulator of cell morphogenesis and cell wall metabolism
BAA196NC_3424	*prpB*	0.46	1.19	-1.55	-1.31	4.14	0.41	2-methylisocitrate lyase
BAA196NC_3285	*apt*	1.08	-1.05	2.35	0.87	3.53	0.80	Adenine phosphoribosyltransferase
BAA196NC_0363	*yhfA*	1.13	-1.00	0.97	-0.80	3.31	0.12	Hypothetical protein
BAA196NC_1896	*rnd*	-0.13	-0.22	1.69	-1.38	3.00	-0.64	Ribonuclease D
BAA196NC_1828	*yecD*	1.85	-0.28	0.00	-0.95	2.93	-0.47	Predicted hydrolase
BAA196NC_1845	*edd*	2.54	0.29	1.82	0.60	2.93	-0.89	Phosphogluconate dehydratase
BAA196NC_0538	*secG*	0.30	-1.59	-0.35	-0.39	2.84	0.92	Protein-export membrane protein
BAA196NC_1115	*trxC*	0.00	-2.10	2.70	0.86	2.70	1.75	Thioredoxin 2
BAA196NC_1971	*ydjN*	2.26	-3.20	0.98	0.16	2.52	0.25	Predicted transporter
BAA196NC_3339	*nusB*	0.67	-1.51	1.53	-1.87	2.24	-0.96	Transcription antitermination protein NusB
BAA196NC_2424	*ribA*	1.47	-1.66	1.26	-1.01	2.13	-0.59	GTP cyclohydrolase II protein
BAA196NC_0218	*yhiR*	2.32	-1.48	2.08	-0.88	1.89	-1.23	Predicted DNA (exogenous) processing protein
BAA196NC_1345	*yfdH*	-1.15	-2.80	-0.27	-1.10	1.01	-0.61	CPS-53 (KpLE1) prophage; bactoprenol glucosyl transferase
BAA196NC_1181	*ndk*	-0.06	-2.43	-0.26	-2.10	1.94	-0.25	Nucleoside diphosphate kinase
BAA196NC_4408	*rpmH*	-1.01	-2.31	-1.13	-1.61	1.45	0.31	50S ribosomal protein L34

BAA196NC_0067	*rpmB*	-2.01	-1.66	-1.39	-1.77	1.45	-0.87	50S ribosomal protein L28
BAA196NC_3712	*rpsT*	-0.66	-1.58	-2.31	-1.41	1.55	-0.77	30S ribosomal protein S20
BAA196NC_0596	*tdcD*	-0.61	-3.52	-0.75	-4.21	-3.37	-6.04	Propionate kinase/acetate kinase C, anaerobic
BAA196NC_1672	*rfbX*	-0.80	-3.15	-2.22	-0.51	-0.28	-0.32	Predicted polisoprenol-linked O-antigen transporter
BAA196NC_4364	*trkD*	-1.67	-2.66	-1.96	-0.56	-0.63	-0.78	Potassium transporter
BAA196NC_2816	*infA*	-2.11	-2.42	-0.93	-1.94	0.16	-1.13	Translation initiation factor IF-1
BAA196NC_4443	.	-1.31	-2.27	-3.39	-2.85	0.25	1.46	Aminoglycoside 3"-nucleotidyltransferase
BAA196NC_4191	*rpmE*	-2.84	-1.04	-2.35	-1.42	0.31	-0.73	50S ribosomal subunit protein L31
BAA196NC_0594	*tdcB*	-3.82	-3.28	-1.29	-2.85	-5.61	-1.77	Threonine dehydratase
BAA196NC_0753	*ansB*	-1.95	-1.38	-2.71	-0.73	-4.98	-0.69	Periplasmic L-asparaginase II
BAA196NC_3036	*sdhD*	-1.54	-1.74	-0.59	-0.83	-4.37	-1.06	Succinate dehydrogenase cytochrome b556 small membrane subunit
BAA196NC_3977	*frdA*	-2.96	-0.42	-1.29	-0.65	-3.82	-2.18	Fumarate reductase
BAA196NC_3994	*aspA*	-2.72	-0.78	-1.40	-0.77	-3.61	-0.60	Aspartate ammonia-lyase
BAA196NC_1956	*astE*	-1.66	-0.98	-0.04	-1.13	-3.47	-1.47	Succinylglutamate desuccinylase
BAA196NC_2710	*cspG*	-2.95	-0.33	-2.19	-0.49	-3.12	-3.28	DNA-binding transcriptional regulator
BAA196NC_0556	*yhbS*	-2.23	-1.47	-1.68	-0.01	-3.01	-0.93	Predicted acyltransferase with acyl-CoA N-acyltransferase domain
BAA196NC_2657	*ymdC*	-1.21	-0.58	-2.22	0.17	-2.99	-0.44	Predicted hydrolase
BAA196NC_1324	*yfdE*	-1.07	-0.87	-3.01	0.00	-2.82	0.10	Predicted CoA-transferase, NAD(P)-binding
BAA196NC_4026	*phnB*	-1.21	-1.02	-3.21	-1.17	-2.07	0.60	Hypothetical protein
BAA196NC_2474	*narG*	-3.81	1.18	-4.48	1.43	-6.58	1.33	Nitrate reductase 1, alpha subunit
BAA196NC_4144	*thiG*	-0.96	1.13	-0.40	-0.13	-5.66	-0.41	Thiazole synthase
BAA196NC_4141	*thiE*	0.22	0.61	0.32	0.09	-5.09	-0.41	Thiamine-phosphate pyrophosphorylase
BAA196NC_1495	*napA*	-3.94	0.55	-2.31	0.74	-4.65	-0.86	Nitrate reductase, periplasmic, large subunit
BAA196NC_3098	*rihA*	-1.80	0.34	-1.96	-0.92	-4.56	-0.41	Ribonucleoside hydrolase 1
BAA196NC_3978	*frdB*	-2.14	-0.31	-1.03	0.35	-4.29	-1.87	Fumarate reductase (anaerobic), Fe-S subunit
BAA196NC_3337	*pgpA*	-2.14	-0.96	-0.76	0.27	-3.92	-0.28	Phosphatidylglycerophosphatase A
BAA196NC_1955	*astB*	-2.08	0.76	-0.04	-0.50	-3.90	-0.73	Succinylarginine dihydrolase
BAA196NC_2473	*narH*	-2.84	-0.48	-2.40	0.75	-3.73	-0.30	Nitrate reductase 1, beta (Fe-S) subunit
BAA196NC_1953	*astA*	-0.08	0.63	-0.69	-2.00	-3.59	-2.07	Arginine succinyltransferase
BAA196NC_2873	*yliA*	-1.78	0.23	-1.30	1.43	-3.58	0.50	Fused predicted peptide transport subunits of ABC superfamily: ATP-binding components
BAA196NC_3023	*ybgT*	-0.56	-0.33	-1.65	0.95	-3.37	-0.80	Hypothetical protein
BAA196NC_3096	*gltK*	-1.49	-0.71	-1.05	0.26	-3.27	0.13	Glutamate and aspartate transporter subunit
BAA196NC_2475	*narK*	-2.94	1.21	-3.07	1.25	-3.20	2.56	Nitrate/nitrite transporter
BAA196NC_0353	*nirB*	-1.28	0.92	-2.26	1.27	-3.04	1.45	Nitrite reductase, large subunit, NAD(P)H-binding
BAA196NC_3378	*sbmA*	0.18	1.26	-2.79	1.57	-2.59	1.01	Predicted transporter
BAA196NC_0164	*yhjX*	-0.80	2.02	0.45	1.80	-7.34	1.22	Predicted transporter
BAA196NC_2687	*putA*	1.31	1.51	1.06	0.91	-5.32	0.04	Fused DNA-binding transcriptional regulator/proline dehydrogenase/pyrroline-5-carboxylate dehydrogenase
BAA196NC_3326	*cyoD*	1.07	1.91	0.01	1.99	-5.29	0.66	Cytochrome o ubiquinol oxidase subunit IV
BAA196NC_3303	*amtB*	2.34	-0.90	1.85	0.47	-4.81	0.64	Ammonium transporter

BAA196NC_4261	*glnG*	0.74	0.12	0.86	1.43	-4.62	0.51	Fused DNA-binding response regulator in two-component regulatory system with GlnL: response regulator/sigma54 interaction protein
BAA196NC_0271	*ggt*	0.15	1.54	0.97	0.03	-3.51	-0.04	Gamma-glutamyltranspeptidase periplasmic precursor
BAA196NC_4260	*glnL*	2.20	0.28	1.90	2.50	-3.33	0.75	Sensory histidine kinase in two-component regulatory system with GlnG
BAA196NC_1434	*yfbB*	0.76	0.98	-0.40	1.83	-2.80	0.87	Predicted peptidase
BAA196NC_3445	*betA*	0.33	2.26	0.03	1.18	-2.50	0.42	Choline dehydrogenase
BAA196NC_3401	*frmB*	0.46	1.92	1.08	0.73	-2.34	1.14	Predicted esterase
BAA196NC_3982	*blc*	-0.46	1.70	-0.04	2.16	-2.33	1.79	Outer membrane lipoprotein (lipocalin)
BAA196NC_3155	*entB*	-0.40	2.57	0.81	1.01	-2.24	-0.37	Isochorismatase
BAA196NC_2897	*fiu*	0.52	2.44	0.28	3.21	0.09	1.35	Predicted iron outer membrane transporter
BAA196NC_2441	*trpA*	1.23	2.75	-1.53	3.11	-0.36	0.04	Tryptophan synthase subunit alpha
BAA196NC_2440	*trpB*	1.96	2.85	1.06	2.66	0.09	-0.43	Tryptophan synthase subunit beta
BAA196NC_2919	*moaC*	0.76	1.88	0.94	2.54	0.39	1.27	Molybdenum cofactor biosynthesis protein C
BAA196NC_0418	*rpmD*	1.10	1.41	1.17	2.51	-1.43	0.73	50S ribosomal protein L30
BAA196NC_3459	*ykgM*	2.14	0.16	1.61	2.48	-0.42	3.43	50S ribosomal protein L31
BAA196NC_0736	*glcB*	-0.01	3.39	0.52	2.10	-0.59	0.06	Malate synthase
BAA196NC_2052	*nemA*	1.62	2.55	1.57	1.99	0.11	1.74	N-ethylmaleimide reductase, FMN-linked
BAA196NC_3001	*modA*	0.87	2.73	-0.87	1.82	-1.11	2.16	Molybdate transporter subunit
BAA196NC_3400	*frmA*	1.31	1.68	1.99	1.49	-1.24	1.04	Alcohol dehydrogenase class III/glutathione-dependent formaldehyde dehydrogenase
BAA196NC_1043	*ygaV*	3.26	0.85	1.16	1.20	-1.64	1.99	Predicted DNA-binding transcriptional regulator
BAA196NC_3891	*pyrB*	3.14	1.92	3.01	0.83	-3.07	-2.00	Aspartate carbamoyltransferase catalytic subunit
BAA196NC_3781	*yjiY*	-0.63	4.82	-1.79	3.57	-3.71	0.14	Predicted inner membrane protein

Table S2. Upregulated and downregulated genes in *S. aureus* ATCC BAA-39 (HMPRNC0000) in response to treatments; KS25, KS33 and KS51 during the lag growth phase. Upregulated genes are represented in positive values and downregulated genes are represented in negative values. Statistically reliable changes of gene expressing (≥2 Log_2FC; p-value ≤ 0.05) are highlighted by yellow (upregulation) or green (downregulation) shading. Genes are ordered by clusters with similar patterns of expression.

Locus tag	Gene	Compounds and growth phases						Annotation
		KS25		KS33		KS51		
		Lag	Log	Lag	Log	Lag	Log	
HMPRNC0000_1008	*clpB*	3.94	2.73	3.45	3.18	0.61	1.61	Protein disaggregation chaperone
HMPRNC0000_2350	*zitB*	3.76	3.32	3.56	4.21	3.05	4.50	Zinc transporter ZitB
HMPRNC0000_2201	*groS*	2.99	1.81	2.35	1.88	0.42	-1.07	Co-chaperonin GroES
HMPRNC0000_2200	*groL*	3.40	3.61	3.13	3.31	1.44	2.18	Chaperonin GroEL
HMPRNC0000_0035	*zntA*	3.54	2.19	2.73	2.00	0.63	0.67	Zinc, cobalt and lead efflux system
HMPRNC0000_1711	*grpE*	2.71	4.28	1.79	4.39	-0.80	2.35	Heat shock protein
HMPRNC0000_2838	*copA*	2.86	1.78	1.77	2.09	0.34	0.67	Copper transporter
HMPRNC0000_2632	*treB*	2.44	4.54	3.12	4.28	-0.83	2.27	Fused trehalose(maltose)-specific PTS enzyme: IIB component/IIC component
HMPRNC0000_1755	*yhbW*	2.44	3.98	1.82	4.13	-0.39	1.54	Luciferase-like monooxygenase
HMPRNC0000_0772	*fruA*	2.48	5.02	2.29	5.23	0.68	0.94	Fused fructose-specific PTS enzymes: IIBcomponent/IIC components
HMPRNC0000_1708	*dnaJ*	2.56	2.52	1.99	2.70	0.47	0.65	Chaperone Hsp40, co-chaperone with DnaK
HMPRNC0000_0769	*ygbI*	2.26	5.56	2.59	4.52	-0.09	-0.66	Predicted DNA-binding transcriptional regulator
HMPRNC0000_0856	*clpP*	1.39	2.97	1.58	3.99	-0.01	3.41	ATP-dependent Clp protease proteolytic subunit
HMPRNC0000_0487	*gltB*	4.60	2.27	4.10	2.45	-3.61	-2.39	Glutamate synthase, large subunit
HMPRNC0000_0488	*gltD*	4.70	2.13	4.21	1.75	-3.49	-3.07	Glutamate synthase, 4Fe-4S protein, small subunit
HMPRNC0000_0477	*metN*	6.34	3.10	6.07	3.30	-0.93	0.00	DL-methionine transporter subunit
HMPRNC0000_0479	*metQ*	5.05	3.50	5.39	2.30	0.16	0.43	DL-methionine transporter subunit
HMPRNC0000_0476	*metB*	4.29	2.73	4.22	3.40	3.83	0.00	Cystathionine gamma-synthase
HMPRNC0000_2204		4.44	0.68	4.61	-0.10	0.74	-1.88	Nitroreductase family protein
HMPRNC0000_0478	*metI*	5.37	0.68	6.20	0.73	2.19	-0.47	DL-methionine transporter subunit
HMPRNC0000_0224	*ggt*	3.83	1.04	3.73	0.00	1.86	0.00	Gamma-glutamyltranspeptidase periplasmic precursor
HMPRNC0000_0474	.	3.82	-0.84	3.83	0.00	-1.46	0.00	Sodium-dependent transporter
HMPRNC0000_2219	*yeeD*	4.34	1.61	3.72	0.59	0.72	0.43	Hypothetical protein
HMPRNC0000_0969	*yuiF*	2.90	1.66	2.56	1.25	-1.00	-0.52	Histidine permease YuiF
HMPRNC0000_2892	*gabT*	2.84	-1.31	2.18	-1.79	-2.95	-2.22	4-aminobutyrate aminotransferase
HMPRNC0000_2984	*hisA*	3.99	0.70	2.96	1.32	-0.07	0.00	1-(5-phosphoribosyl)-5-[(5-phosphoribosylamino)methylideneamino] imidazole-4-carboxamide isomerase
HMPRNC0000_2989	*hisD*	2.80	-1.43	2.83	-2.25	-0.83	-1.92	Histidinol dehydrogenase
HMPRNC0000_2982	*hisI*	2.84	-0.60	2.26	-1.67	-1.80	-1.36	Bifunctional phosphoribosyl-AMP cyclohydrolase/phosphoribosyl-ATP pyrophosphatase protein
HMPRNC0000_2235	*ilvC*	2.66	-1.83	3.12	-2.95	-0.06	-3.49	Ketol-acid reductoisomerase (NADP(+))
HMPRNC0000_2231	*ilvD*	4.24	-0.51	4.49	-2.70	0.48	-2.35	Dihydroxy-acid dehydratase
HMPRNC0000_2233	*ilvI*	2.68	-1.32	3.03	-1.01	-1.44	-2.21	Acetolactate synthase III large subunit

HMPRNC0000_2236	*leuA*	2.59	1.56	2.12	0.59	-2.12	0.00	2-isopropylmalate synthase
HMPRNC0000_1423	*thrA*	2.13	-1.66	1.53	-2.44	-0.81	-6.08	Homoserine dehydrogenase
HMPRNC0000_1425	*thrB*	0.63	-1.16	1.19	-0.86	-3.04	-4.41	Homoserine kinase
HMPRNC0000_2404	*betT*	-1.67	-1.45	-0.87	-1.23	-1.67	-4.37	Choline transporter of high affinity
HMPRNC0000_1020	*oppC*	-2.69	-2.82	-0.97	-1.40	-0.91	-4.79	Oligopeptide transporter subunit
HMPRNC0000_1021	*oppD*	-1.12	-2.29	-0.78	-2.24	-0.18	-4.19	Oligopeptide transporter ATP-binding component
HMPRNC0000_1473	*trpB*	-0.64	-0.97	1.13	0.59	-1.35	3.46	Tryptophan synthase subunit beta
HMPRNC0000_2570	*hutI*	-0.16	0.26	-0.53	-0.78	3.32	0.86	Imidazolonepropionase
HMPRNC0000_0597	*tdh*	-2.15	-1.12	-1.18	-1.14	1.40	1.58	L-threonine 3-dehydrogenase
HMPRNC0000_2416	*rpiB*	-0.45	0.00	-1.16	0.00	0.48	0.00	Ribose-5-phosphate isomerase B
HMPRNC0000_2572	*hutU*	-0.69	-0.13	-0.35	0.29	3.68	1.43	Urocanate hydratase
HMPRNC0000_2644	*narK*	-2.97	-2.55	-1.47	-1.41	0.45	-3.84	Nitrate/nitrite transporter
HMPRNC0000_1928	*pck*	-1.08	0.77	-0.73	0.49	3.54	1.39	Phosphoenolpyruvate carboxykinase
HMPRNC0000_1099	*purE*	-2.39	-2.83	-0.65	-4.83	2.16	-2.55	Phosphoribosylaminoimidazole carboxylase catalytic subunit
HMPRNC0000_2285	*tenA*	-1.92	0.00	-1.07	0.00	3.32	1.84	Thiaminease II involved in salvage of thiamine pyrimidine moiety
HMPRNC0000_0008	*hutH*	-3.38	-0.83	-2.02	-0.36	1.64	-0.25	Histidine ammonia-lyase
HMPRNC0000_2415	*pfkB*	-1.34	0.00	-0.27	0.00	-0.59	0.00	6-phosphofructokinase II
HMPRNC0000_2282	*thiE*	-1.03	-1.51	0.10	0.00	6.12	3.95	Thiamine-phosphate pyrophosphorylase
HMPRNC0000_2284	*thiD*	-0.93	-1.51	0.25	0.00	5.77	3.14	Phosphomethylpyrimidine kinase
HMPRNC0000_2283	*thiM*	-1.84	-3.36	-1.49	-1.67	5.66	2.98	Hydroxyethylthiazole kinase

Table S3. Pathways and biological processes of genes expressed during the lag and log phase (≥2 Log_2FC, p-value 0.05) in *E. coli* strain ATCC BAA-196 in response to KS25, KS33 and KS51. Genes that were strongly upregulated (≥5 Log_2FC) are highlighted in yellow and genes strongly downregulated are highlighted in green. For each pathway, associated genes are listed.

	KS25		KS33		KS51	
Pathways/ Biological processes	Upregulated genes	Downregulated genes	Upregulated genes	Downregulated genes	Upregulated genes	Downregulated genes
Protein biosynthesis						
RNA maturation/processing		*rnr*			*greA*	
tRNA charging	*argS*				*cysS, hemA*	
Ribosomal proteins/assembly	*rpsR*	*rpmE, sra, yhbY*	*rpmD*	*rmpE, sra*	*rpsU, ykgM, ykgO,*	*rplF*
Methyltransferase activity	*yjcD*		*yjcD*			
tRNA modification/processing					*ygfZ, rnd*	*hypB, rnpB*
Protein folding and maturation						
tRNA modification			*ygfZ*		*ygfZ*	*yeaZ*
Translation initiation/activation		*infA, yhbJ*		*infA*		
Transcription elongation					*greA*	
Translation termination/inhibition						
Transcription antitermination					*nusB*	
Transcription termination					*rof*	
tRNA-dihydrouridine synthase		*dusB*				
Trans-translation mechanisms		*ssrA*				
tRNA-uridine 2-thiolation selenation	*iscS*		*yhdL*	*dnaT*		
Amino acid biosynthesis/Degradation						
L-tyrosine biosynthesis						
L-asparagine biosynthesis	*iscS*			*ansB*	*aspC*	*ansB,*
L-tryptophan biosynthesis	*trpA, trpB*		*trpABCD*			*rbsK*
L-glutamine biosynthesis	*glnA*		*glnAPQ*		*glnB*	*glnA*
L-methionine biosynthesis				*mtnNJ*	*yebR*	*metE*
L-threonine degradation		*tdcB*	*ltaE*	*tdcBC*		*tdcABCDEF*
L-glutamate degradation		*aspA*			*aspC*	*aspA*
L-arginine degradation						*astABD*
L-lysine degradation						*ldcC, yfiQ*
Aminopropylcadaverine biosynthesis						*ldcC*
L-tryptophan degradation				*tnaA*		*tnaA*
L-glutamate biosynthesis	*gltBD, glnA*		*glnA*			
Modulation of ribosome activity				*yfiA*		
L-aspartate degradation	*glnA*	*aspA*	*glnA*			
L-alanine biosynthesis	*iscS*					

L-serine degradation		*tdcB*		*tdcBD*		
L-glutamine degradation			*carAB*			*carA*
L-arginine biosynthesis			*carAB*			*carA*
Amino acid degradation		*hflD*				
L-leucine biosynthesis				*lrp*		
L-cysteine degradation				*tnaA*		
Amino acid salvage						*ggt*
L-lysine degradation						*gabD*
Cofactor, secondary metabolite						
Molybdenum cofactor biosynthesis		*yagR*	*moaABC, sbp*			
Iron-sulfur clusters/Iron uptake	*entB, iscS*		*fiu*		*exbB*	
Riboflavin biosynthesis						
Protoporphyrin-IX biosynthesis					*ribA*	
Porphyrin-containing compound metabolism					*hemA*	
Ubiquinone and cofactor biosynthesis						
Thiamine diphosphate and cofactor biosynthesis					*ubiA, thiCEFH*	
Hydrogenase maturation pathway						*hypD*
Biotin and cofactor biosynthesis					*fabB*	*bioA*
Ethanolamine degradation						*eutCL*
Cobalamin (vitamin 12) transport	*btuB*					
Transport of β-D-cellobiose + chitobiose		*chbBC*				
Pyridoxal 5'-phosphate biosynthesis cofactor (Vitamin B6)			*pdxJ*			
Transport of iron(III)-enterobactin complex					*exbB*	
Methylerythritol phosphate pathway					*fldA*	
Fatty acid, lipids, membranes and Peptidoglycan biosynthesis		*gpsA*				*pgpA*
Murein precursor, activator and maturation		*mltD*		*mltD*	*mltD*	*lpp*
Membrane biogenesis/maintenance		*rfbDX, wbbH*				
Fatty acid biosynthesis					*fabAB*	*accC*
Fatty acid beta-oxidation/degradation		*fadH*		*fadD, yfcY,*		*fadI*
Phosphatidylglycerol biosynthesis						*pgpA*
Phospholipid biosynthesis		*gpsA*				
Cell wall/peptidoglycan biosynthesis		*mltD*		*mltD*	*mltD, ftsN*	
DNA and nucleotide biosynthesis						
Cytochrome c biogenesis	*secF*				*secG*	
Pyrimidine and purine biosynthesis/ metabolism	*pyrBI, purCM*		*pyrBCI, purNMT*			
Pyrimidine salvage pathway	*codA*		*pyrBCI, purNMT, codAB*			

Purine salvage and metabolism		cdd	*codAB*		*apt, seqA*	*rbsK, codA, pyrB, purK,*
Replication and cell division	*holC*	*rnr*			*rnd*	*rihA*
de novo UMP biosynthesis	*Ihr, pyrBI*	*cdd*	*carAB, codAB, pyrBCI,*			*carA*
5-aminoimidazole ribonucleotide			*purNMT*			
Cell division inhibitor	*ttk*					
UMP biosynthesis l	*pyrBI*		*pyrBCI*			
Guanosine nucleotide biosynthesis			*guaB*			
4-aminobenzoate biosynthesis I (folate synthesis)			*pabA*			
Purine catabolic pathway						*ygeW*
Response to stimuli and repair						
General stress	*rpoS*	*hns, uspE, pspA, gadWX, clcA*	*ycfR rseB, ycfR*	*lsrR, hns* *cspA*	*uspG, ycfR, yciEF, ydhm, osmY*	
Recovery from glucose phosphate stress		*dksA*				
Cold/Heat/phage shock/peroxidase		*cspACE*	*ibpA*		*ibpAB, groS, osmY*	*osmB, cspAB*
Methylglyoxal degradation lll	*yqhD*		*yqhD*		*yhcN*	
Copper/zinc/lead/mercury transport	*cueO, copA, yobA*	*zur*	*cueO, copA, zupT*		*copA, zupT*	
Acidity/ acid tolerance			*frc*	yddV	*ymgB*	
General/DNA repair/SOS			*ruvC*	*yicR, yebG, mutY*		*uvrC, tatD*
Phage degradation						*hflD*
Thiol-oxidative stress	*azoR*				*azoR*	
Glycine betaine transport	*proX*					
Toxin-antitoxin systems		*yhaV*				*fic*
Two-Component Signal Transduction System		*evgS*				
Detoxification of toxic formaldehyde			*frmA*			
Carbon starvation induced regulation			*csiR*			*frmA*
Ubiquinone biosynthesis					*yubiA*	
Energy and Cellular respiration						
Glyoxylate cycle bypass, and glycolate dehydrogenase activity	*glcBDEFG, aceAB,*		*glcBE, aceAB*			
Glycolysis						*glgA, gapA*
Gluconeogenesis	*pck, pps*		*pps*			*pcka, gapA*
Carbohydrate/ pyruvate metabolism		*gpsA,sfsA*			*kdgK*	*pck*
Pentose phosphate pathway						*galK, gatZ*
Carbohydrate degradation		*rbsD*		*melR*		*rbsK*
ATP biosynthesis	*atpG*					
Entner-doudoroff pathway catabolism			*gntR*			
Glycogen biosynthesis pathway						*glgA*
CMP-3-deoxy-D-manno-octulosonate biosynthesis						*kdsC*
Formate-independent degradation						
Acetate and pyruvate metabolism						*ygeV, tdcE*

Propionate metabolism: 2-methylcitrate cycle I					*prpB*	
Anaerobic-associated processes						*fdoH*
Nitrate reduction pathway					*norR, narK*	*narH, napACG*
Nitrogen metabolism					*norR*	
Threonine degradation						*tdcE*
C4-dicarboxylate transporter						*dcuC*
Anaerobic metabolism						*hybAO*
Anaerobic respiration/ Mixed Fermentation		*frdA*				*frdAB, hyaAD, dmsAC, tdcE, hybAO*
Propionate metabolism					*prpB*	*gapA*
Isoprenoid biosynthesis					*fldA*	
Aerobic-associated processes						*fdoH*
The citric acid cycle (TCA)	*sucC, sdhAB, glcBCGFE, aceAB*		*sdhA*			*sdhBD*
Oxidative phosphorylation	*sdhAB, sucC, glcBCGFE, aceAB*		*sdhA*			
Cytochrome bo oxidase electron transfer						*cyoD, cydB*
Sulfur metabolism	*cysN*		*cysD, pspE, sbp*			
Sulfur degradation				*csdA*		
Resistance-associated genes						
Antimicrobial/multi-drug resistance		*aacA6*	*marB*	*aacA6, aadA-1, aph3*	*terE, marA*	*yhjX, mdtE, evgS*
Efflux pump/transporter	*copA*		*copA, cueO, zupT*		*zupT*	*yjcQ*
Inner/outer membrane proteins	*yqjF, yjiY*	*ychH, yecN, yniB*	*yjiY, yebE, yqjE*	*ychH, ylaC*	*yqjF, tolA, yqjF, slp, slyB*	*yjiY, ychH*
Toxin/Antitoxin		*dinJ*	*chpR*		*chpR*	
Plasmid/Transposase						*insH-3*
Degradation of toxins	*nemA*		*nemA*			
Detoxification of alcohols and aldehydes						*aldA*
Virulence-associated genes						
Biofilm formation	*yjgI*	*yjfO, ylaB, yjcC*	*yjgI, ydeH*	*yliH, lsrR,* yddV, *csgDG*	*yjgI, ymgB, yeaJ*	*flu, yjfO*
Motility		*irhA*				
Virulent toxins	*cvpA*		*cvpA*	*yhaV*		
Plasmids/Transposase						*insH-3*
Adhesion		*ylaB*				
Transport						
Formate transporter						*focA*
Phosphate transporter/uptake			*phoBRU, psts*		*pstS*	
MFS superfamily transporter					*ycaD*	
Carbohydrate/Sugar transport system		*chbBC, mltR*		*chbB*		*manX, lamB*

Nitrate/Nitrite transporter					*narK*	
Zinc uptake						
Hexose phosphate transporter						*uhpA*
L-cysteine sodium transporter					*ydjN*	
Potassium transport						*kdpABCDE*
Glutamate and aspartate transporter			*glnPQ*			*glnHQ*
Proton-coupled chloride transporter						
Cobalamin (vitamin B12) transporter	*yjcD*					
Nucleoside transporter		*nupC*	*uraA*			
Periplasmic and amino acid transport		*gcvB*			*ycaD*	
ABC organic solvent transporter			*yrbD*			
Outer membrane transport mediation				*ompCF*		
Autoinducers and quorum sensing		*lsrC*		*lsrABCR*		*lsrAB,*
Signalling/sensory proteins					*sixA*	
Transcriptional regulators	*Ttk, rpoS*	*dksA, gadX, hns*	*csiR, rseB*	*melR, lrp, hns*	*ydhM*	*ygeV,*
Transcriptional activators		*gadW*	*phoB*	*csgD*		
Transcriptional repressor		*mltR, irhA, zur*	*gntR*	*metJ, lsrR*	*frmR*	

Table S4. Pathways and biological processes of genes expressed during the lag and log phase (≥2 Log_2FC, p-value 0.05) in *S. aureus* strain ATCC BAA-39 in response to KS25, KS33 and KS51. Genes that are strongly upregulated are highlighted in yellow and genes strongly downregulated are highlighted in green. For each pathway, associated genes are listed.

	KS25		**KS33**		**KS51**	
Pathway/ Biological processes	Upregulated genes	Downregulated genes	Upregulated genes	Downregulated genes	Upregulated genes	Downregulated genes
Protein biosynthesis						
RNA synthesis/maturation	*rnjA*					*rpoA,*
Aminoacyl-tRNA synthetases	*valS, thrS*	*glyS*	*valS*	*glyS*		
Ribosomal protein/maturation	*prmA, rplL3*	*rpmB*			*rpmG*	*rplV, rplJ, rplL, rplO, rpsE, rplR, rplF, rpsH, rplN, rplP, rpsS*
Transcription		*veg*				*pnp, veg*
mRNA/ tRNA processing/binding	*gidA*	*rnpA*				
Protein catabolism	*yrrO*		*yrrO*			
Transcription termination						
Translation termination/inhibition		*srp*				*cggR*
Aminotransferase	*gabT*					
tRNA Methyltransferase	*trmB*					
tRNA wobble base modification						
Amino acid biosynthesis/Degradation						
Amino acid catabolism/degradation	*acoB, bkdA*	*gabP*				
L-lysine biosynthesis				*thrA*		
L-arginine biosynthesis	*argGH*		*argGH*			*dapBD, ywfG,*
L-glutamate biosynthesis	*gltBD*	*gltS, pnbA*	*gltBD*			*gltB*
L-threonine degradation	*tcyA*	*tdh*				
L-glycine biosynthesis	*serAC*	*pnbA*				
Glycine degradation	*gcvP2*		*gcvP2*		*gcvP2*	
Amino transferases	*gabT*		*gabT*			
Isoleucine biosynthesis	*ilvBCD*		*ilvB*			
Valine biosynthesis	*ilvBCD*		*ilvB*			
Threonine synthesis						*thrC*
L-leucine biosynthesis	*leuA2, ilvBCD*		*leuA2, leuC*			
Amino acid-proton transporter		*prsA2*		*prsA2*		
L-serine, glycine, threonine metabolism		*betB*				
Valine, leucine, isoleucine degradation	*acoB, bkdA*			*pct*		*pct*
L-glutamine synthesis		*glnB*				
Protein synthesis inhibition		*srp*				

L-alanine catabolism		*ald*				
L-Histidine biosynthesis	*hisABCDEGHZ*		*hisE*	*putA*		
Histidine catabolism		*hutHIU*			*hutIU*	
Arginine and proline metabolism						*glxK*
Serine/glutamate/threonine degradation		*tdh*				
Amino acid salvage	*ggt*					
L-cysteine biosynthesis	*metC2*					
L-glycine biosynthesis	*merA2*, *serA*		*merA2*			
L-methionine biosynthesis	*metINCQ2*					
Fatty acid, lipids, membranes and Peptidoglycan biosynthesis						
Peptidoglycan hydrolyses						*ltyM, glmU*
Lipoteichoic acid biosynthesis					*dltBD*	
Aerobic fatty acid beta oxidation		*menE*			*fadA*	
Fatty acid biosynthesis						
Cell wall/Peptidoglycan biosynthesis		*murQ*				*uppS, ftsW*
Lipid catabolic process		*lip2*			*lip2*	
DNA and nucleotide biosynthesis						
Pyrimidine and purine biosynthesis		*purEFKLQS, pyrPBC*		*pyrBC*	*purACDEFHKLMNQ, pyrE*	*purDHLM*
Pyrimidine nucleobases salvage		*upp*				
Purine salvage/metabolism						*relA*
Guanosine nucleotide de novo biosynthesis		*guaC*			*guaC*	
Folate biosynthesis	*folC*		*folC*			
Uptake of purine bases						
DNA/Nucleic acid binding	*nrnA*					*nrnA*
Nucleotide-sugar biosynthesis		*hup*				*glmU*
Cell division and DNA replication	*dinB*	*mraZ*		*mraZ*		*ylaQ, mraZ, dnaX, recQ*
Adenosine ribonucleotides de novo biosynthesis					*purAD*	*purD*
5-aminoimidazole ribonucleotide biosynthesis I					*purFLMN*	*purLM*
Inosine-5'-phosphate biosynthesis I					*purCEHKO*	*purH*
UMP biosynthesis					*pyrE*	
Response to stimuli and repair						
General stress	*mcsB*		*mcsB*		*uspAB, spxA, degP/htrA, mcsB*	*yugI, vraS*
Cold/Heat shock/ Chaperones	*grpE, hrcA, groLS*		*groLS, hrcA*		*groL*	*cspAB, cspA2*
Oxidative stress caused by reactive oxygen species	*bshC*	*msrR*		*msrR*	*katE, ahpCF, merR*	
Copper/zinc ion transport/homeostasis	*mco, copA*		*copA*			
Cadmium ion transport	*cadABC*		*cadABC*			
Zinc ion or cobalt transport/homeostasis	*zitB*		*zitB*		*zitB*	

Alkaline shock protein/tolerance		*asp*	*asp*	*phoB*		
Chaperone/Protein folding	*hslO, dnaJK*		*hslO, dnaJK*			
	clpBCPX		*clpBCPX*			
General/DNA repair	*uvrB/uvrC, yeeS*	*hsdS*	*uvrB/uvrC*	*hsdS*		*recAQ, uvrB/uvrA, lexA*
DNA Protection during starvation	*dps*		*dps*		*dps*	
Defence against phagocytosis	*hlgB*		*hlgB*			
Immunogenic protein	*ssaA*					
Defence against neutrophil killing						*srrB*
Plasmid	*pre*					
Protection against thiol-specific stress	*azoR*					
Phosphate starvation	*yitU*					
Thioredoxin pathway			*trxB*			
Energy and cellular respiration						
Glyoxylate cycle		*pdxB*				
Fructose and mannose metabolism	*pfkB, fruA*		*pfkB, fruA*			
Pyruvate generation		*ald*				
D-gluconate degradation		*gntP*				*gntKRP*
Pentose phosphate pathway					*tkt*	
Sugar/carbohydrate metabolism	*treP, gatD, gntP*	*lacCE*				*trePR, ispE, gntKR, manA*
Nitrate reduction/nitrogen metabolism		*narHK, nirB*				
Gluconeogenesis	*pfkB, gpmA*	*gapA, pckA*	*fbp, pfkB*		*pckA*	*gapA*
Methylglyoxal degradation					*aldA*	
Glycolysis	*gmpA*				*gap, fba*	*gap*
Electron transport chain						*hepT*
Trehalose degradation						*treC*
Acetate and pyruvate metabolism	*pta*		*pta*		*pta*	
Embden-Meyerhof-Parnas	*pfkB*		*pfkB*			
Anaerobic-associated processes						
Nitro-reductase family proteins		*narHK, nirB*	*frp*			*narG*
Mixed fermentation	*gmpA, pta*		*pta*		*frdAB*	*idhA*
NADH dehydrogenases						*nuoF*
Aerobic-associated processes						
The citric acid cycle (TCA)	*ccpAE, merA2*	*sucC, icd*	*merA2*	*sucABCD*	*sdhABC*	
Glycerol uptake/degradation		*glpFQ4*	*glpD*		*glpKD,*	*uhpT*
Cytochrome bo oxidase electron transfer	*cydA*					*qoxA*
NADH dehydrogenases						*nuoF*
Sulfur transport/metabolism	*fdhD*					
Degradation of aromatic compounds					*yfmJ*	
Resistance-associated genes						
Antimicrobial resistance	*fmtB1, marR*		*marR*	*tcaA*	*mecA,*	
Efflux pump/transporter	*copA, zitB*					

Membrane barriers						
Copper, zinc efflux	*copA, zitB, zntA*		*copA, zntA*		*zntA, copA*	
Acid resistance/tolerance						*speA_1*
Carotenoid biosynthesis		*crtQ*		*crtN*		*crtQ*
Cadmium stress proteins	*cadABC*		*cadABC*			
Virulence-associated genes						
Biofilm formation	*mcsB*		*mcsB*		*sasG, mcsB*	
IgG-binding protein	*sbi*		*sbi*		*sbi*	
Invasion	*fnbAB*		*fnbAB,*		*saeRS*	
Adhesion	*sraP, lysM*	*spa, sdrC, clfAB*			*sarRS, saeRS*	*clfB, ebh, sasC*
Surface colonization	*lysR*		*efb*		*efb*	
Secreted proteins/toxins	*hlgAB*		*isaA*		*isaA, hly, cap5F, hlgAB*	*yqfA*
Autolysis	*sarV*	*sasH*				
Transport						
L-cysteine transport	*tcyAP*		*tcyACP*			
Sodium transporter	*sdcS*		*sdcS*			
Sugar/carbohydrate transport system	*fruA, scrA, treP, gntP*	*lacE*	*fruA, scrA*	*malK*		*ptsG, manA*
Methionine transport	*metINCQ2*		*metN2, metI*			
Histidine permease ABC transporter	*yuiF*		*yuiF*			
Glutamine transport	*glnQ*		*glnQ*			
Maltodextrin ABC transporter				*mdxE*		
Uracil symporter				*pyrP*		
D-serine/D-alanine/glycine transporter		*cycA*				
Manganese ABC transporter	*mntH*	*sitAB*				*sitB*
Oligopeptide/Choline ABC transporter	*opuCC*	*oppD, oppC3*	*opuCC*	*oppBD*	*opuCD, opuCC, proV*	*oppD, oppA2*
Nucleotide transporter						*nupCG*
Nitrate ABC transporter		*narK*				
Glutamate symporter		*gltS*				
Amino acid transporter	*yisU, ybeC*					*gabP*
Zinc ion transporter	*zitB*		*zitB*		*zitB*	
Potassium transport					*kdpBC*	
Translocase pathway						*secY*
L-lysine transporter						*lysP*
ABC transporter	*Wzt*		*mntC*			*ecsA, tagH*
Thiamine ABC transporter		*ykoDE*			*ykoDE*	
Spermidine/putrescine transporter				*ecsA*	*potA*	
L-lactate transmembrane transporter						*lctP*
Gluconate transporter						*gntP*
Secondary metabolites and co-factors						
Dephospho-CoA kinase	*coaE*					
Thiamine biosynthesis		*thiDEM*			*thiEM*	
Molybdenum cofactor	*fdhD*				*moeB*	*fdhD*
	folk					

Tetrahydrofolate and cofactor biosynthesis (vitamin B6) Shikimate pathway Thiamine salvage pathway Pyridoxine biosynthesis (vitamin B6) Iron clusters assembly/storage/uptake	*serC*	*aroK* *tenA* *ftnA*	*paaD,*			
Autoinducers and quorum sensing Signalling proteins		*cbix*		*cbiX*	*saeRS*	
Transcriptional regulators	*ctsR, sarV, marR, lysR, ccpE*		*ctsR, marR*		*merR*	
Transcriptional repressor	*lacR2, hrcA, czrA*		*lacR2, hrcA*			*gntR, lexA*

Table S5. Fold change comparison values of homologous genes differentially expressed in *E. coli* BAA-196 (BAA196NC) in comparison to *S. aureus* BAA-39 (HMPRNC0000) under the effect of three iodine-containing complexes, KS25, KS33 and KS51, in Lag and Log growth phases. Upregulated genes are represented in positive values and downregulated genes are represented in negative values. Statistically reliable changes of gene expressing (≥2 Log_2FC; p-value ≤ 0.05) are highlighted by yellow (upregulation) or green (downregulation) shading. Genes are ordered by clusters with similar patterns of expression.

Locus tag		**Gene**	**Model microorganisms, treatments and growth phases**												**Annotation**
			***E. coli* ATCC BAA-196**						***S. aureus* ATCC BAA-39**						
			KS25		**KS33**		**KS51**		**KS25**		**KS33**		**KS51**		
			Lag	Log	Lag	Log	Lag	Log	Lag	Log	Lag	Log	Lag	Log	
BAA196NC_3269	HMPRNC0000_2838	*copA*	5.32	3.86	5.77	3.71	2.65	0.98	2.86	1.78	1.77	2.09	0.34	0.67	Copper transporter
BAA196NC_3990	HMPRNC0000_2200	*groL*	2.01	2.18	1.43	3.22	1.55	2.47	3.40	3.61	3.13	3.31	1.44	2.18	Chaperonin GroEL
BAA196NC_0249	HMPRNC0000_0035	*zntA*	1.15	0.39	0.69	1.11	-1.65	0.07	3.54	2.19	2.73	2.00	0.63	0.67	Zinc, cobalt and lead efflux system
BAA196NC_2850	HMPRNC0000_0426	*nfsA*	-0.82	1.46	0.22	0.79	-1.36	-0.35	1.78	0.29	0.91	1.28	-0.02	1.17	Nitroreductase A, NADPH-dependent, FMN-dependent
BAA196NC_1600	HMPRNC0000_2283	*thiM*	0.22	0.61	0.32	0.09	-5.09	-0.41	-1.84	-3.36	-1.49	-1.67	5.66	2.98	Hydroxyethylthiazole kinase
BAA196NC_1601	HMPRNC0000_2284	*thiD*	-1.18	-3.73	-0.29	-0.25	-1.28	-0.63	-0.93	-1.51	0.25	0.00	5.77	3.14	Phosphomethylpyrimidine kinase
BAA196NC_4141	HMPRNC0000_2282	*thiE*	1.05	0.14	0.99	-0.77	-1.69	-0.69	-1.03	-1.51	0.10	0.00	6.12	3.95	Thiamine-phosphate pyrophosphorylase
BAA196NC_1963	HMPRNC0000_2410	*chbC*	1.29	-1.11	1.50	0.74	-1.81	-0.96	-1.94	-0.96	-0.99	-0.98	-1.82	-1.55	N,N'-diacetylchitobiose-specific enzyme IIC component of PTS
BAA196NC_1977	HMPRNC0000_2415	*pfkB*	0.00	-1.36	0.66	-1.51	0.22	-0.76	-1.34	0.00	-0.27	0.00	-0.59	0.00	6-phosphofructokinase II
BAA196NC_3232	HMPRNC0000_1099	*purE*	-2.94	1.21	-3.07	1.25	-3.20	2.56	-2.39	-2.83	-0.65	-4.83	2.16	-2.55	Phosphoribosylaminoimidazole carboxylase catalytic subunit

BAA196NC_1964	HMPRNC0000_2413	*chbA*	0.91	0.58	0.81	1.10	0.49	0.23	0.68	-2.46	0.26	-1.67	1.84	-1.36	N,N'-diacetylchitobiose-specific enzyme IIA component of PTS
BAA196NC_2475	HMPRNC0000_2644	*narK*	0.40	-1.61	0.40	-1.04	-0.28	-1.07	-2.97	-2.55	-1.47	-1.41	0.45	-3.84	Nitrate/nitrite transporter
BAA196NC_4201	HMPRNC0000_1367	*glpK*	-2.84	-0.48	-2.40	0.75	-3.73	-0.30	-1.26	0.14	-0.75	0.34	1.97	1.79	Glycerol kinase
BAA196NC_4043	HMPRNC0000_2416	*rpiB*	-3.81	1.18	-4.48	1.43	-6.58	1.33	-0.45	0.00	-1.16	0.00	0.48	0.00	Ribose-5-phosphate isomerase B
BAA196NC_2473	HMPRNC0000_2652	*narH*	-3.82	-3.28	-1.29	-2.85	-5.61	-1.77	-1.42	-1.17	-1.41	-1.46	0.92	-2.84	Nitrate reductase 1, beta (Fe-S) subunit
BAA196NC_2474	HMPRNC0000_2655	*narG*	-1.80	0.34	-1.96	-0.92	-4.56	-0.41	-2.34	-1.83	-1.45	-1.38	-1.15	-3.55	Nitrate reductase 1, alpha subunit
BAA196NC_0594	HMPRNC0000_1548	*tdcB*	-1.78	0.23	-1.30	1.43	-3.58	0.50	0.48	-0.26	2.05	0.74	0.16	0.06	Threonine dehydratase
BAA196NC_3098	HMPRNC0000_0263	*rihA*	-2.95	-0.33	-2.19	-0.49	-3.12	-3.28	-1.42	-2.11	-0.83	-2.45	-0.60	-0.70	Ribonucleoside hydrolase 1
BAA196NC_2873	HMPRNC0000_0219	*yliA*	-1.87	-0.06	-1.14	1.44	-1.37	-0.04	1.60	1.32	1.64	1.23	-0.83	0.65	Fused predicted peptide transport subunits of ABC superfamily: ATP-binding components
BAA196NC_2710	HMPRNC0000_1509	*cspG*	-0.10	-1.15	-1.17	0.49	0.82	0.47	-2.49	-1.01	-0.82	-0.53	-2.16	-2.68	DNA-binding transcriptional regulator
BAA196NC_3442	HMPRNC0000_2404	*betT*	0.00	0.00	0.00	0.00	0.22	0.00	-1.67	-1.45	-0.87	-1.23	-1.67	-4.37	Choline transporter of high affinity
BAA196NC_3536	HMPRNC0000_0477	*metN*	-0.89	0.16	-0.56	0.23	-0.11	0.16	6.34	3.10	6.07	3.30	-0.93	0.00	DL-methionine transporter subunit
BAA196NC_3389	HMPRNC0000_0177	*tauC*	-0.23	-1.94	2.12	-0.94	1.80	-0.75	5.83	0.27	5.12	0.72	1.84	-1.55	Taurine transporter subunit
BAA196NC_3538	HMPRNC0000_0479	*metQ*	0.10	-1.48	-1.86	-1.94	1.20	-0.31	5.05	3.50	5.39	2.30	0.16	0.43	DL-methionine transporter subunit
BAA196NC_1685	HMPRNC0000_2984	*hisA*	0.15	1.54	0.97	0.03	-3.51	-0.04	3.99	0.70	2.96	1.32	-0.07	0.00	1-(5-phosphoribosyl)-5-[(5-phosphoribosylamino)methylideneamino] imidazole-4-carboxamide isomerase
BAA196NC_1697	HMPRNC0000_2219	*yeeD*	0.51	-0.46	1.04	0.32	1.55	-0.58	4.34	1.61	3.72	0.59	0.72	0.43	Hypothetical protein

BAA196NC_0271	HMPRNC0000_0224	*ggt*	-1.08	1.97	0.26	1.15	-1.09	2.41	3.83	1.04	3.73	0.00	1.86	0.00	Gamma-glutamyltranspeptidase periplasmic precursor
BAA196NC_4349	HMPRNC0000_2231	*ilvD*	0.00	-0.52	-0.17	-0.22	0.76	-0.46	4.24	-0.51	4.49	-2.70	0.48	-2.35	Dihydroxy-acid dehydratase
BAA196NC_3537	HMPRNC0000_0478	*metI*	-0.92	0.25	0.80	0.42	-2.62	-0.96	5.37	0.68	6.20	0.73	2.19	-0.47	DL-methionine transporter subunit
BAA196NC_2398	HMPRNC0000_2892	*puuE*	0.40	-0.54	-0.64	-0.41	-1.40	-0.45	2.84	-1.31	2.18	-1.79	-2.95	-2.22	GABA aminotransferase, PLP-dependent
BAA196NC_1048	HMPRNC0000_2892	*gabT*	-0.07	-1.19	-0.54	0.16	0.12	0.09	2.84	-1.31	2.18	-1.79	-2.95	-2.22	4-aminobutyrate aminotransferase
BAA196NC_2767	HMPRNC0000_0175	*ssuB*	0.06	-0.16	-0.21	-0.21	-1.77	-0.25	5.27	1.41	5.81	0.00	0.00	0.00	Alkanesulfonate transporter subunit
BAA196NC_1683	HMPRNC0000_2982	*hisI*	-0.63	0.48	0.09	0.53	-1.40	1.97	2.84	-0.60	2.26	-1.67	-1.80	-1.36	Bifunctional phosphoribosyl-AMP cyclohydrolase/phosphoribosyl-ATP pyrophosphatase protein
BAA196NC_3658	HMPRNC0000_2233	*ilvI*	1.45	0.64	-1.55	0.50	0.17	0.53	2.68	-1.32	3.03	-1.01	-1.44	-2.21	Acetolactate synthase III large subunit
BAA196NC_3991	HMPRNC0000_2201	*groS*	0.38	0.50	0.62	1.37	-0.76	0.34	2.99	1.81	2.35	1.88	0.42	-1.07	Co-chaperonin GroES
BAA196NC_4188	HMPRNC0000_0476	*metB*	1.03	0.56	1.84	0.09	-1.10	-0.41	4.29	2.73	4.22	3.40	3.83	0.00	Cystathionine gamma-synthase
BAA196NC_3012	HMPRNC0000_2350	*zitB*	0.18	1.33	0.28	0.88	-0.21	1.02	3.76	3.32	3.56	4.21	3.05	4.50	Zinc transporter ZitB
BAA196NC_1109	HMPRNC0000_1008	*clpB*	0.34	1.60	-0.29	1.50	-0.70	0.61	3.94	2.73	3.45	3.18	0.61	1.61	Protein disaggregation chaperone
BAA196NC_0249	HMPRNC0000_0035	*zntA*	-0.66	-0.87	0.12	-0.78	0.98	1.16	3.54	2.19	2.73	2.00	0.63	0.67	Zinc, cobalt and lead efflux system
BAA196NC_1090	HMPRNC0000_1711	*grpE*	0.97	2.04	0.21	1.49	-1.09	-0.75	2.71	4.28	1.79	4.39	-0.80	2.35	Heat shock protein
BAA196NC_0499	HMPRNC0000_0487	*gltB*	0.29	1.95	0.24	1.05	0.31	-0.66	4.60	2.27	4.10	2.45	-3.61	-2.39	Glutamate synthase, large subunit
BAA196NC_0498	HMPRNC0000_0488	*gltD*	0.49	-0.14	0.96	0.23	-2.34	1.27	4.70	2.13	4.21	1.75	-3.49	-3.07	Glutamate synthase, 4Fe-4S protein, small subunit
BAA196NC_3896	HMPRNC0000_2632	*treB*	1.96	0.67	0.84	-0.55	0.82	0.14	2.44	4.54	3.12	4.28	-0.83	2.27	Fused trehalose(maltose)-specific PTS enzyme: IIB component/IIC component

BAA196NC_0552	HMPRNC0000_1755	*yhbW*	0.16	-0.85	1.35	-0.31	-0.42	-0.80	2.44	3.98	1.82	4.13	-0.39	1.54	Luciferase-like monooxygenase
BAA196NC_3720	HMPRNC0000_1708	*dnaJ*	-0.80	0.38	-1.47	-0.45	0.59	1.10	2.56	2.52	1.99	2.70	0.47	0.65	Chaperone Hsp40, co-chaperone with DnaK
BAA196NC_0976	HMPRNC0000_0769	*ygbI*	2.00	1.88	0.07	1.44	-0.02	0.88	2.26	5.56	2.59	4.52	-0.09	-0.66	Predicted DNA-binding transcriptional regulator
BAA196NC_3932	HMPRNC0000_0412	*rpsR*	1.92	-0.17	3.95	0.74	1.60	1.10	0.70	1.03	0.60	1.86	1.21	1.44	30S ribosomal protein S18
BAA196NC_3356	HMPRNC0000_1610	*phoB*	3.14	1.92	3.01	0.83	-3.07	-2.00	-1.60	-0.65	-0.40	-0.54	0.15	-0.77	DNA-binding response regulator in two-component regulatory system with PhoR (or CreC)
BAA196NC_3891	HMPRNC0000_1253	*pyrB*	0.47	1.18	0.39	0.84	-2.31	0.39	-2.85	1.17	-2.49	3.06	0.97	-1.36	Aspartate carbamoyltransferase catalytic subunit
BAA196NC_0316	HMPRNC0000_1928	*pck*	5.32	3.86	5.77	3.71	2.65	0.98	-1.08	0.77	-0.73	0.49	3.54	1.39	Phosphoenolpyruvate carboxykinase

Table S6. List of databases and tools used.

List of databases and tools used	URL	Reference
UGENE v.36	http://www.ugene.net/	Okonechnikov *et al*., 2012
Trimmomatic v.0.40	http://www.usadellab.org/cms/?page=trimmomatic	Bolger *et al*.,2014
PheNetic	http://bioinformatics.intec.ugent.be/phenetic/index.html#/index	De Maeyer *et al*., 2013
Pathway Tools v.24.0	http://bioinformatics.ai.sri.com/ptools/	Karp *et al*., 2016
ShinyGO v0.66	http://bioinformatics.sdstate.edu/go/	Ge SX *et al*.,2020

Appendix A

UNIVERSITEIT VAN PRETORIA
UNIVERSITY OF PRETORIA
YUNIBESITHI YA PRETORIA

Faculty of Natural and Agricultural Sciences
Ethics Committee

E-mail: ethics.nas@up.ac.za

07 August 2020

ETHICS SUBMISSION: LETTER OF APPROVAL

Ms S Taukobong
Department of Biochemistry, Genetics and Microbiology
Faculty of Natural and Agricultural Science
University of Pretoria

Reference number: NAS176/2020
Project title: Exploring the gene regulation response of a multi-drug resistant, pathogenic Escherichia coli ATCC BAA-196 exposed to synthesized iodine containing complexes used as potential antimicrobial drugs or disinfectants

Dear Ms S Taukobong,

We are pleased to inform you that your submission conforms to the requirements of the Faculty of Natural and Agricultural Sciences Research Ethics committee.

Please note the following about your ethics approval:

- Please use your reference number (NAS176/2020) on any documents or correspondence with the Research Ethics Committee regarding your research.
- Please note that the Research Ethics Committee may ask further questions, seek additional information, require further modification, monitor the conduct of your research, or suspend or withdraw ethics approval.
- Please note that ethical approval is granted for the duration of the research (e.g. Honours studies: 1 year, Masters studies: two years, and PhD studies: three years) and should be extended when the approval period lapses.
- The digital archiving of data is a requirement of the University of Pretoria. The data should be accessible in the event of an enquiry or further analysis of the data.

Ethics approval is subject to the following:

- The ethics approval is conditional on the research being conducted as stipulated by the details of all documents submitted to the Committee. In the event that a further need arises to change who the investigators are, the methods or any other aspect, such changes must be submitted as an Amendment for approval by the Committee.
- **Applications using Animals:** NAS ethics recommendation does not imply that AEC approval is granted. The application has been pre-screened and recommended for review by the AEC. Research may not proceed until AEC approval is granted.

Post approval submissions including application for ethics extension and amendments to the approved application should be submitted online via the Ethics work centre.

We wish you the best with your research.

Yours sincerely,

Chairperson: NAS Ethics Committee